New Zealand Contributions to Radar Meteors: The Solar System Dust Cloud

Jack Baggaley

Physics & Astronomy Dept.
College of Science
University of Canterbury

UNIVERSITY OF CANTERBURY
Te Whare Wānanga o Waitaha
CHRISTCHURCH NEW ZEALAND

Describing the solar system dust cloud

1. Geometry of the gross dust distribution

Proto-planetary Discs

Hubble NICMOS

Near Infrared Camera & Multi-Object spectrometer 0.8 – 2.5 microns

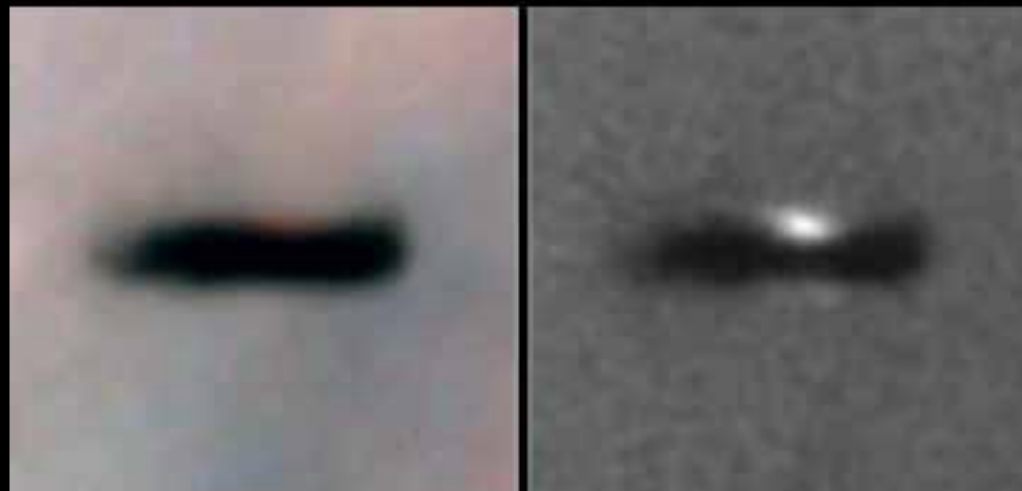

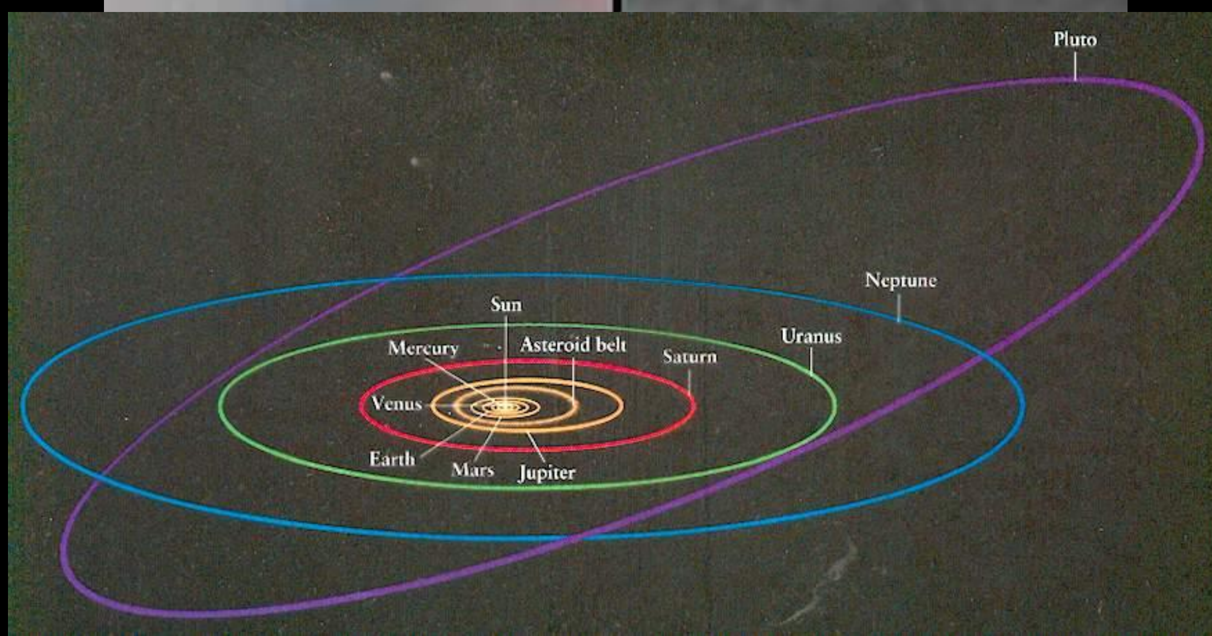

Describing the solar system dust cloud

2. Discrete features within the cloud –
   sources of the dust –
     dust loss from comets near perihelion
     dust associated with asteroids –
         inter-asteroid collisions
         solar wind irradiation of asteroid surface
         levitation via surface charging

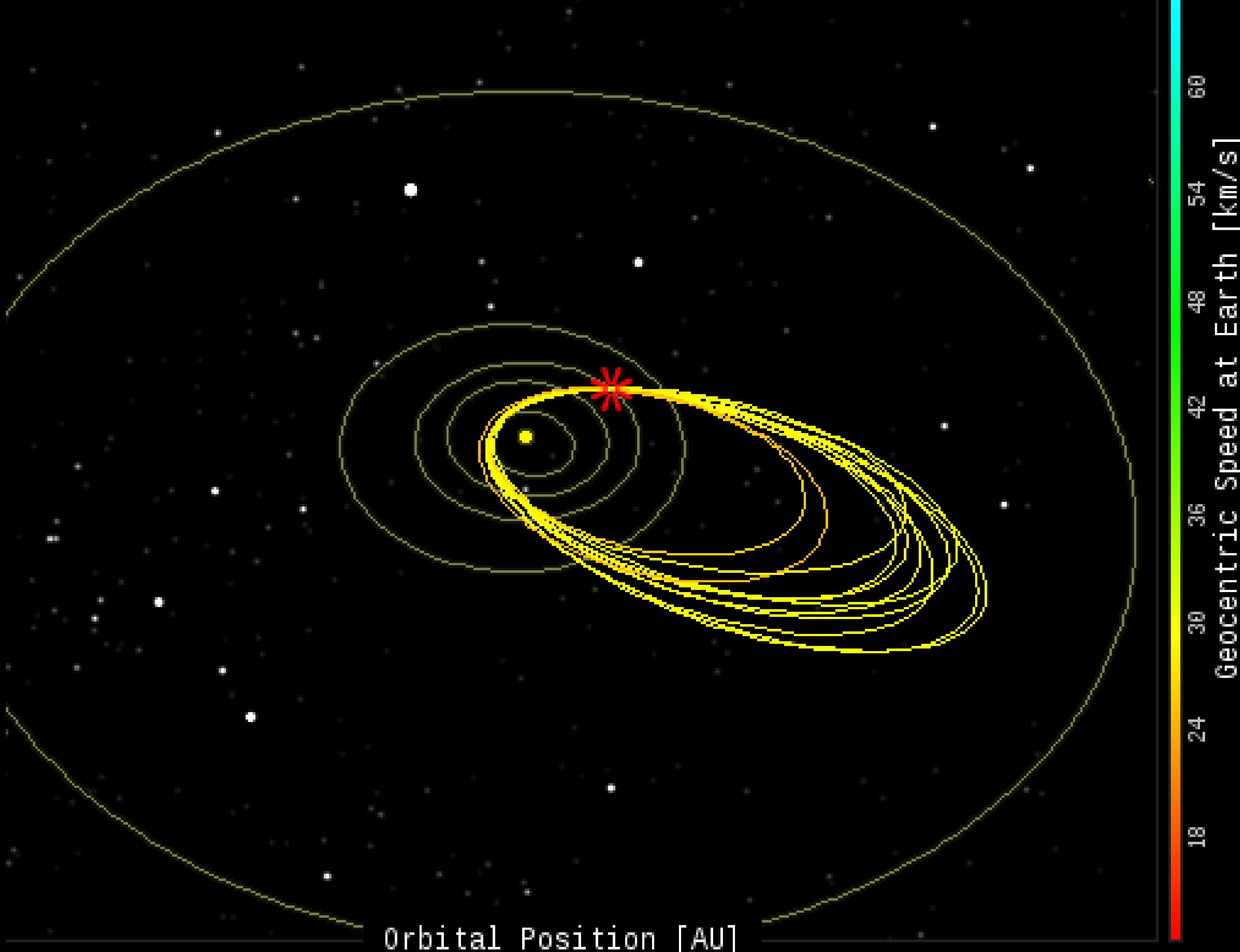
Orbital Position [AU]
Geocentric Speed at Earth [km/s]
18
24
30
36
42
48
54
60

Meteoroid evaporation in the atmosphere – generation of transient plasma

Radar detection of the plasma by scattering of radio waves

First work at Canterbury – 1950 -1970: range/ diurnal/seasonal characteristic

- spatial density of dust particles
- geometry of the macro features of the dust cloud.

Second – 1970 - examination of the phase features of individual echoes -

tells us about velocities – heliocentric orbits

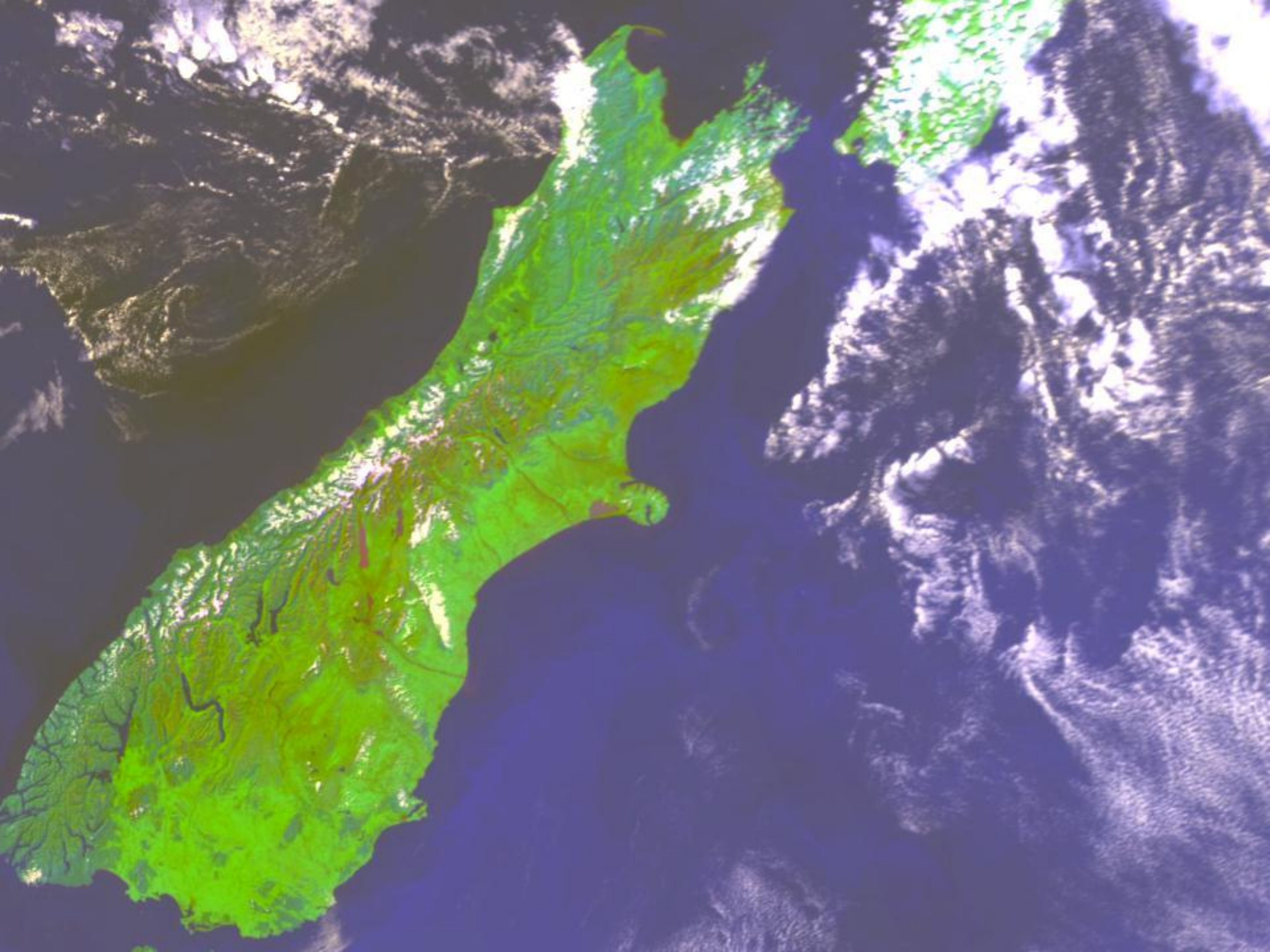

Clif Ellyett

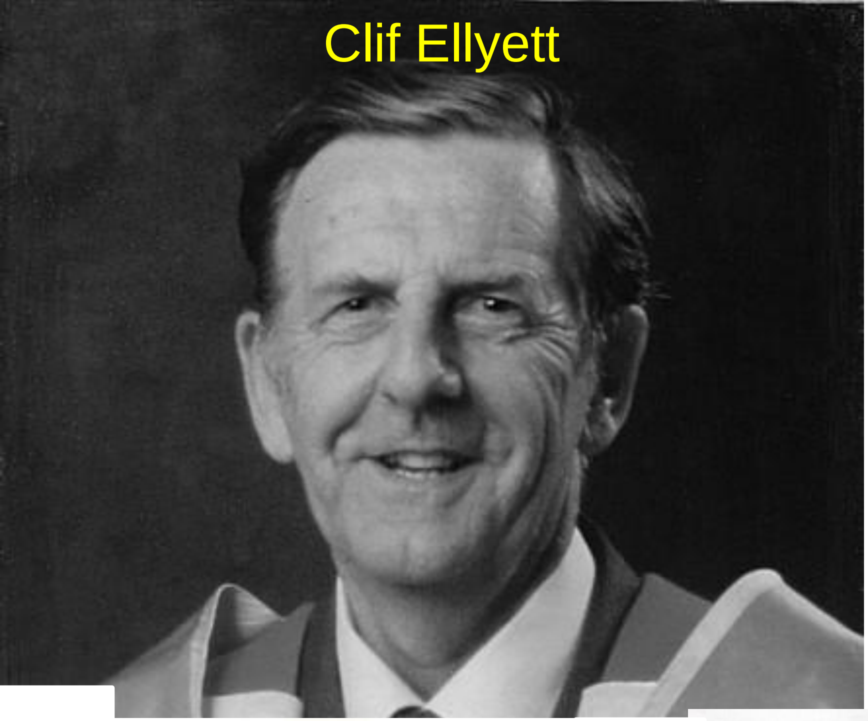

Colin Keay

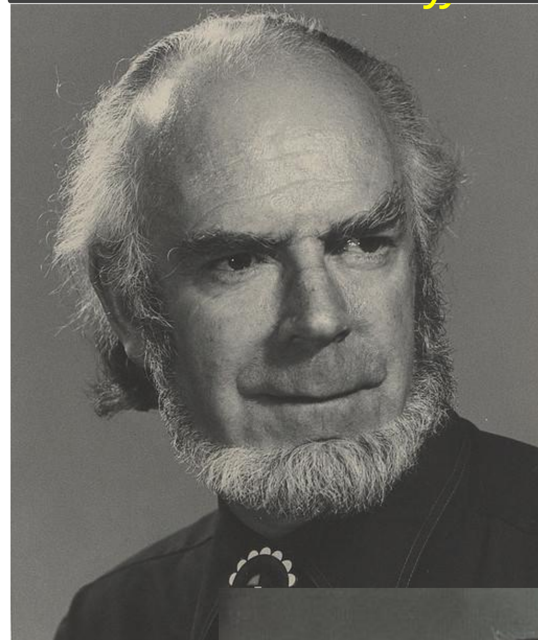

Errol McClauchlan
Peter McNabb

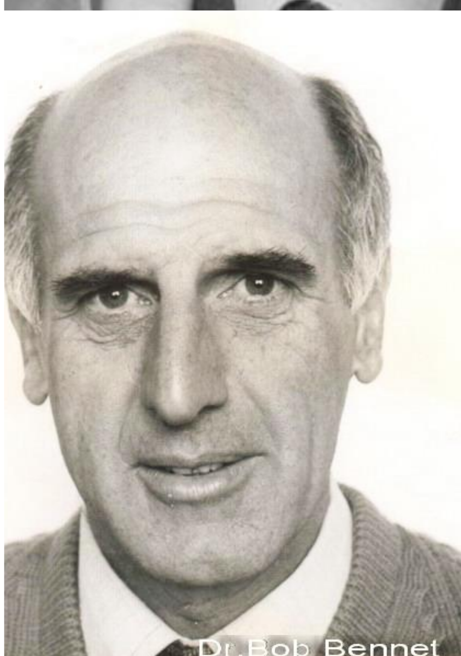

Bob Bennett

Grahame Fraser

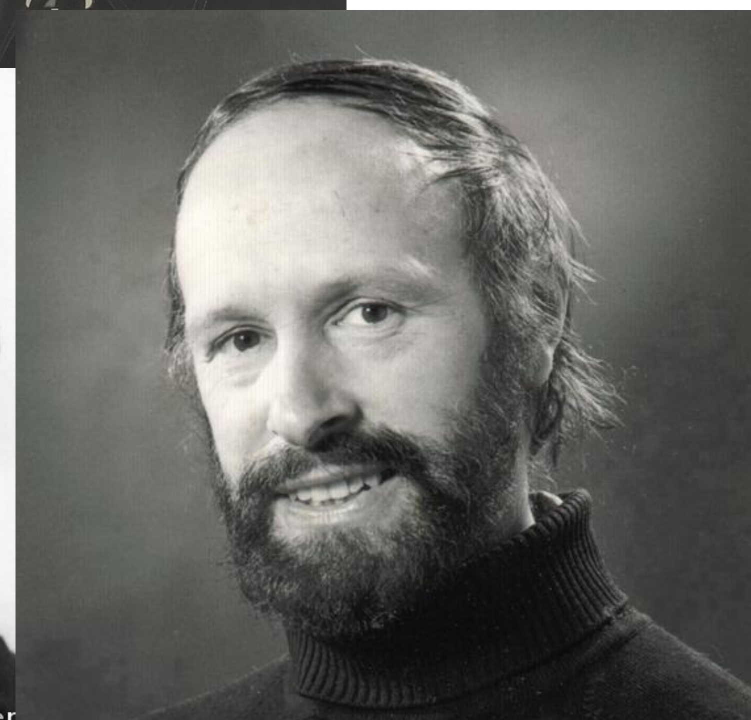

Jack Baggaley

* Pre 1940 visual meteors R.A. McIntosh

1940-43: Clif Ellyett work on ionospheric ionosondes in Christchurch, Campbell Is, Rarotonga, Kermadec Ils – for communication in the S Pacific.

1943: Clif liased between Australia and NZ to coordninate ionospheric work.

1944: Clif attended a meeting in the US on radio propagation and communication.

Some background –

optimum wavelength for meteor plasma studies

Optimum wavelength for detection of meteor plasma

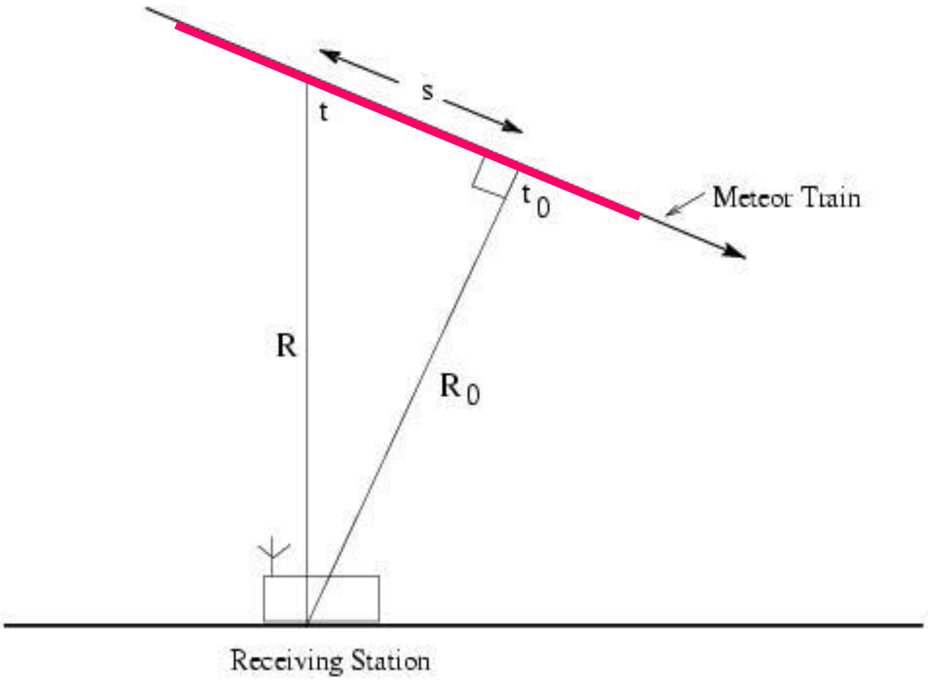

Optimum wavelength for detection of meteor plasma

Fresnel Zone length = $(R_0 \lambda / 2)^{0.5}$

Receiver antenna cross-section ~ λ^2

Echo power ~ λ^3

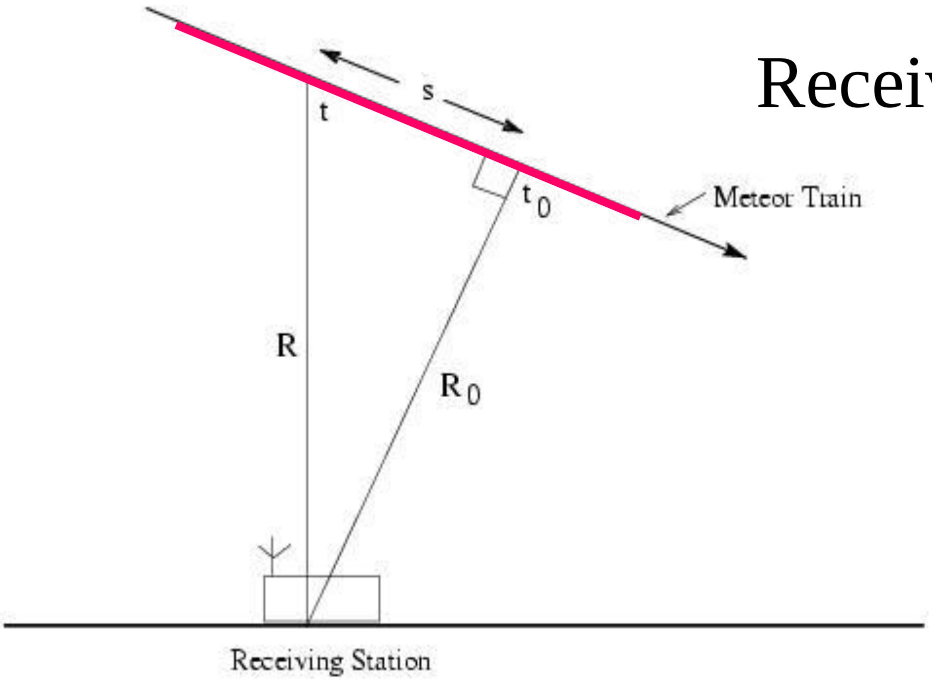

Optimum wavelength for detection of meteor plasma

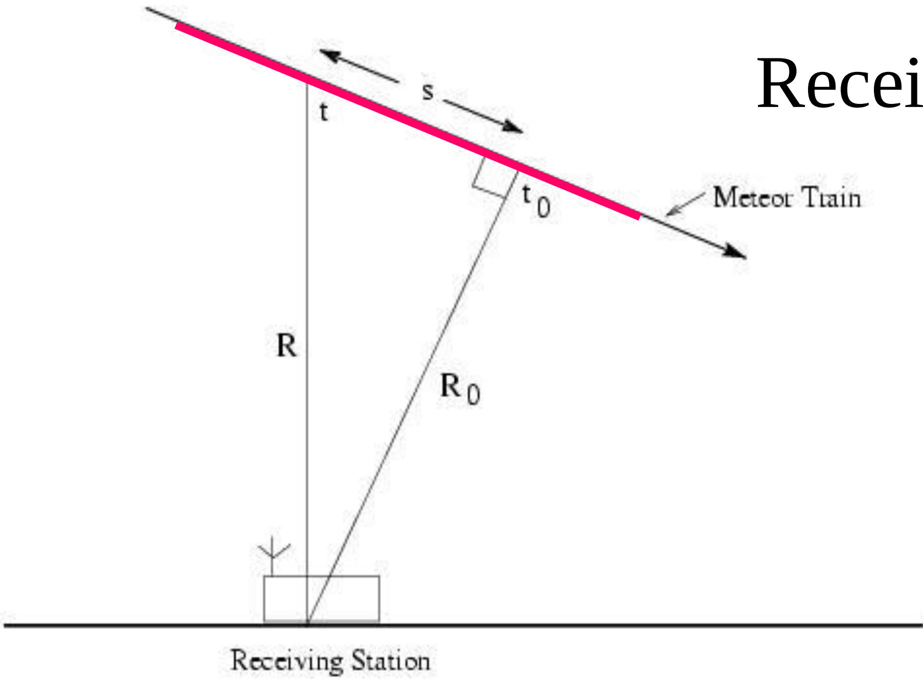

Fresnel Zone length = $(R_0 \lambda / 2)^{0.5}$

Receiver antenna cross-section ~ λ^2

Echo power ~ λ^3

Cosmic noise power ~ λ

Ionospheric reflections

Broadcast interference

Optimum frequency 20 – 60 MHz
15 – 5 metres

Some background –

on radars employed for meteor plasma studies

Chain Home radar network 25 MHz

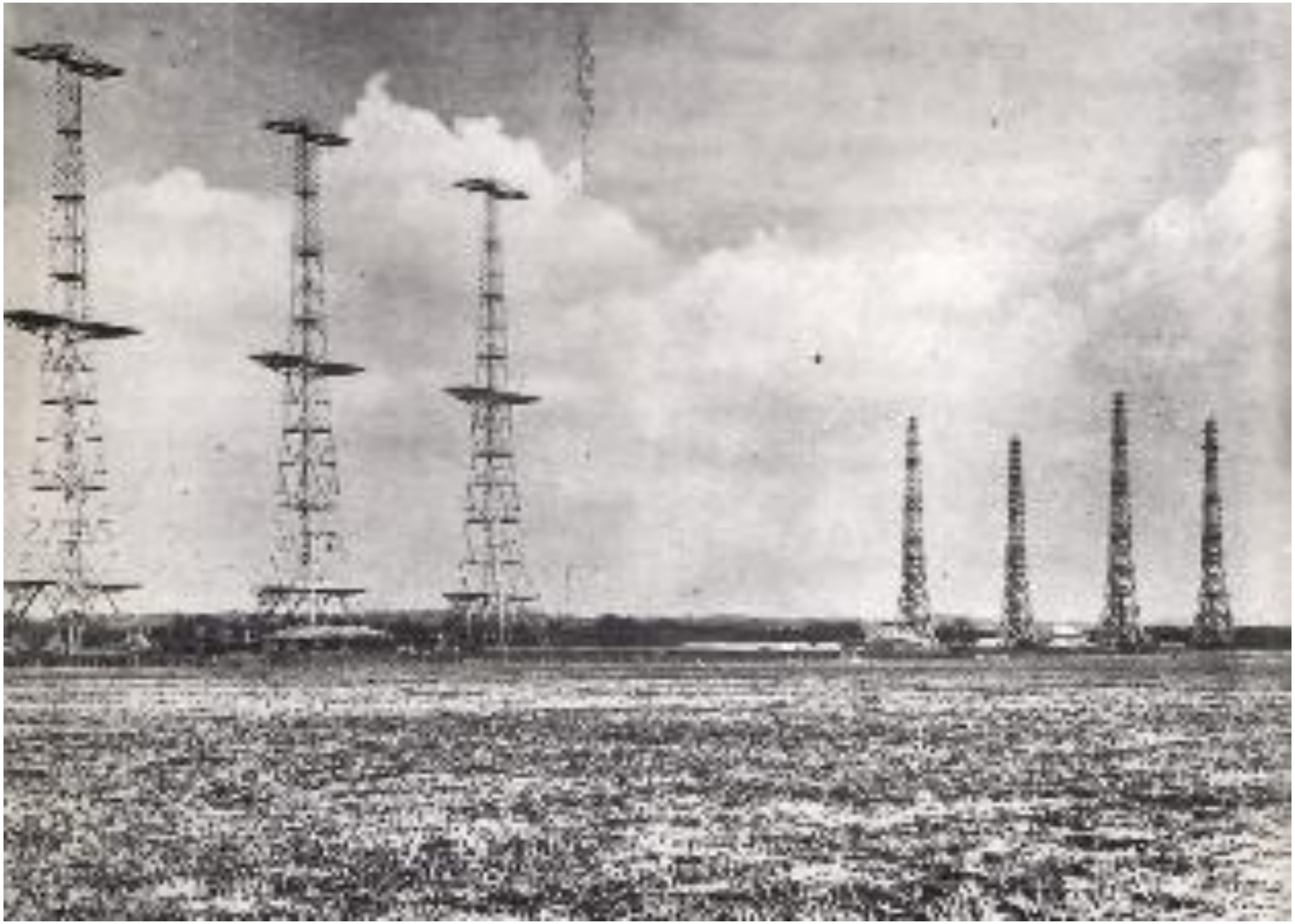

Chain Home radar network 25 MHz

Range-time records ~ 1940 plasma irregularities = meteors

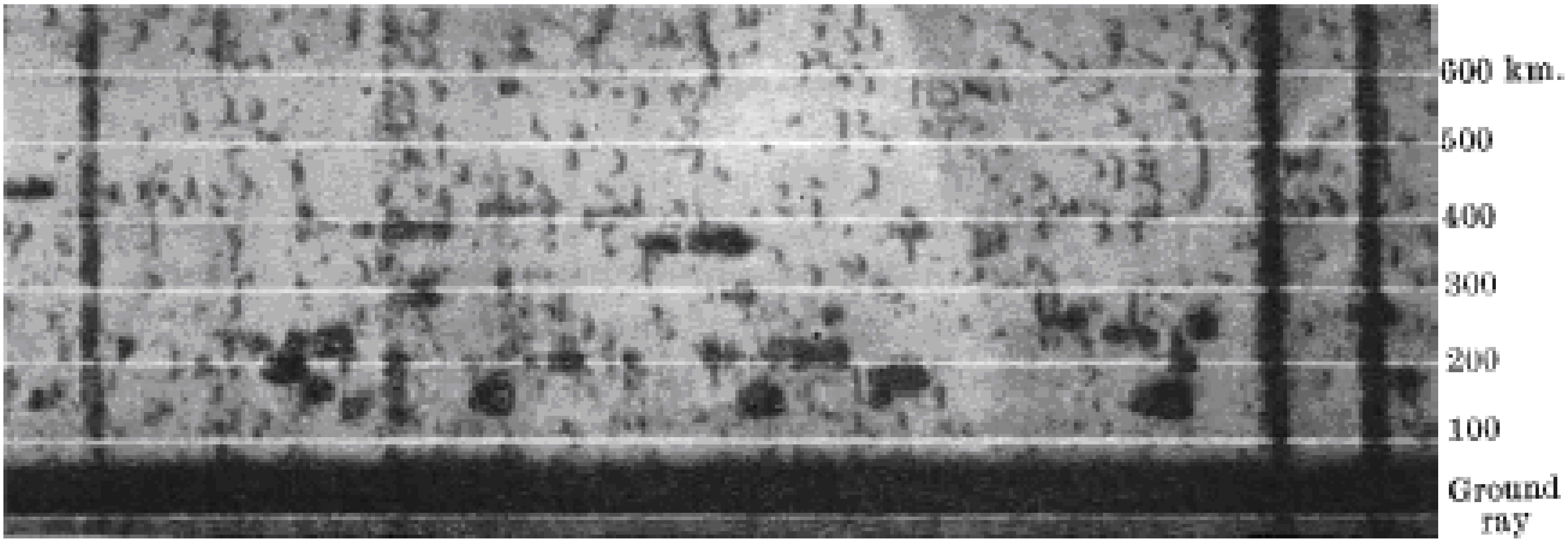

Range-time records ~ 1940 plasma irregularities = meteors

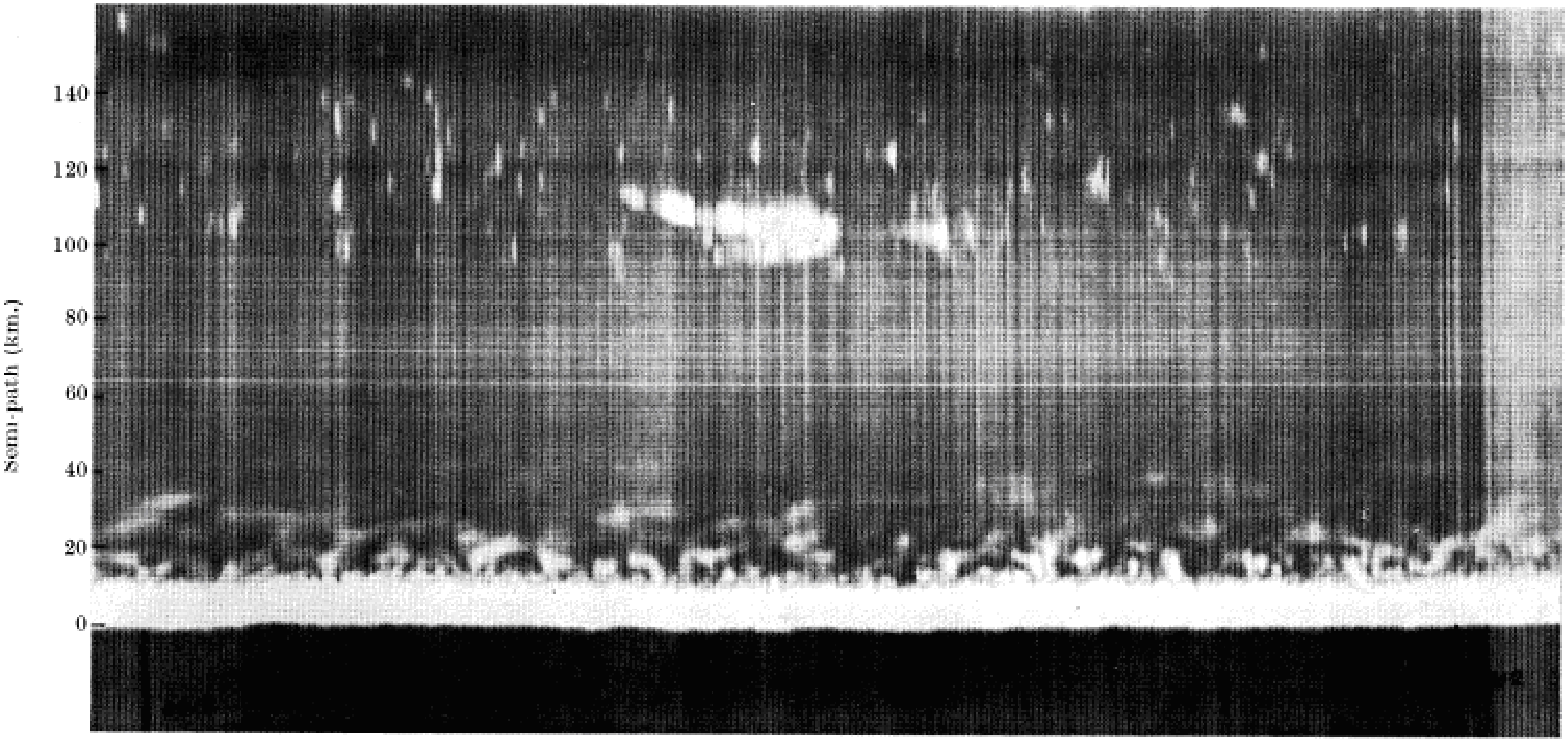

Military Radar units employed for meteor plasma studies

Gun-Laying GL2 ~ 75 MHz Jodrell Bank 1945

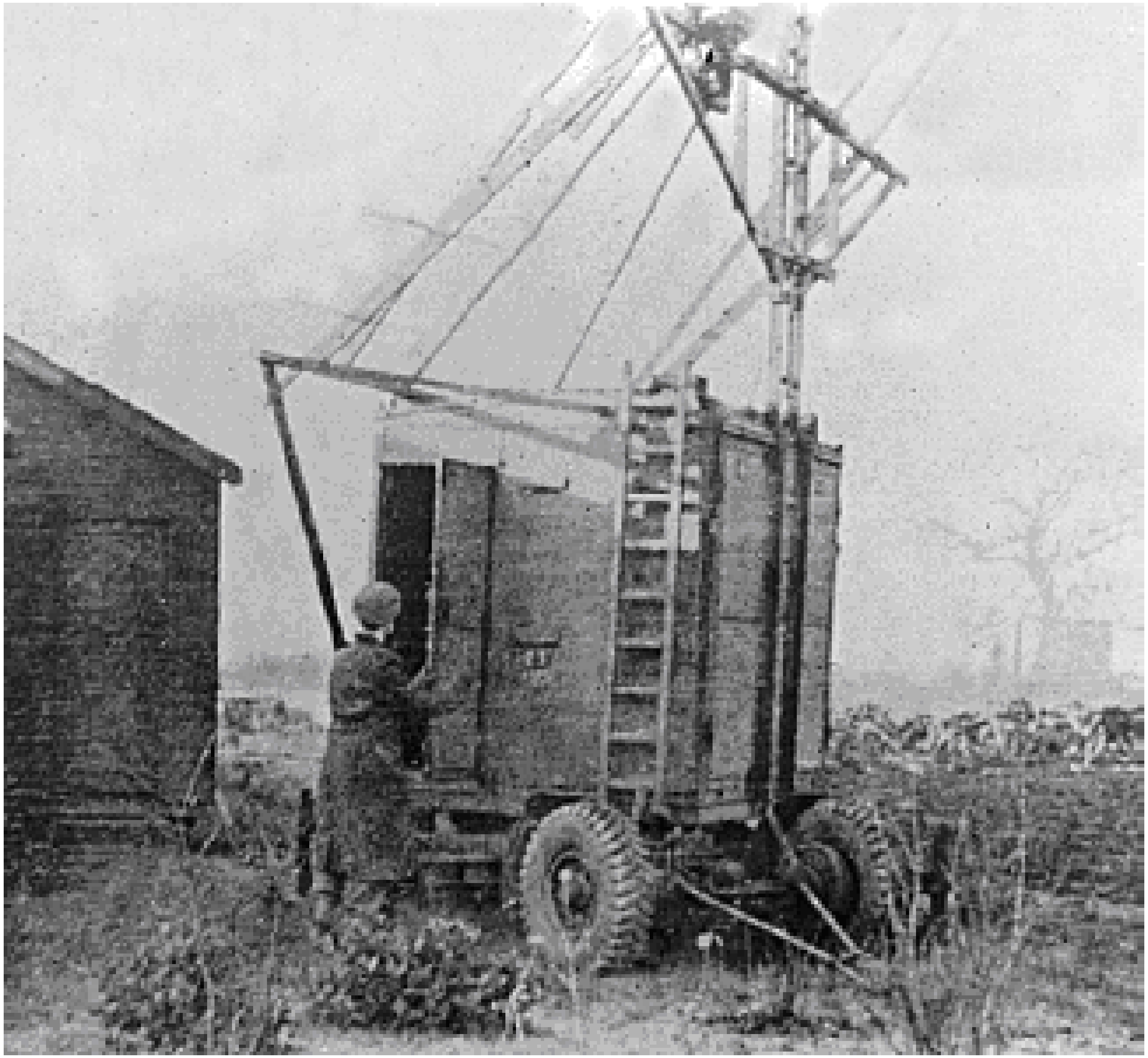

CHL ~ 75 MHz rotating on tower

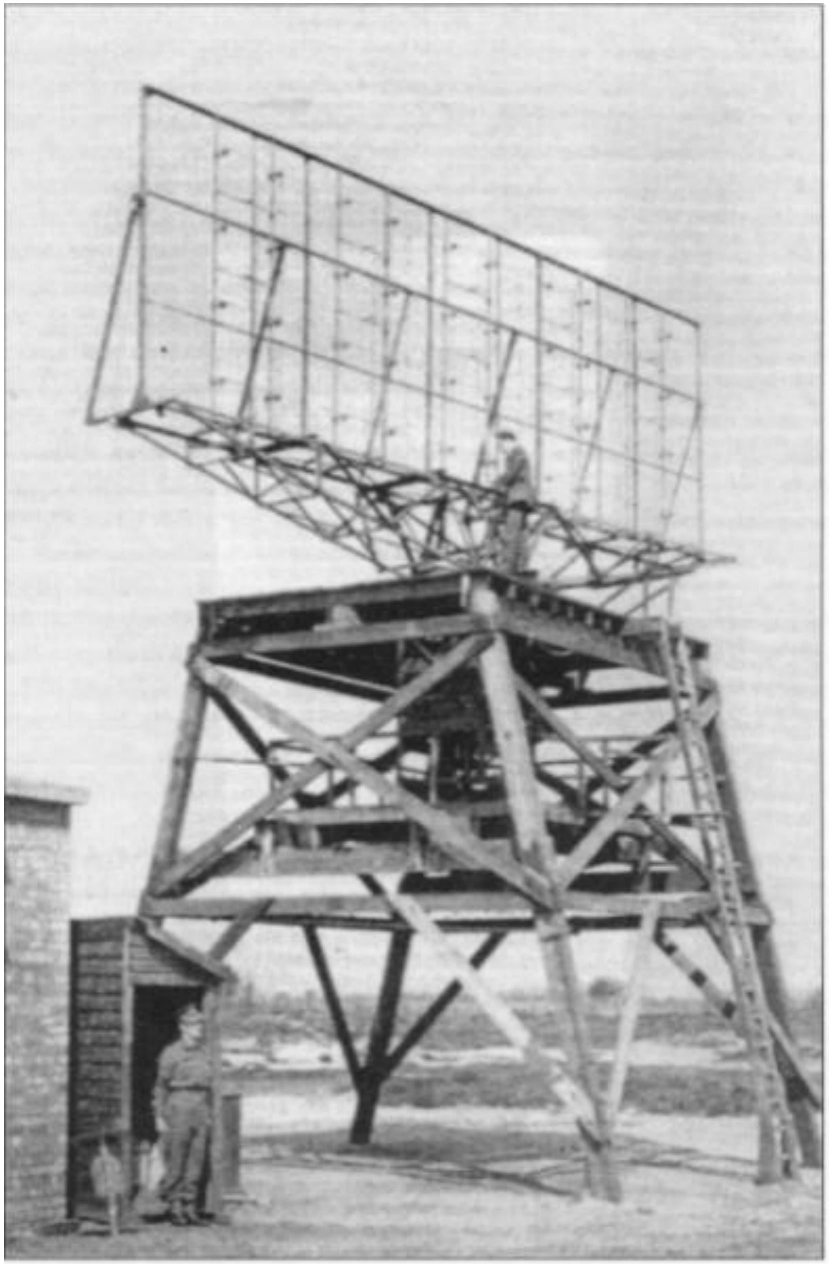

CHL rotating installed on large tower

1942 : John Bamwell with George Bacon & Roland Lees produces Transmit-Receive (T/R) switch

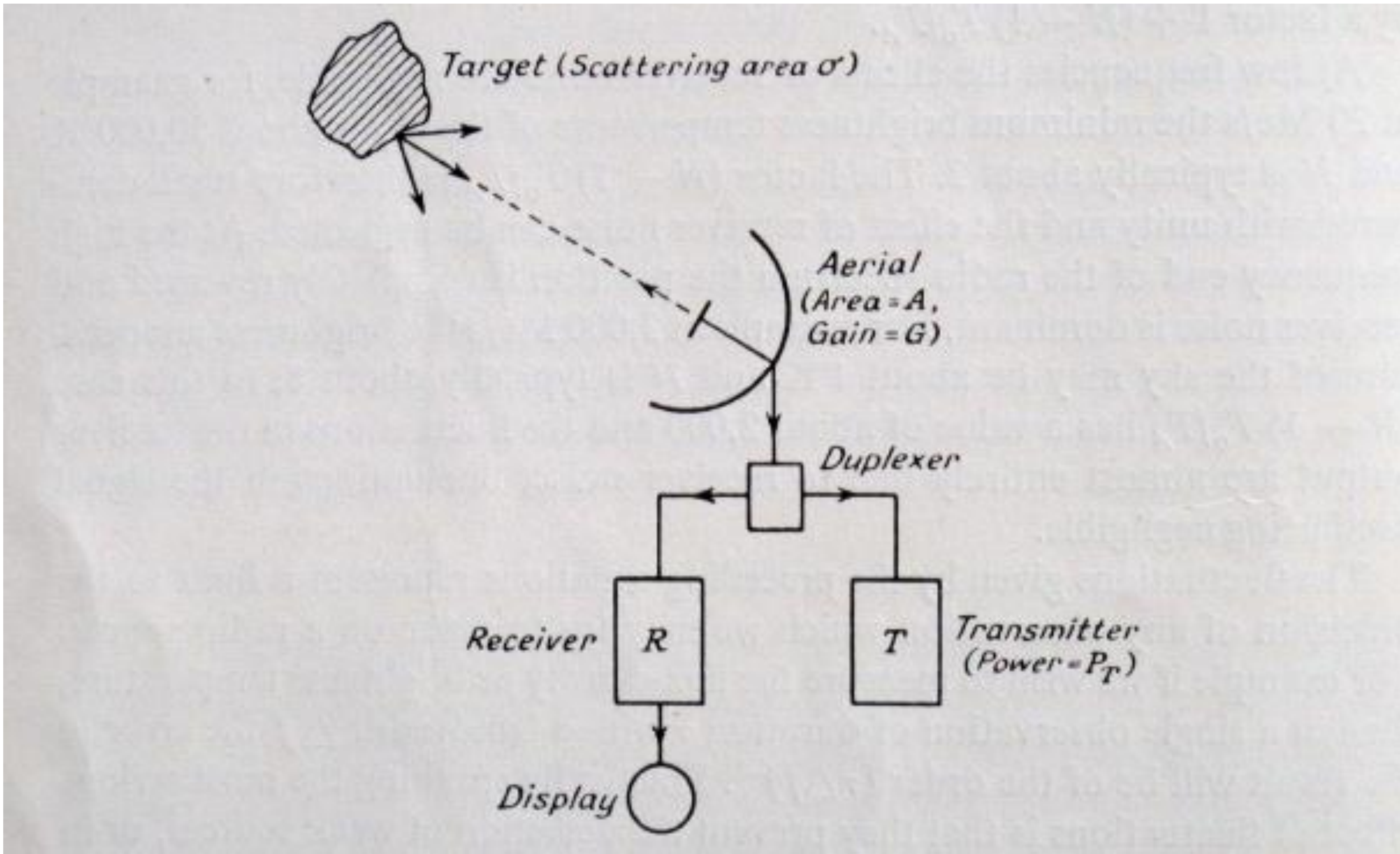

T-R switch

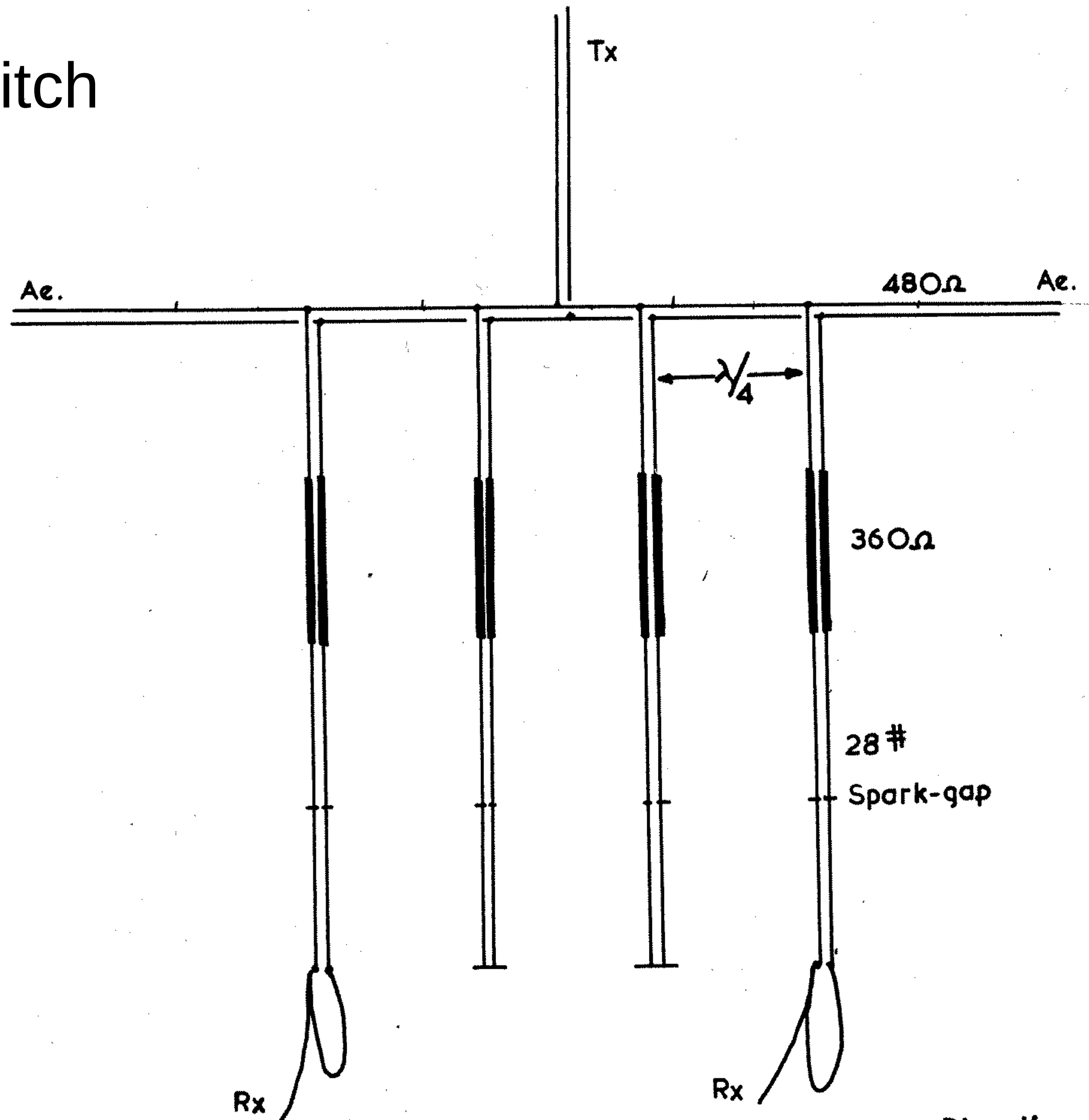

Diag. 11

1946 Giacobinid stream

Earth 1 day before ascending node of stream

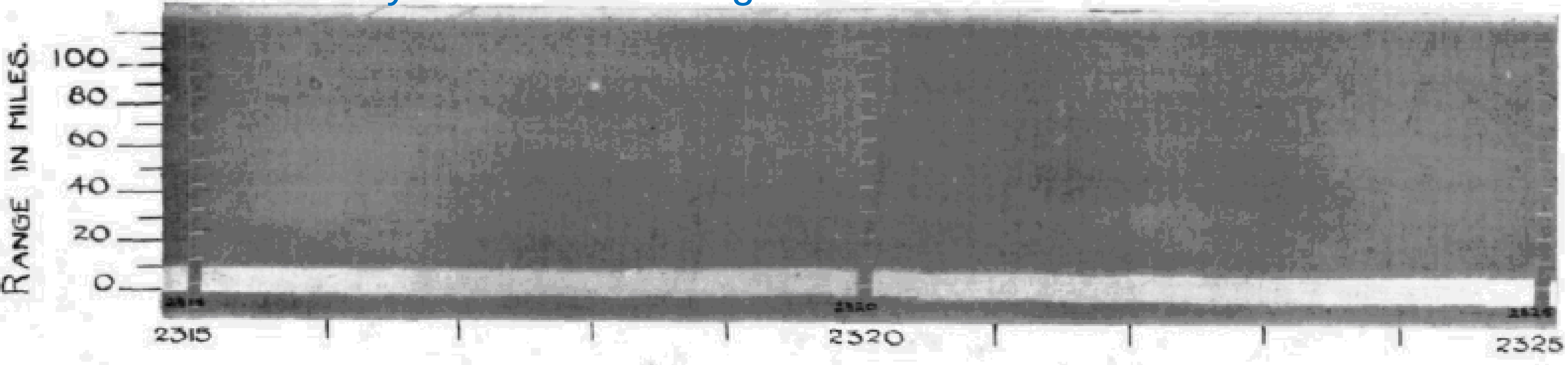

Plate A.

Earth passes through ascending node of stream

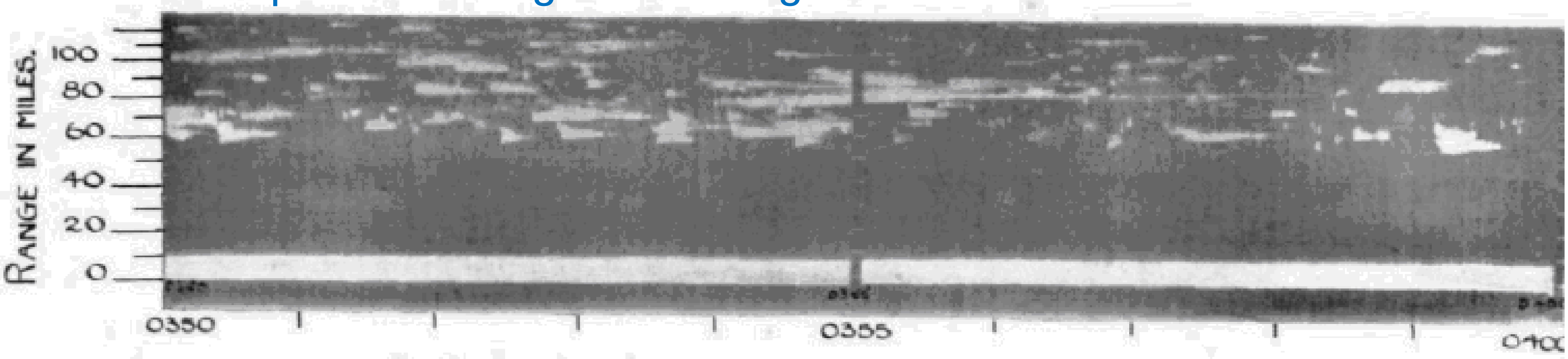

Jodrell Bank Radar Meteor community ~ 1950

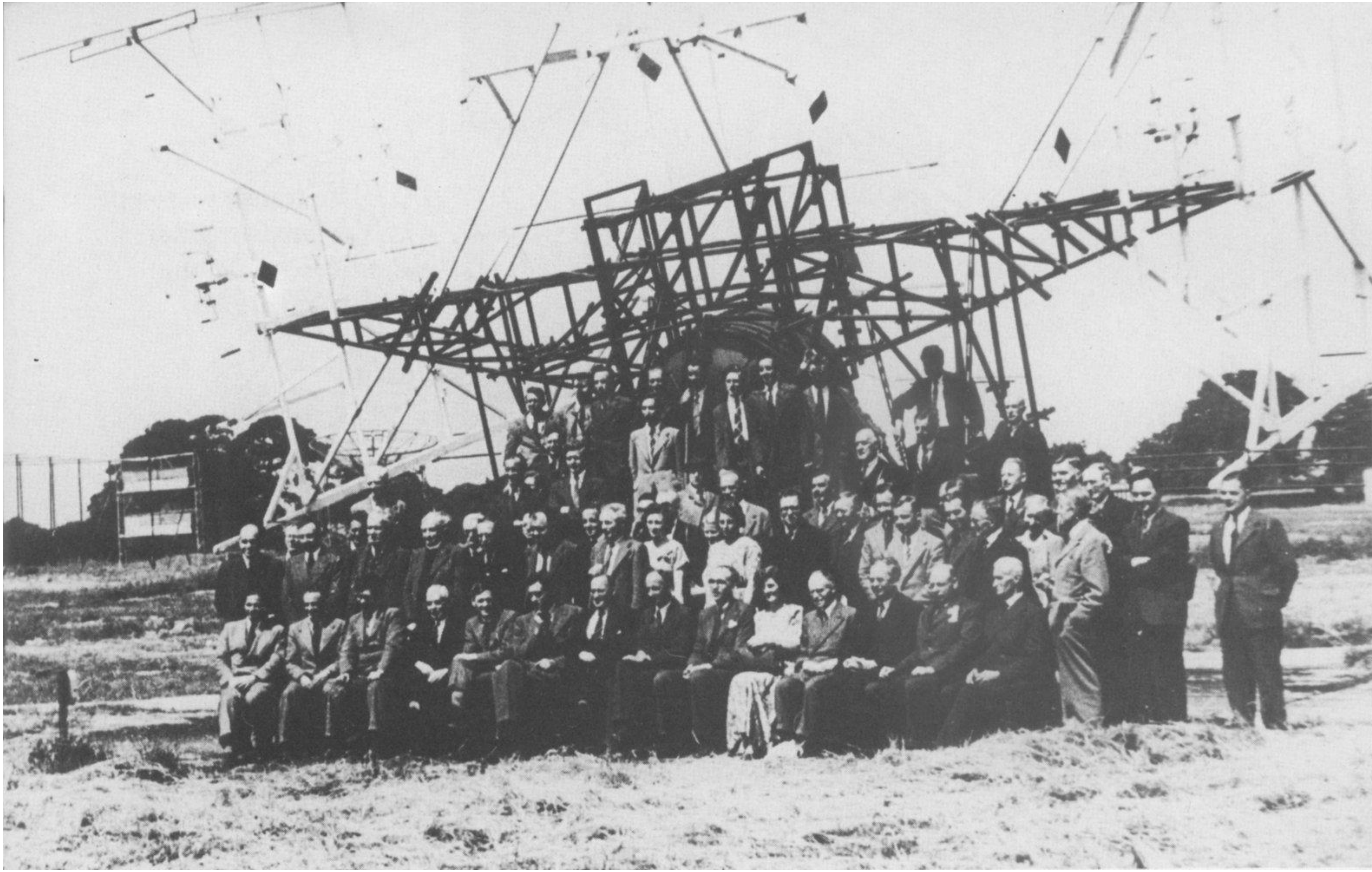

Jodrell Bank Radar Meteor community ~ 1950

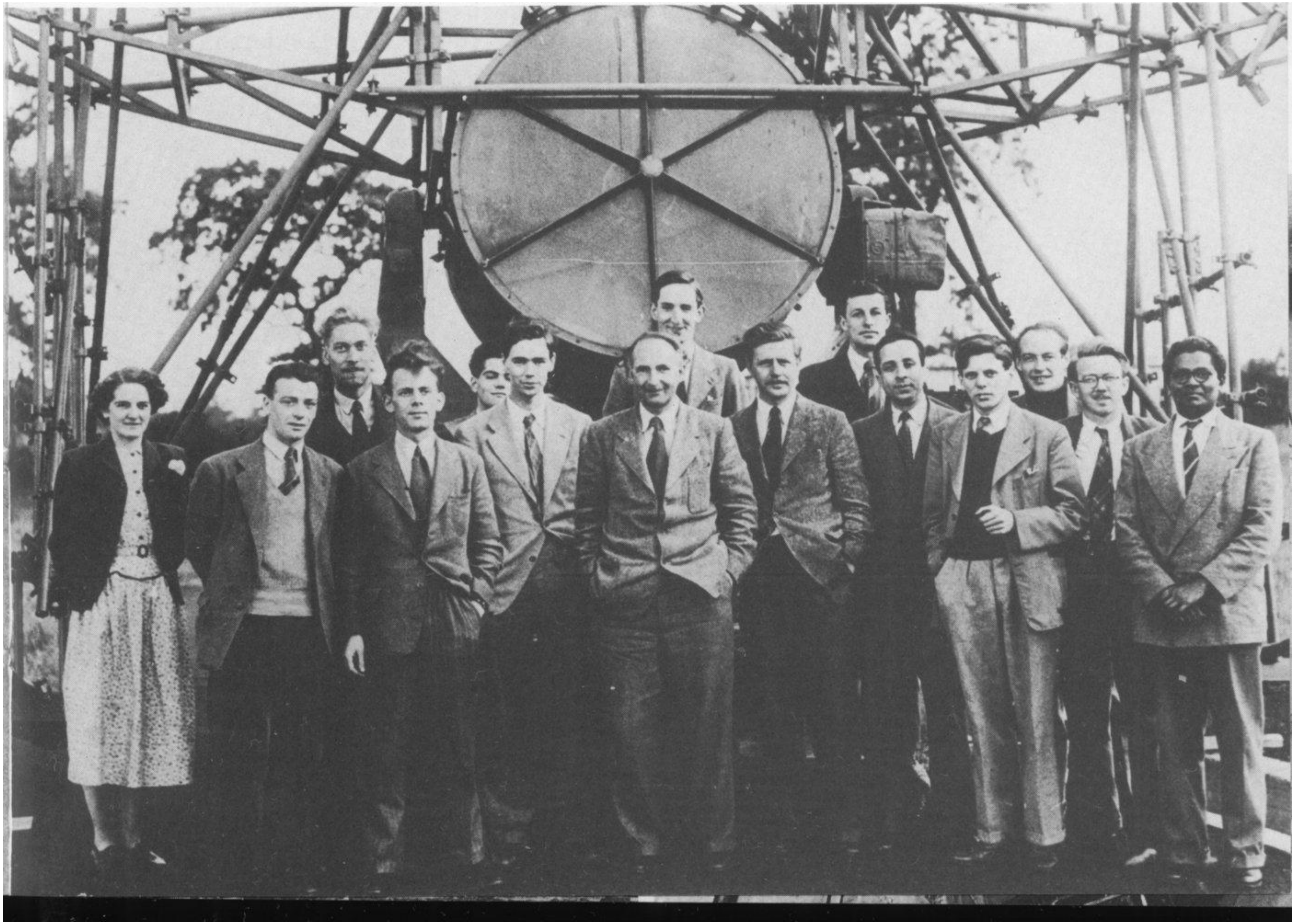

Jodrell Bank crossed Yagi for polarisation ~ 1950

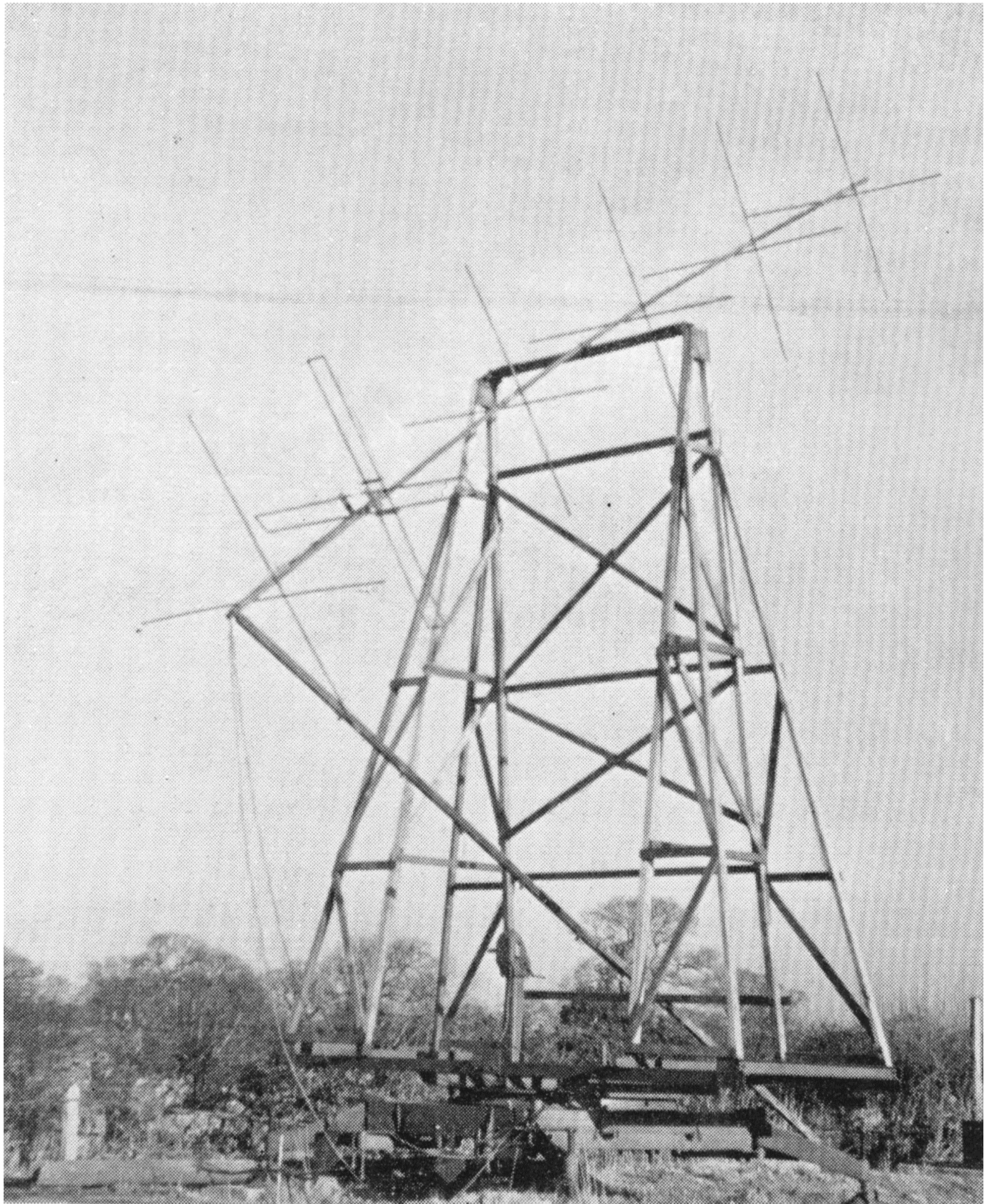

Jodrell Bank rotating twin Yagi ~ 1950

Radiant coordinates of Geminid stream

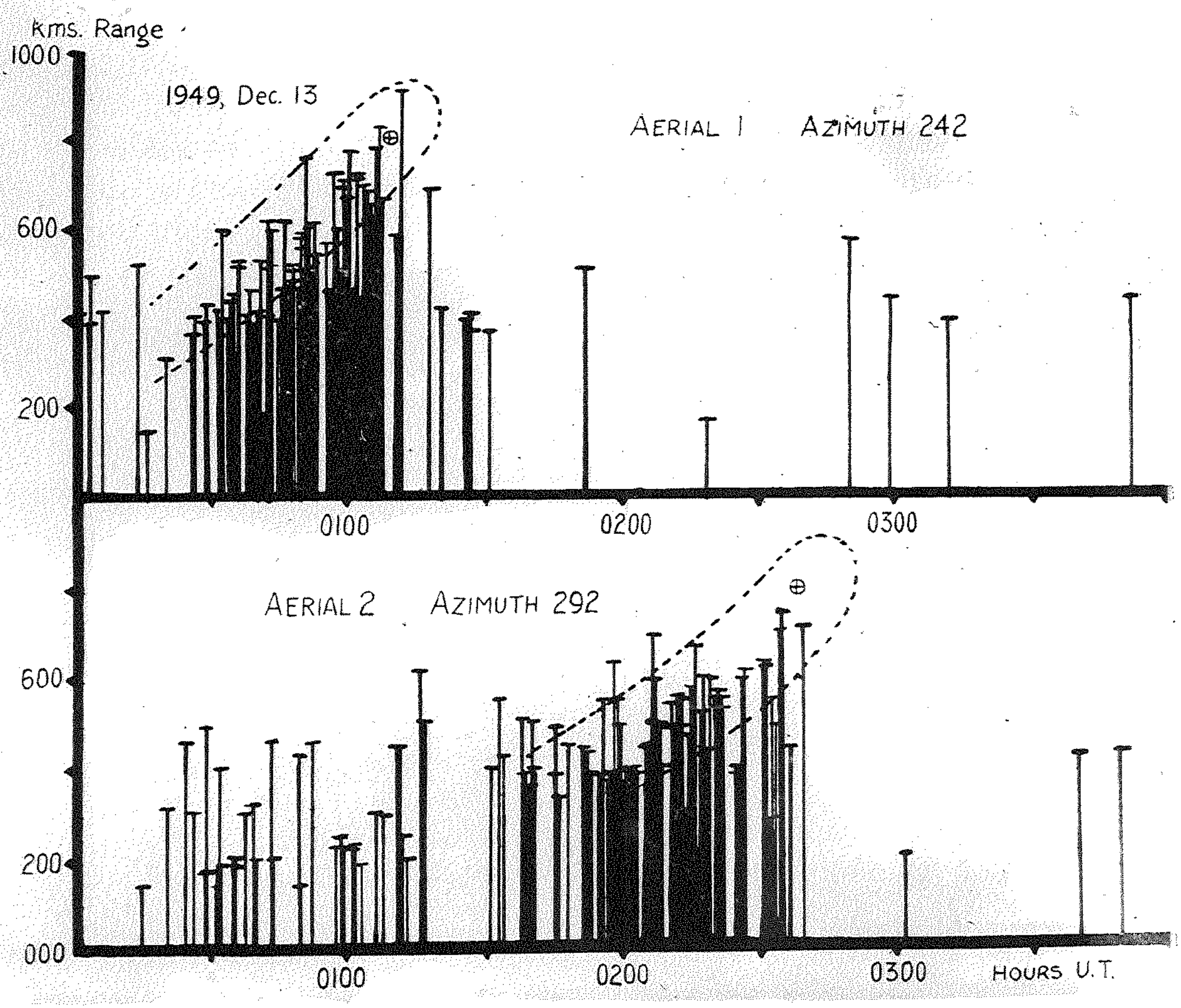

1946: Clif Ellyett won a Government scholarship to study in UK – worked at then Jodrell Bank with Bernard Lovell’s team. He and JG Davies worked out a method of measuring meteoroid speeds:

This fundamental problem…..

‘saw how to employ the diffraction – the radar wavelength being much shorter than the plasma target.

Founding paper……….

Nature **161**, 596-597 (17 April 1948) | doi:10.1038/161596a0;
Velocity of Meteors Measured by Diffraction of Radio Waves from Trails during Formation

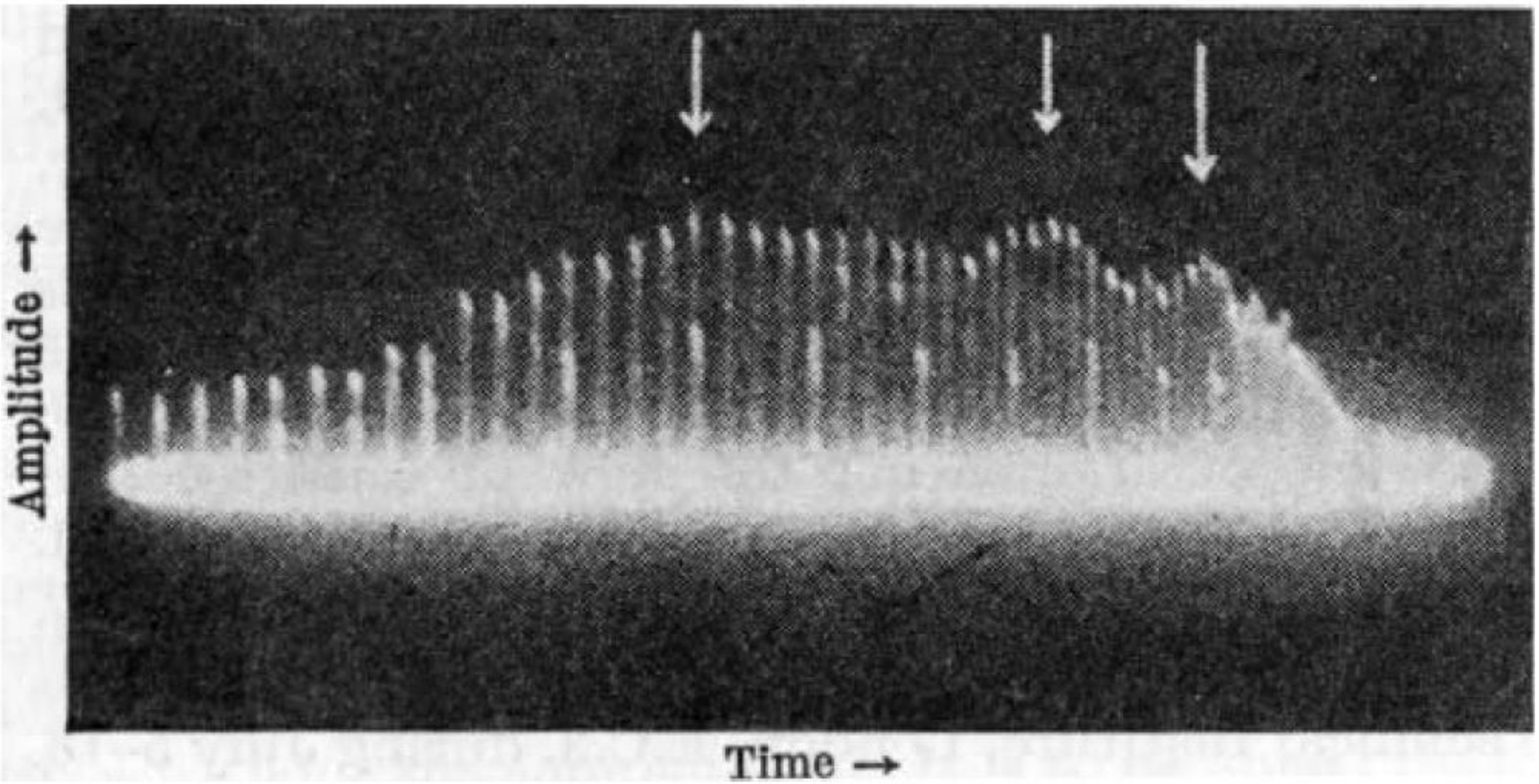

Fig. 1. QUADRANTID METEOR. JANUARY 4, 1948, 05h. 01m. ZONE MAXIMA MARKED BY ARROWS. RANGE 440 KM. MEASURED VELOCITY = 34·7 ± 2·2 KM./SEC. INTERVAL BETWEEN PULSES = 1·6 MILLISEC. EXPONENTIAL TIME BASE

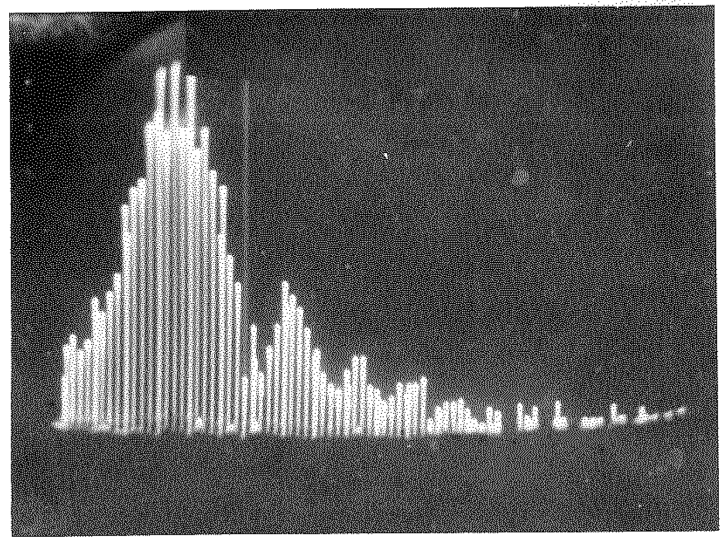

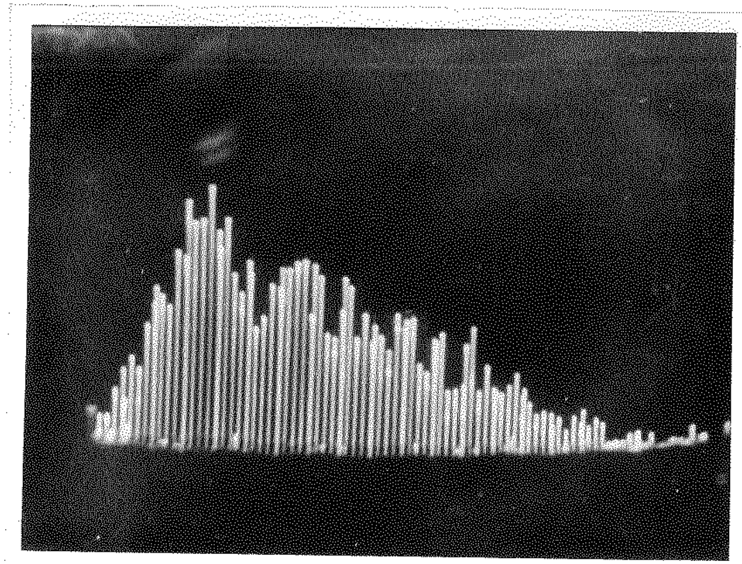

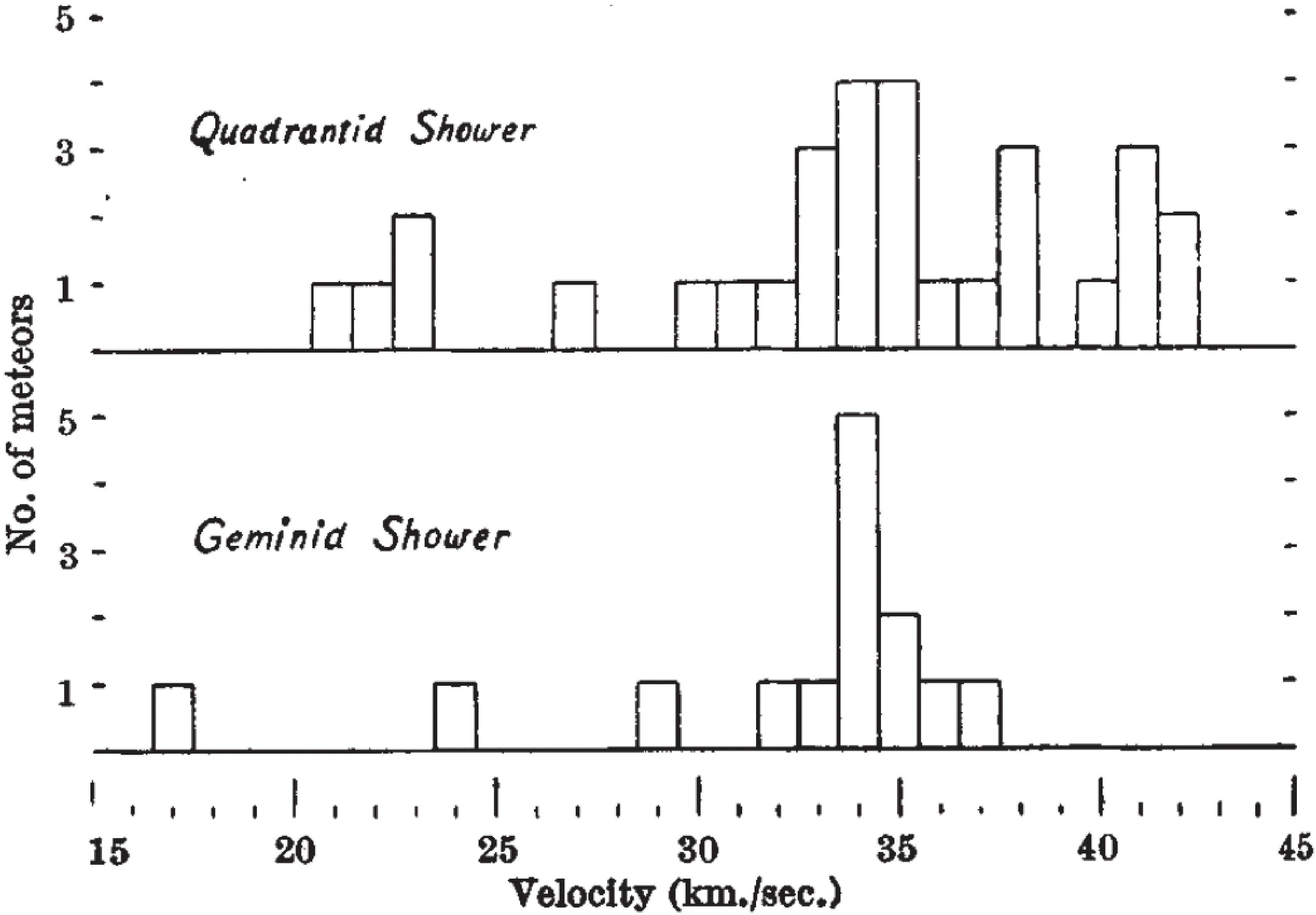
Quadrantid Shower
Geminid Shower
No. of meteors
5
3
1
5
3
1
15
20
25
30
35
40
45
Velocity (km./sec.)

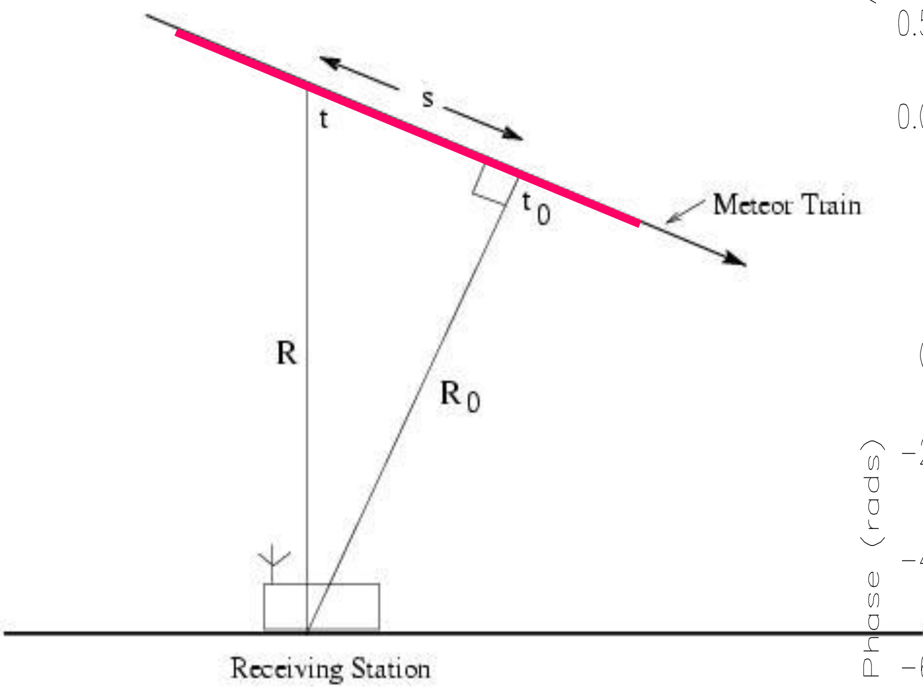

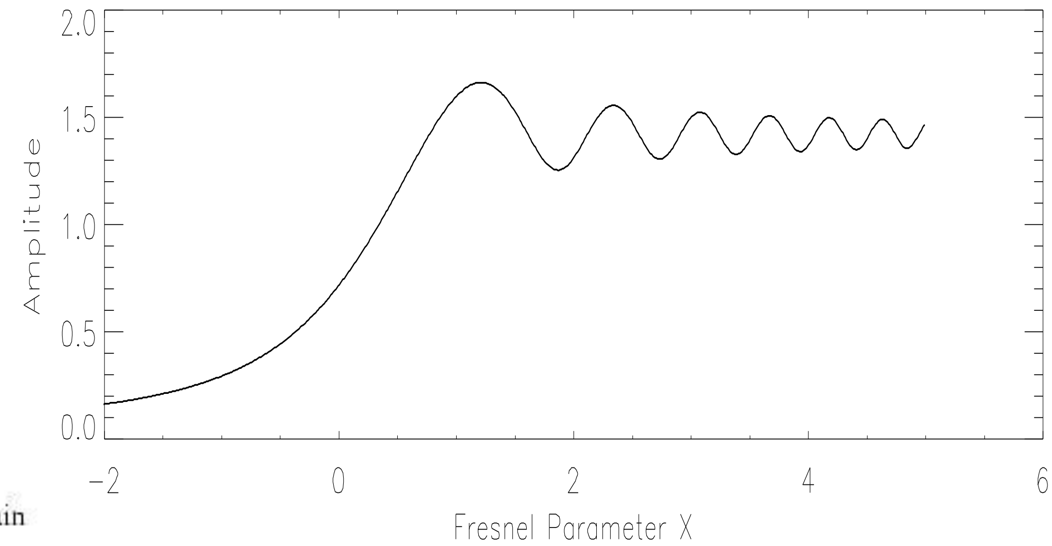

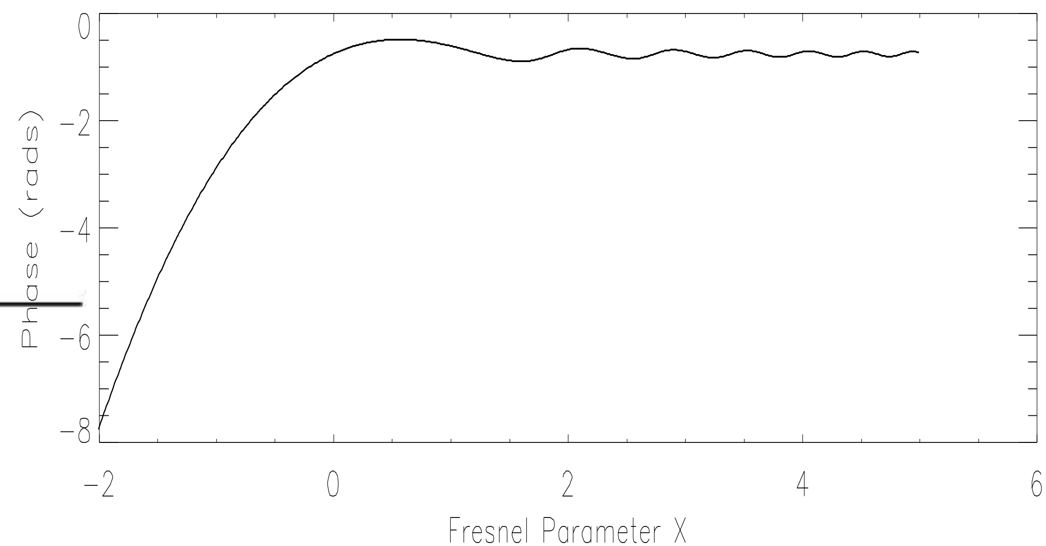

X = in units of Fresnel Zones = $(R_0 \lambda / 2)^{0.5}$

Cornu spiral in the complex plane

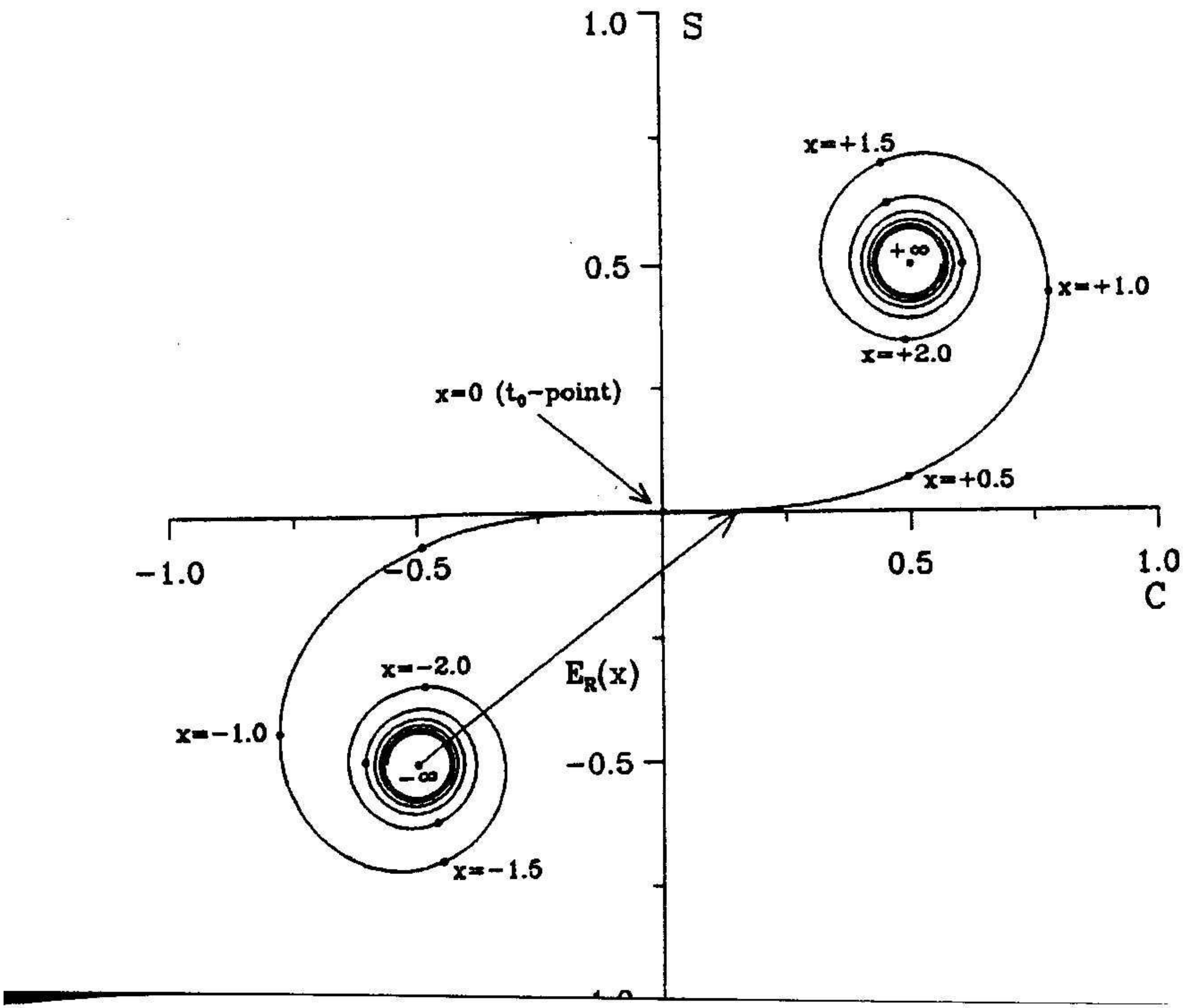

Canterbury diffraction behaviour Bob Bennett ~ 1955

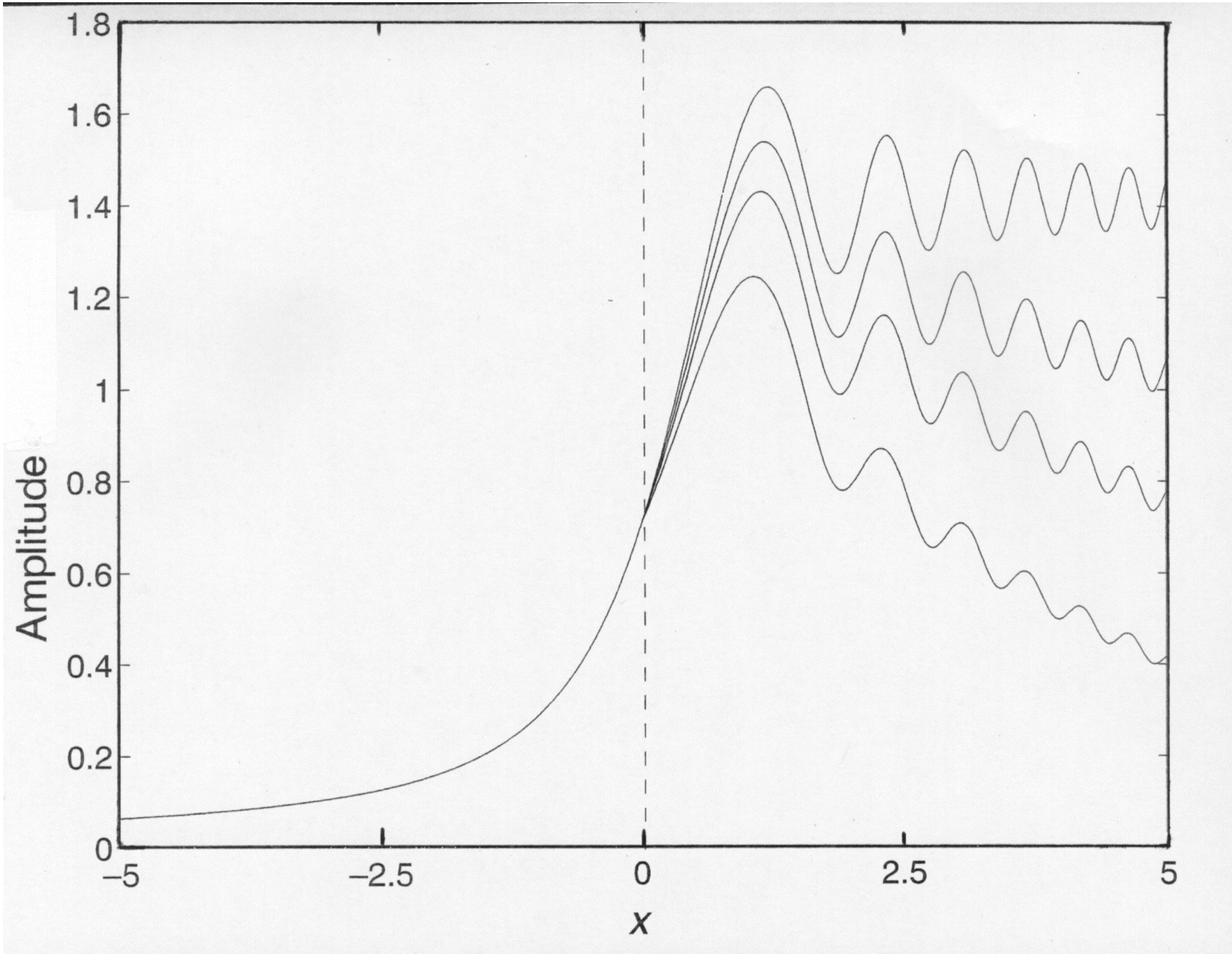

Canterbury diffraction behaviour Bob Bennett ~ 1955

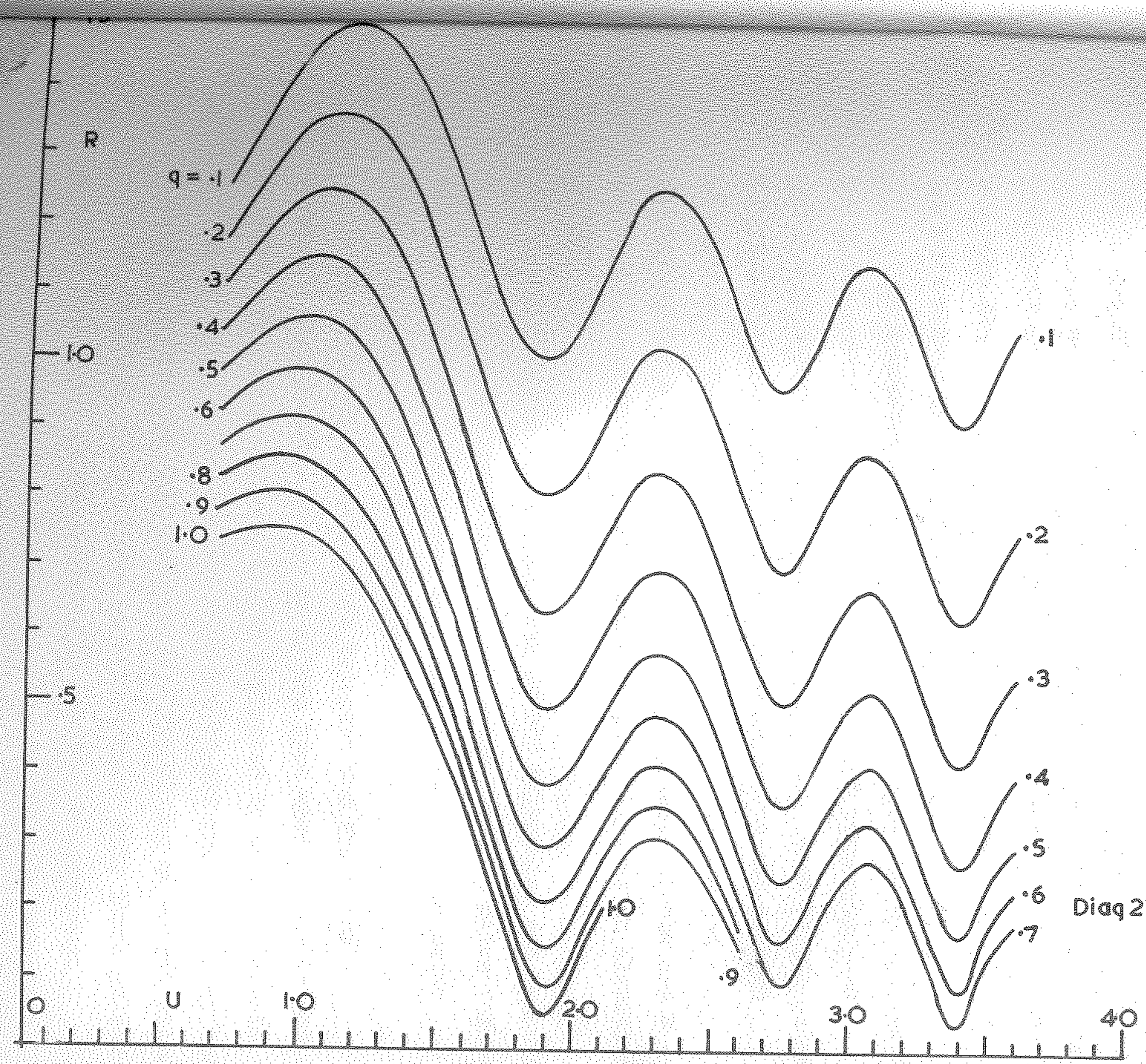

1950: in NZ Ellyett set up radar facility at Rolleston Christchuch. Used CHL TX and rotating antenna.

1954: Prof Chalklin killed Singapore aircrash. : Prof Francis Tarrant appointed – Funding for setting up meteor radar difficult.

1957: McLellan appointed HOD physics. Emphasis on theoretical work left limited support for astronomy.

1958: Clif went to US sort funding from NASA and US Airforce. By 1959 acquired funding US Airforce Cambridge research centre for radar meteor south hemisphere survey.

Rolleston Radar Station (SW of Christchurch) ~ 1960

69 MHz array Rolleston ~ 1960
narrow azimuthal pattern

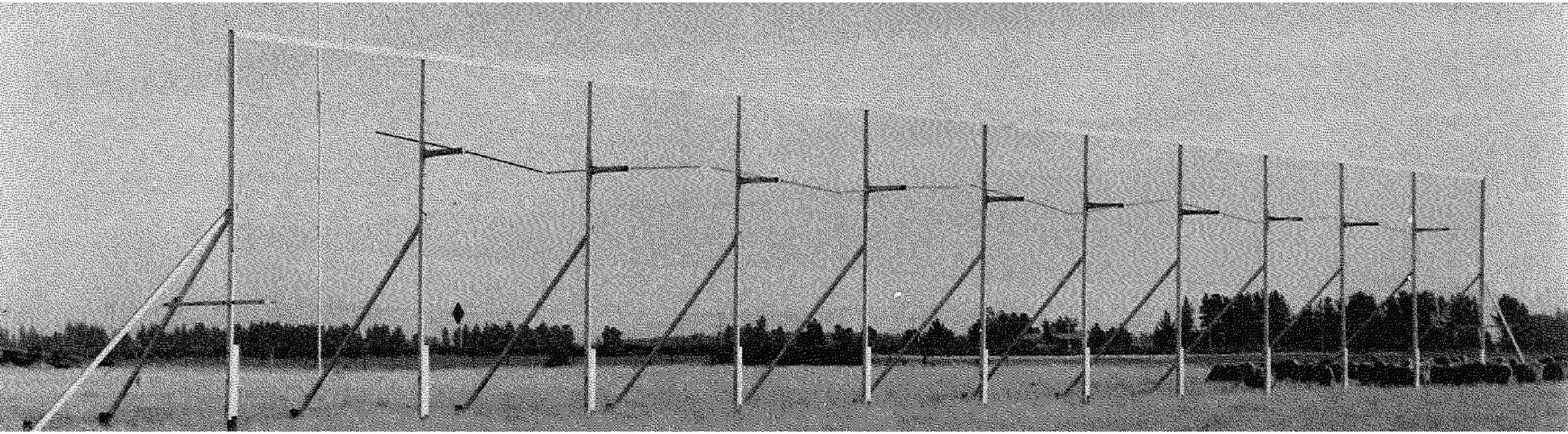

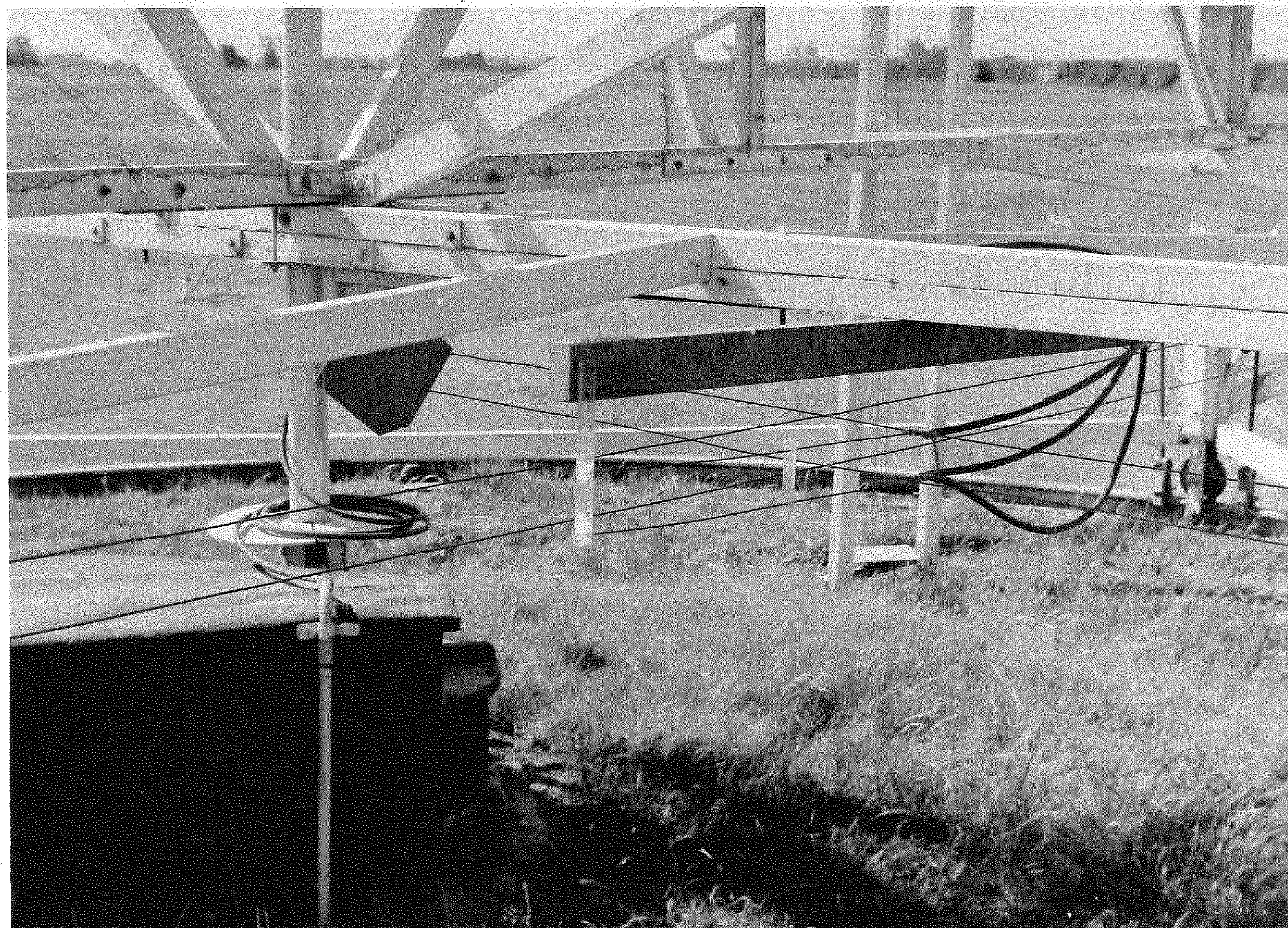

69 MHz radar Rolleston ~ 1960 horizontal stack of 8 Yagis
Meteor stream radiant coordinates.

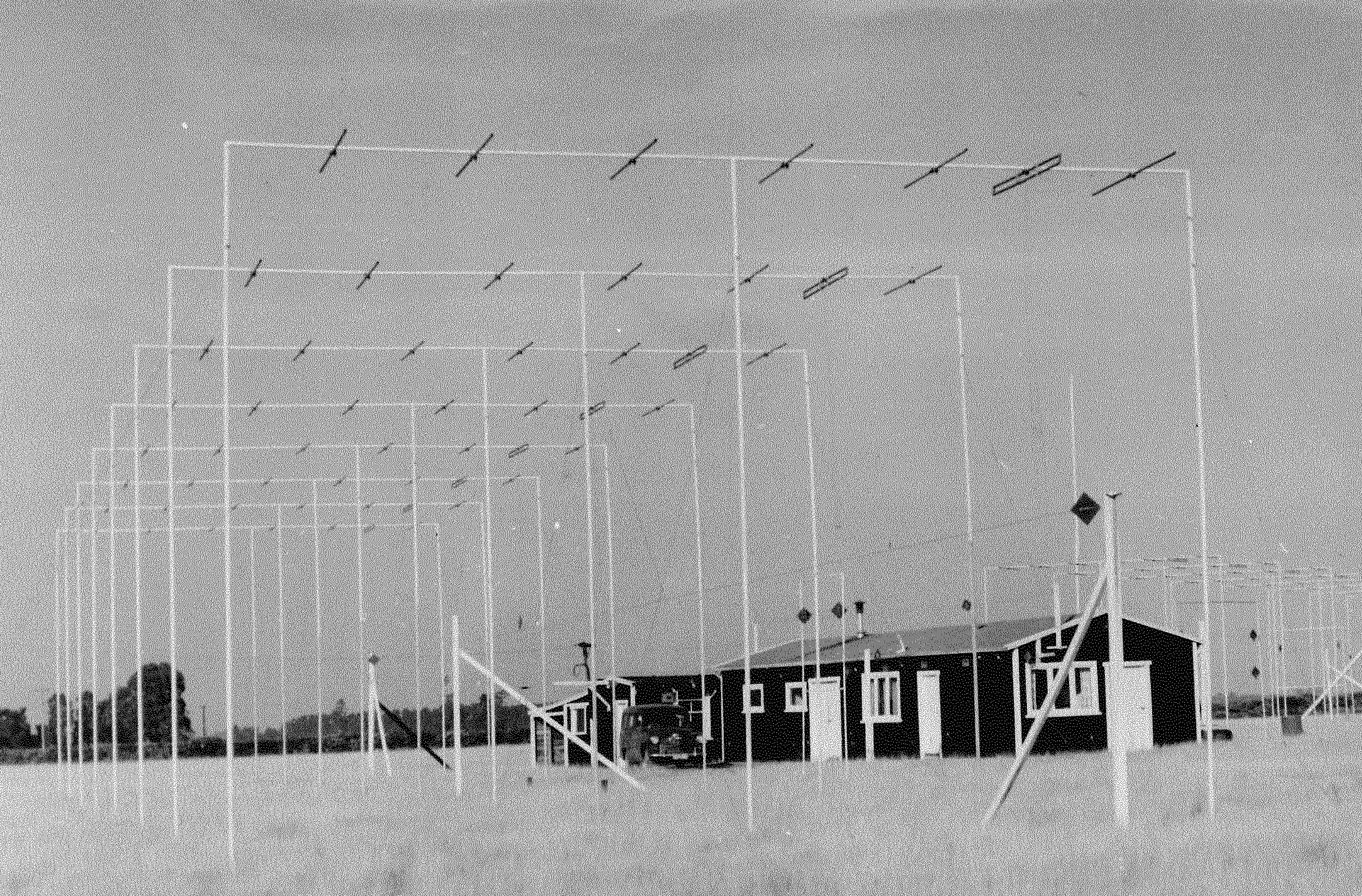

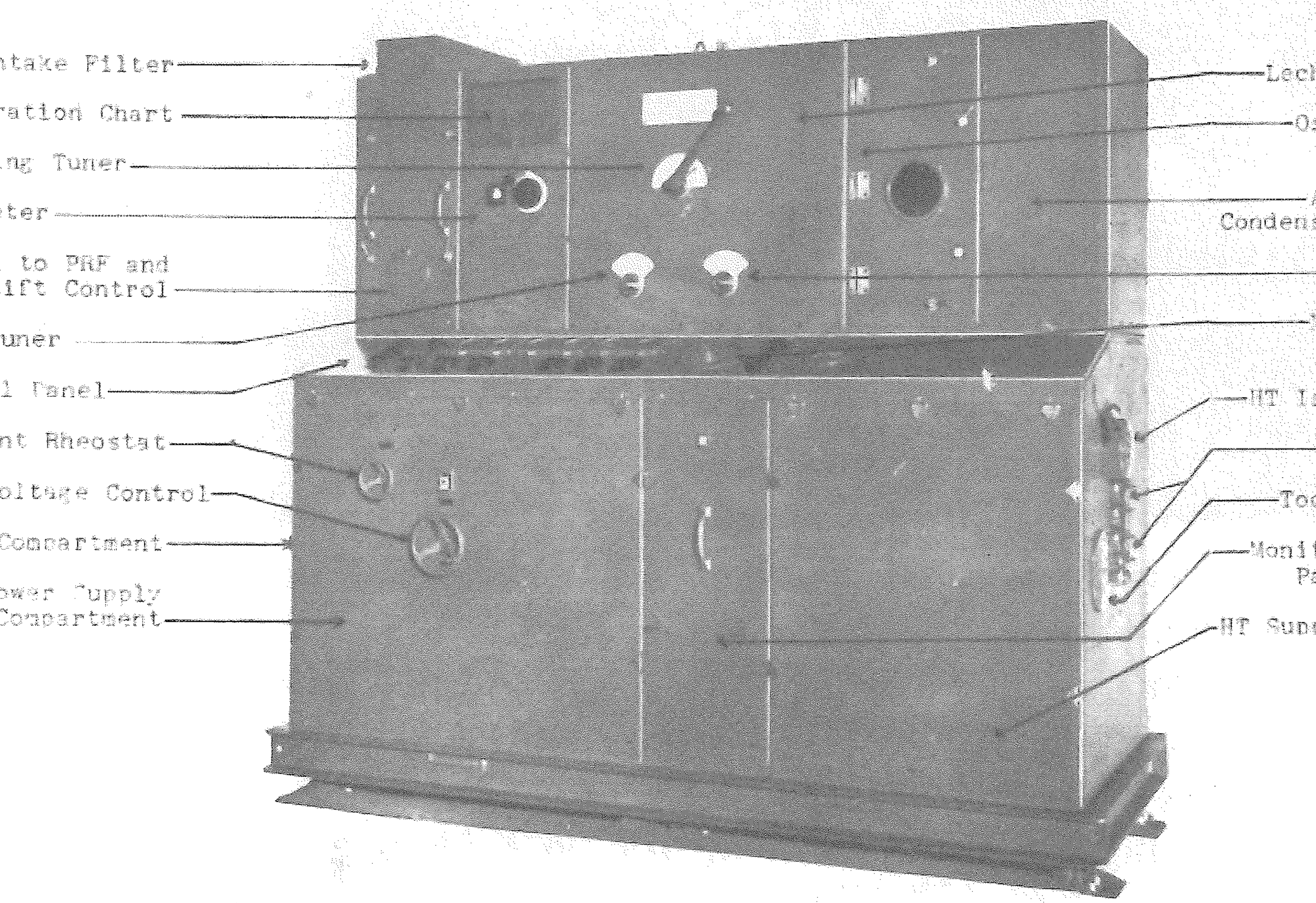

m transmitter as used for CHL and GCI stations.

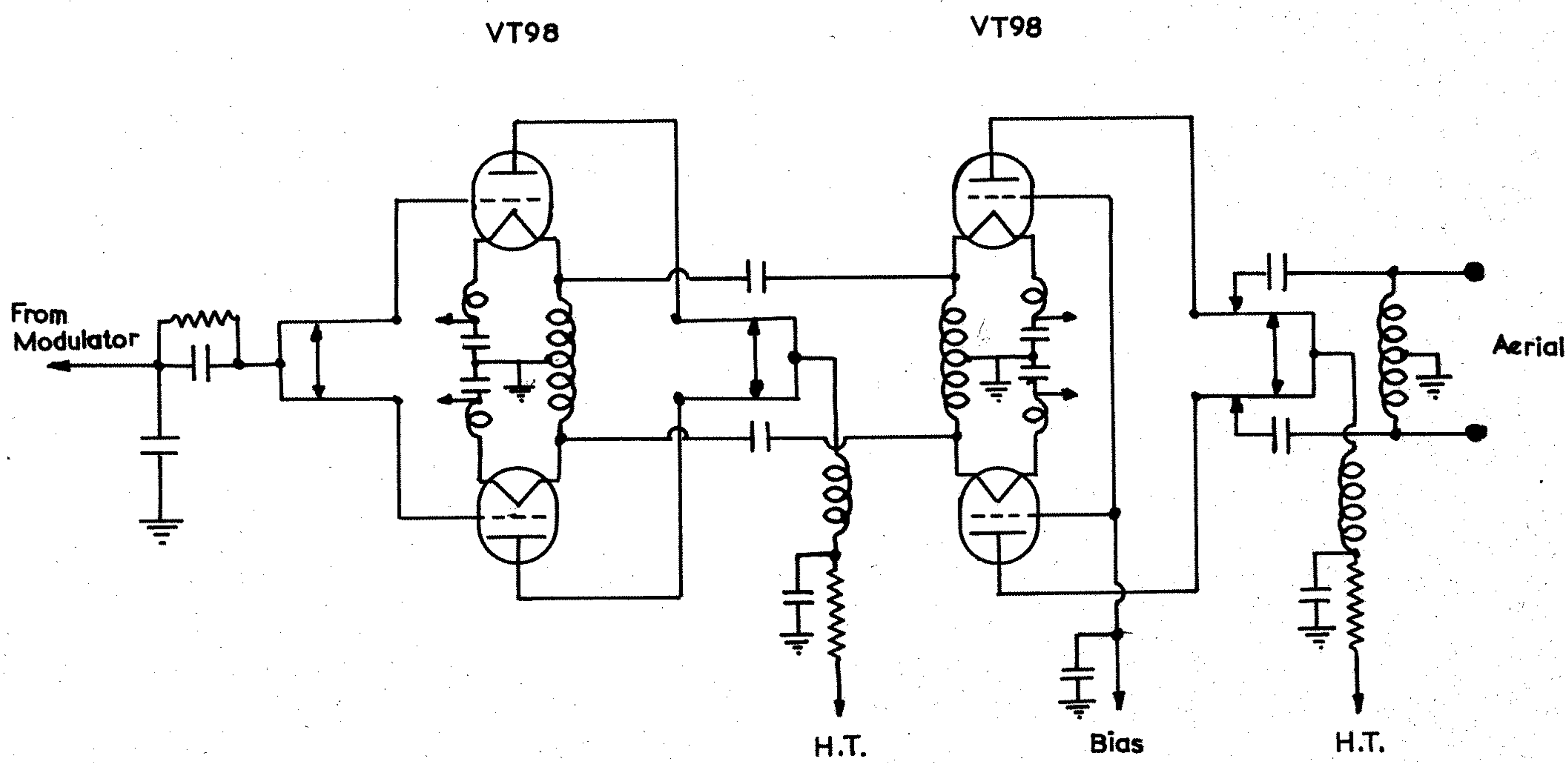

Diag. 7.

Transmitter valve
VT 98

Omni-directional antenna Rolleston. Later made with ground-plane
influx rate gives particle density in space

FIG. 15

Omni-directional RX antenna Rolleston….

separate similar transmitter

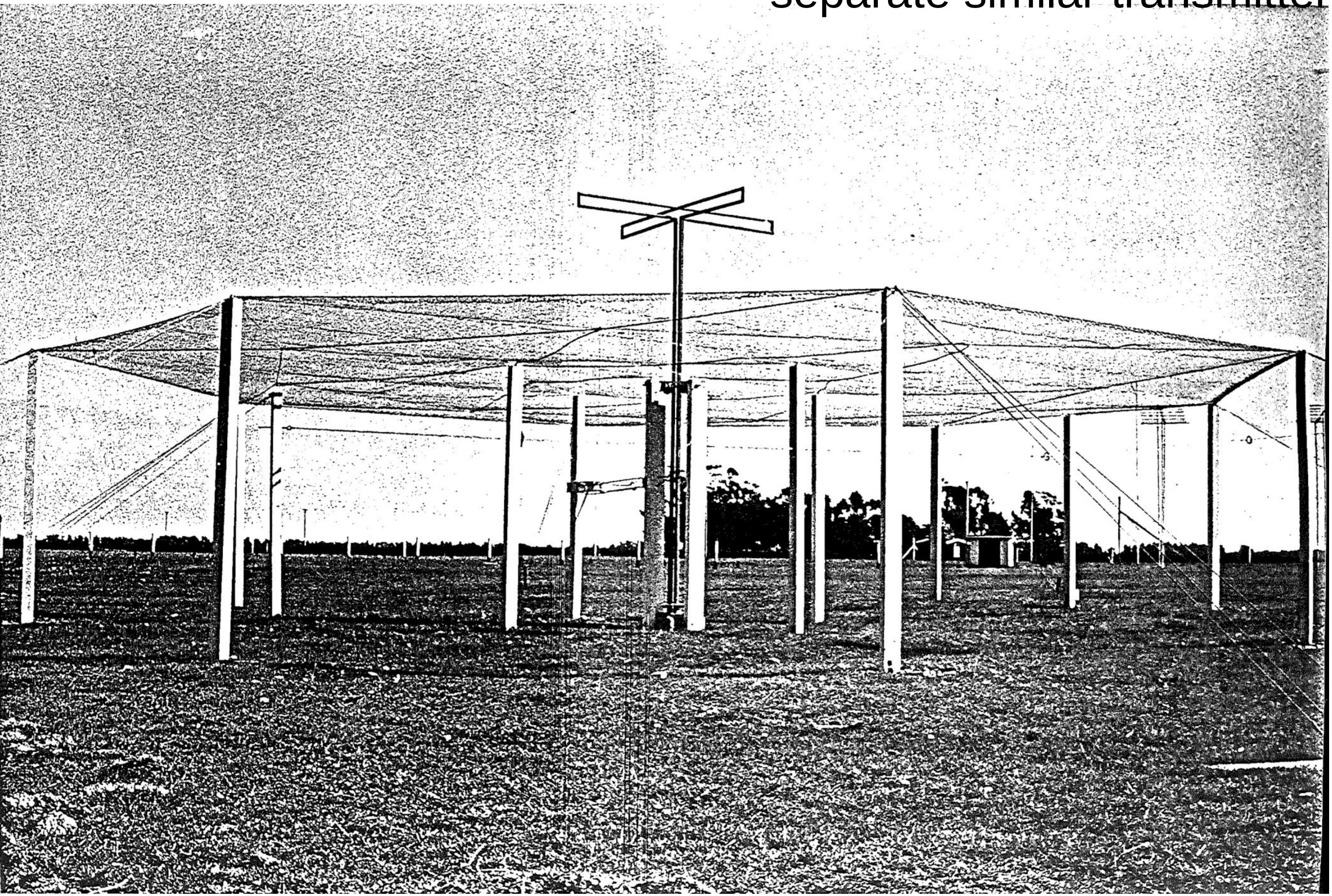

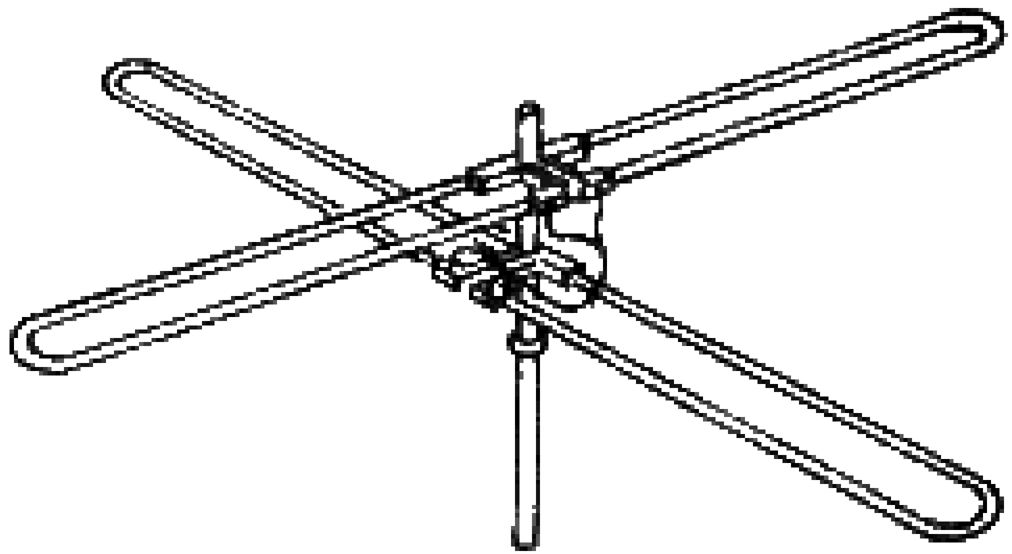

Fully rotatable previous CHL: converted to measurement of meteor radiant coordinates

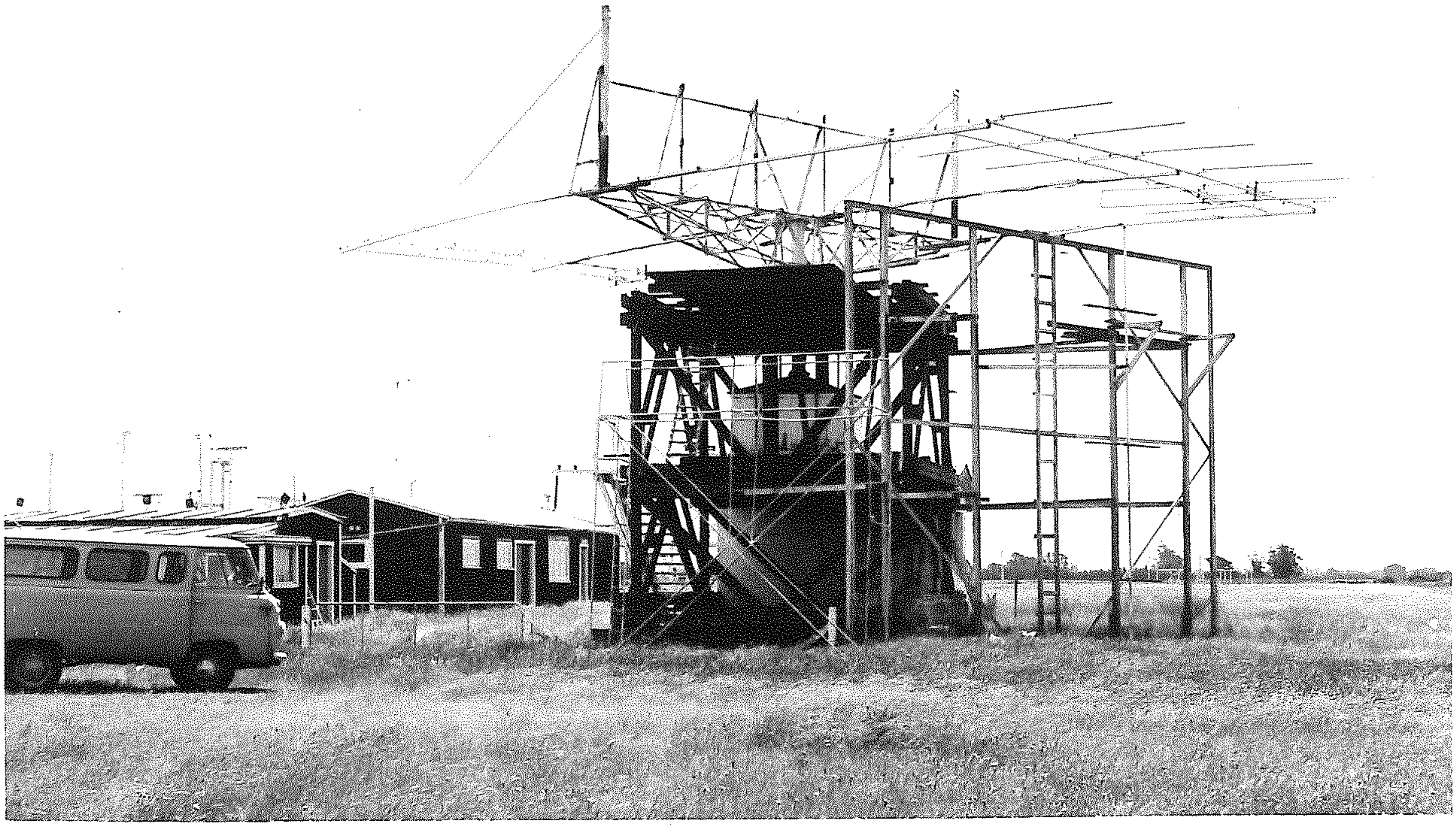

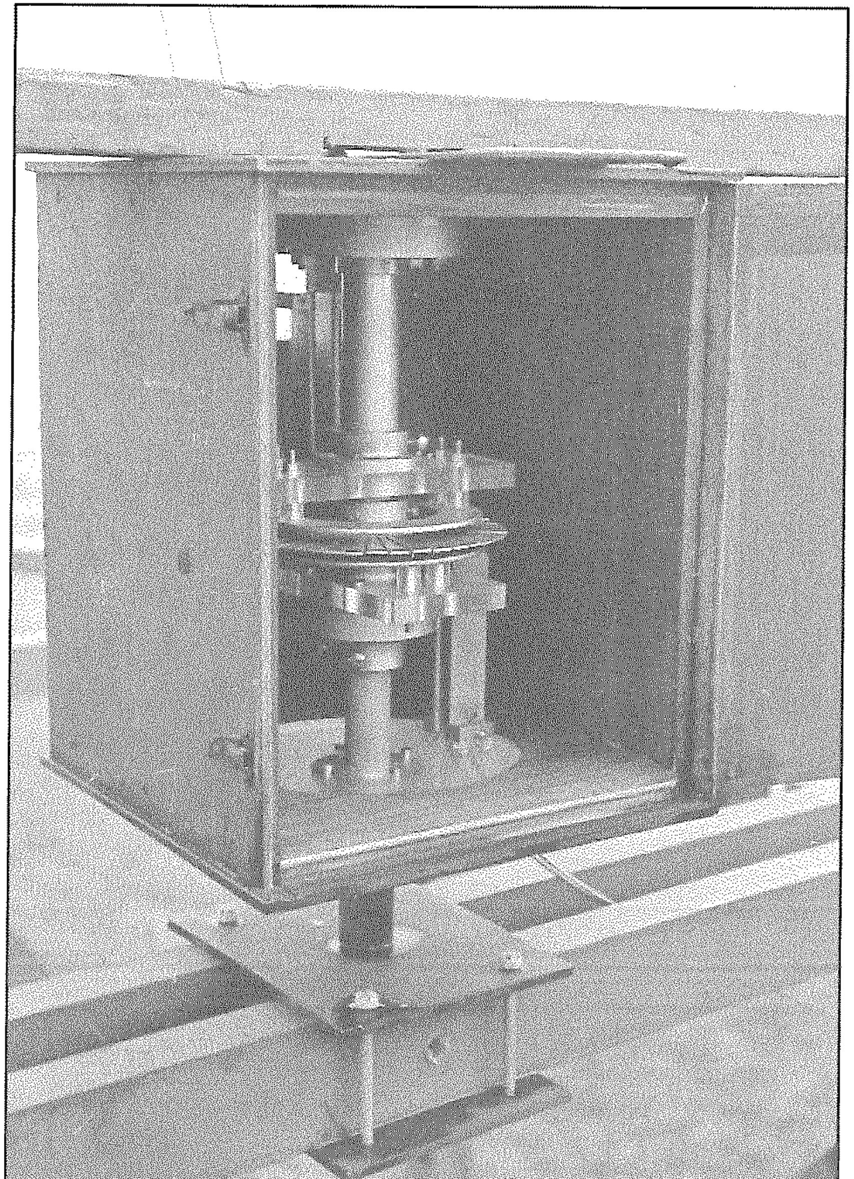

A rotating joint for coupling transmitter power to a rotating aerial array on 1.5 m radars including CHL and GCI. The slotted disc in the centre is the Faraday screen to ensure reasonably constant coupling, irrespective of angle of rotation.

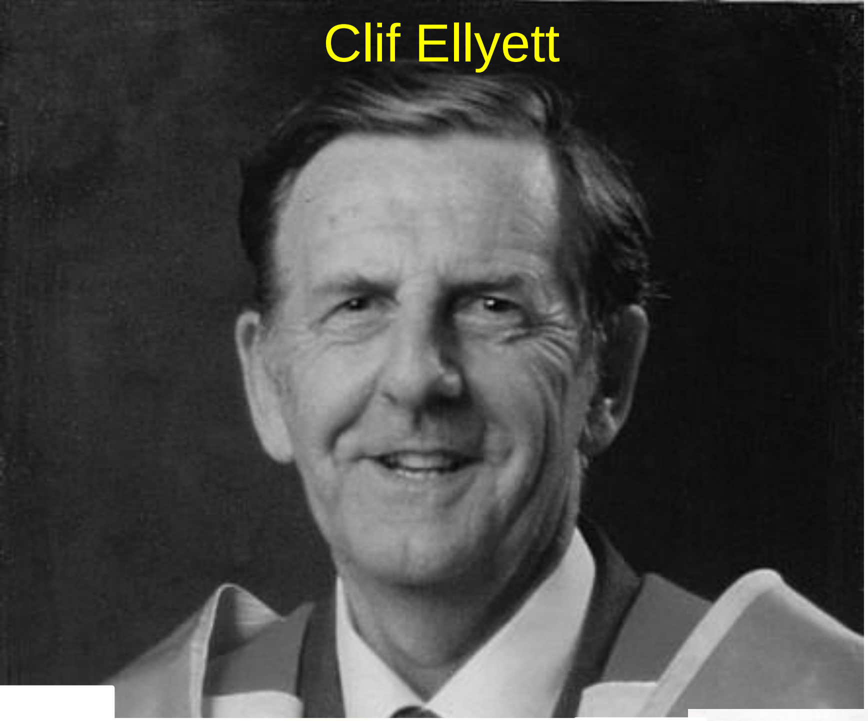

Clif Ellyett

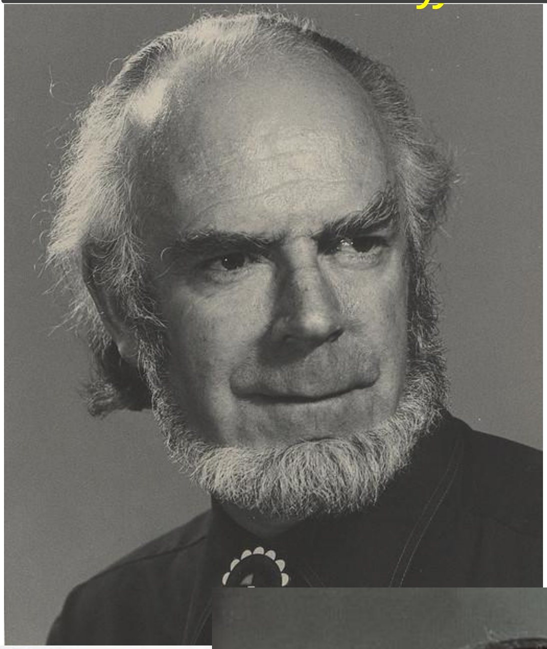

Colin Keay

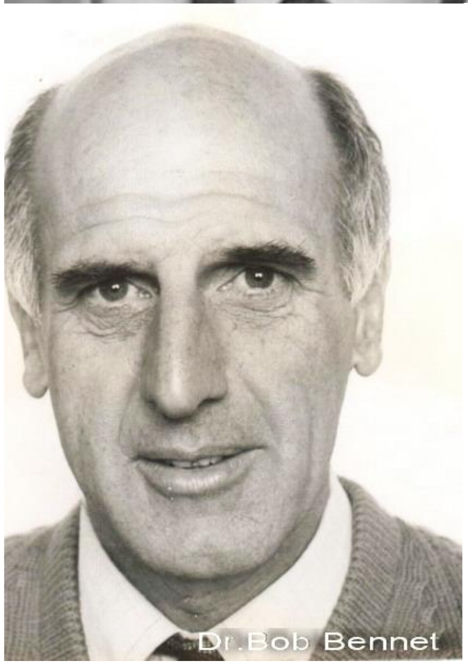

Bob Bennett

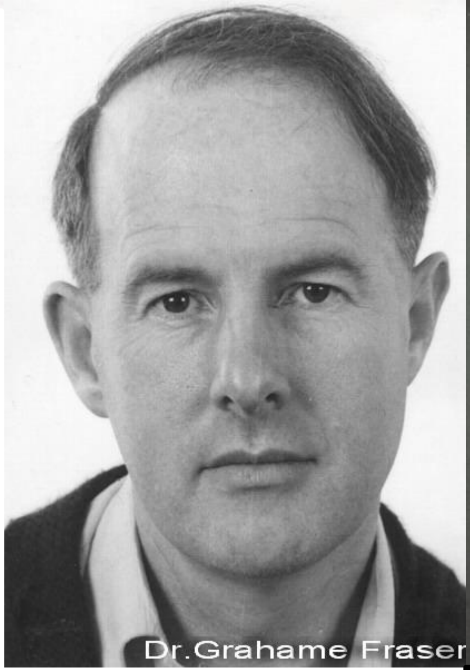

Grahame Fraser

Jack Baggaley

Technology of Vacuum Values

MARGE

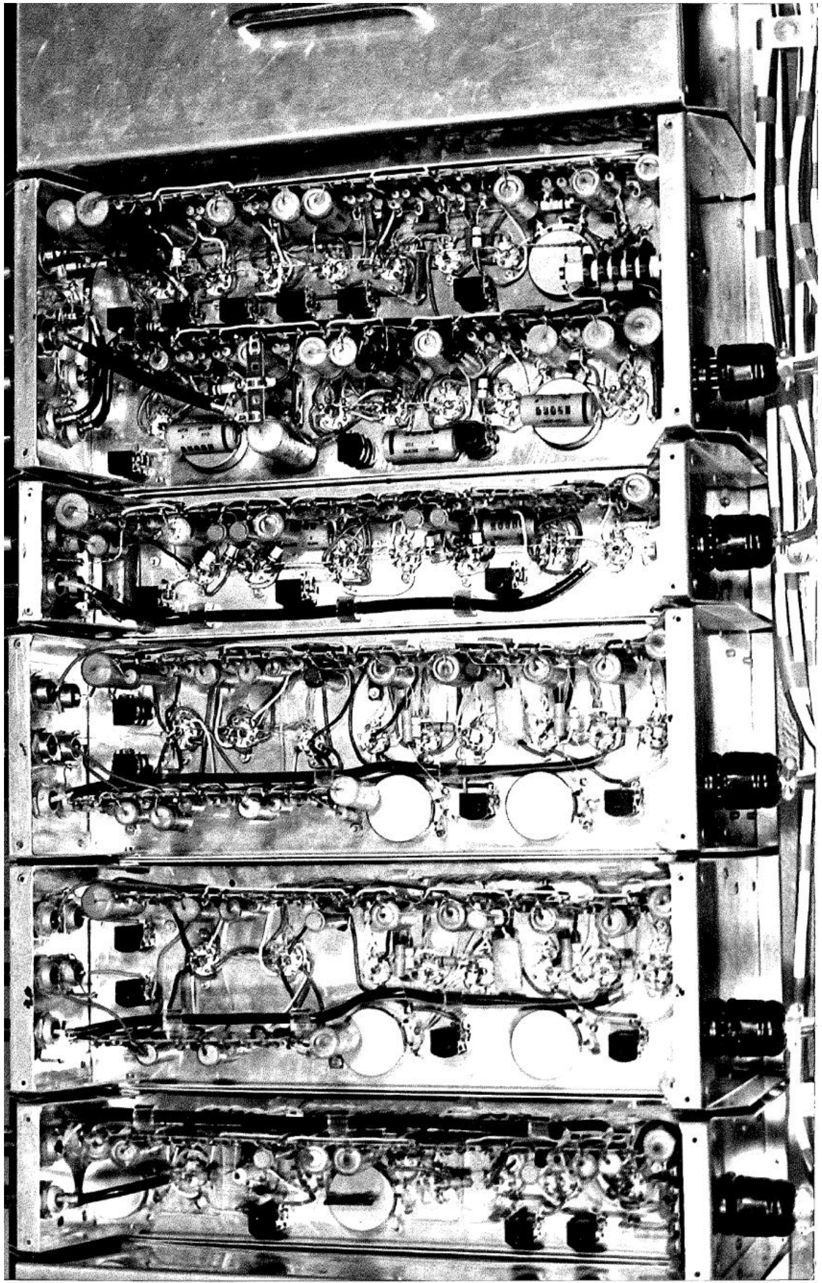

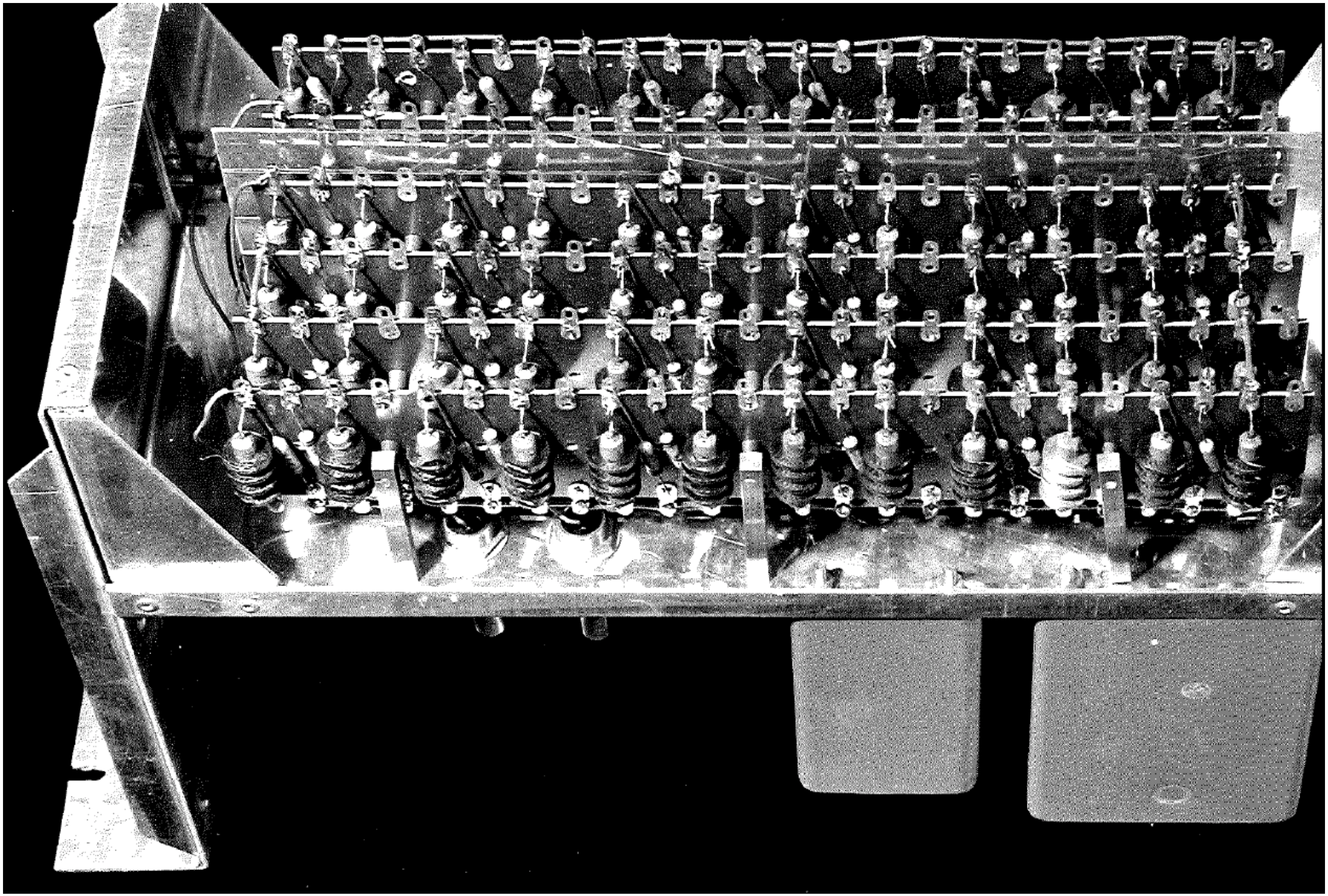

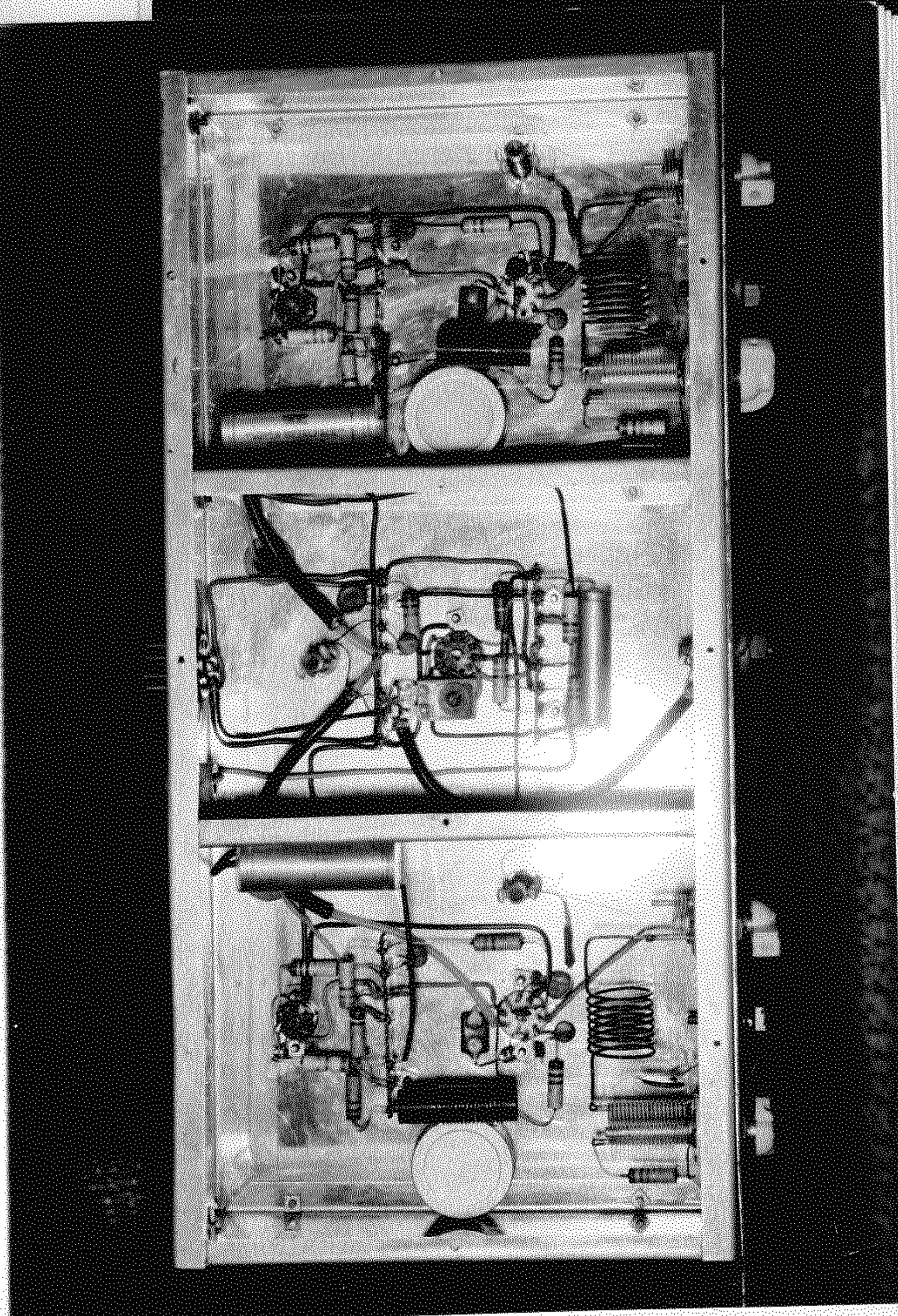

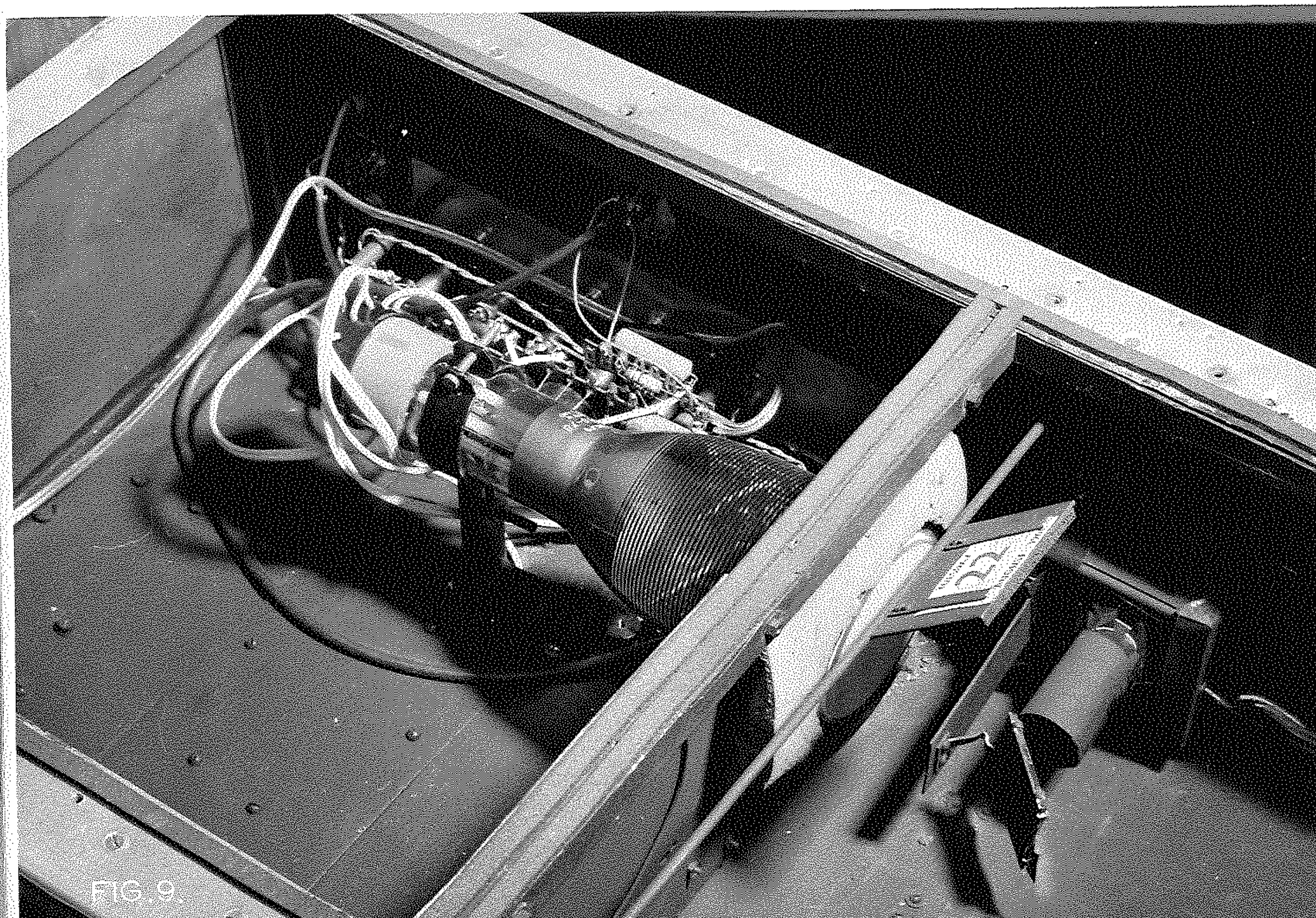

FIG. 9.

FIG. 15

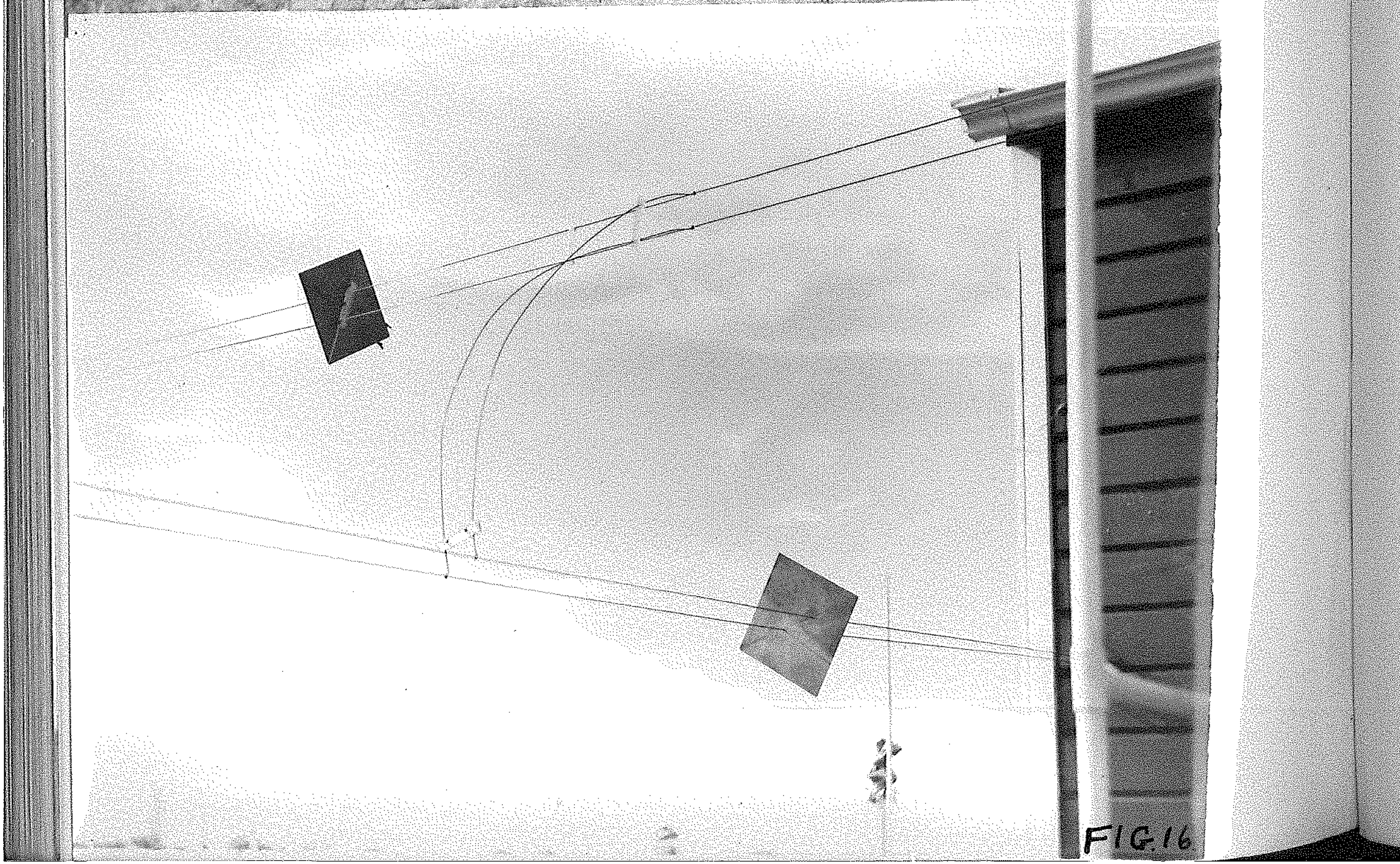

FIG. 16

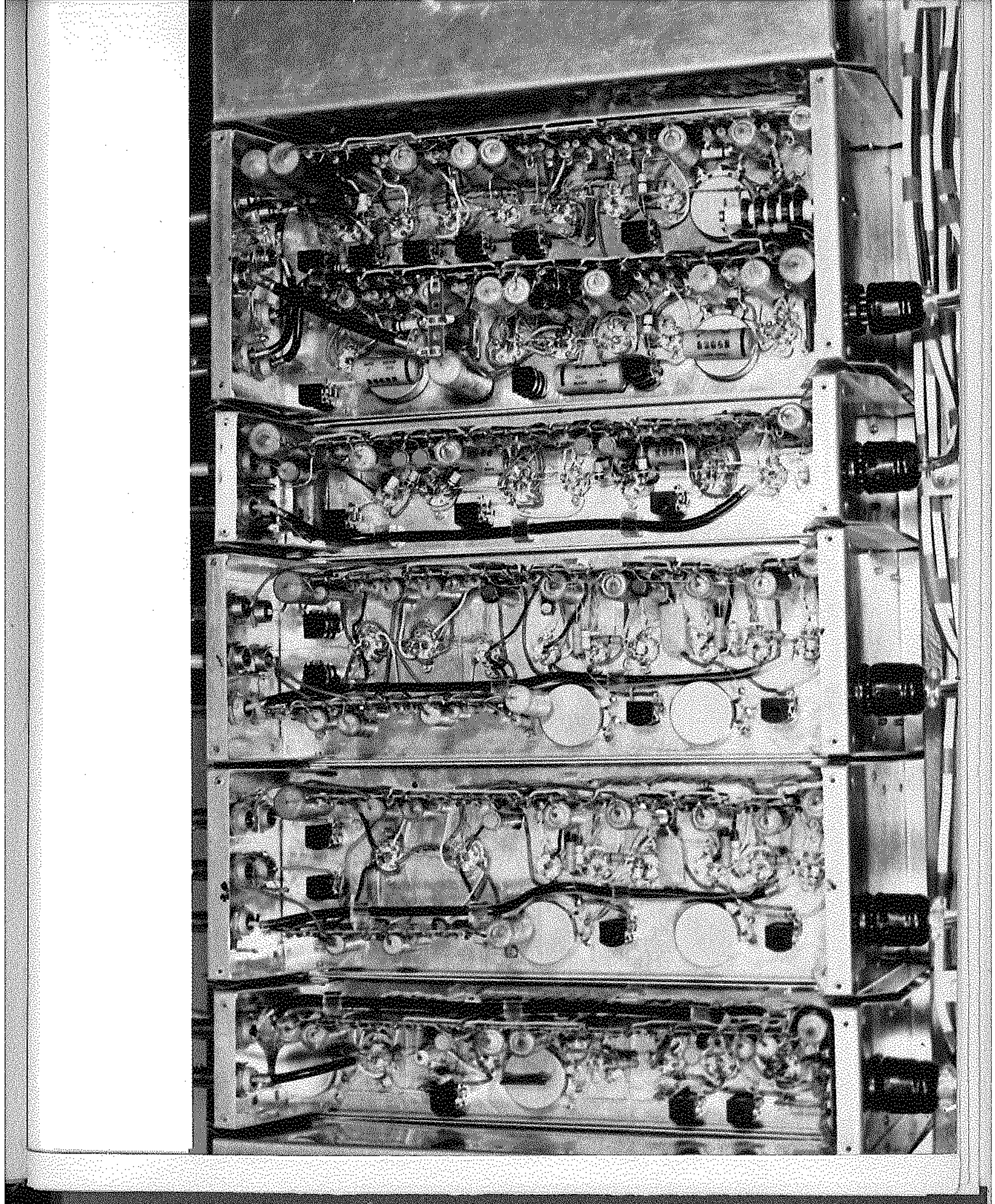

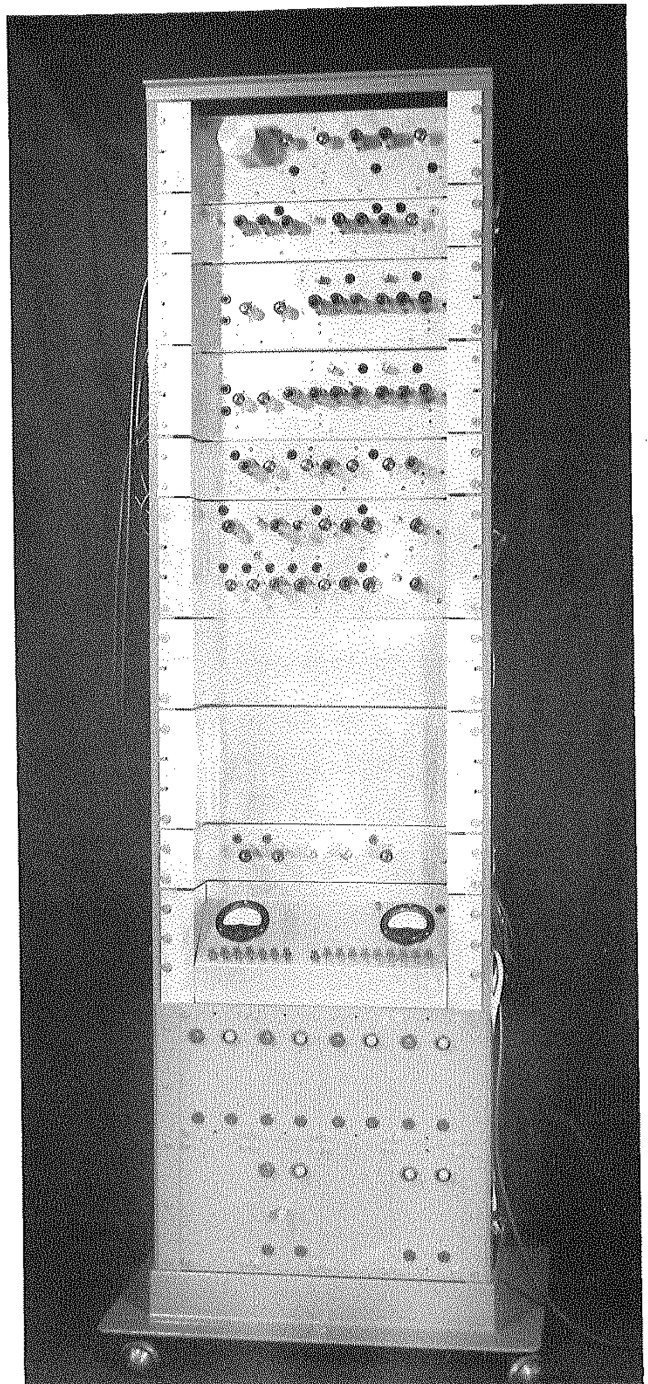

Rolleston: 35mm film recording

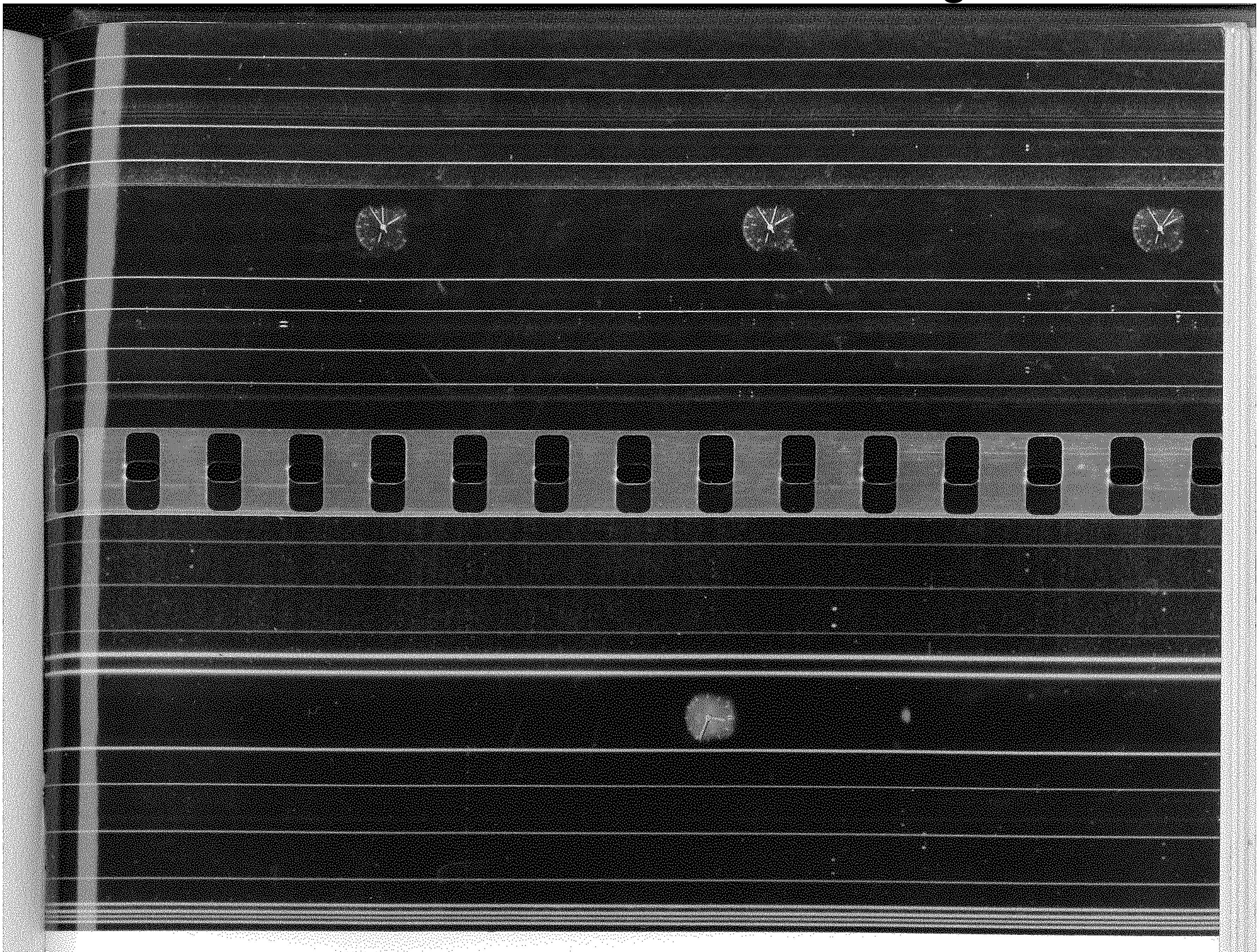

Rolleston: 35mm film recording

Fig. 10 Contd.

(c)

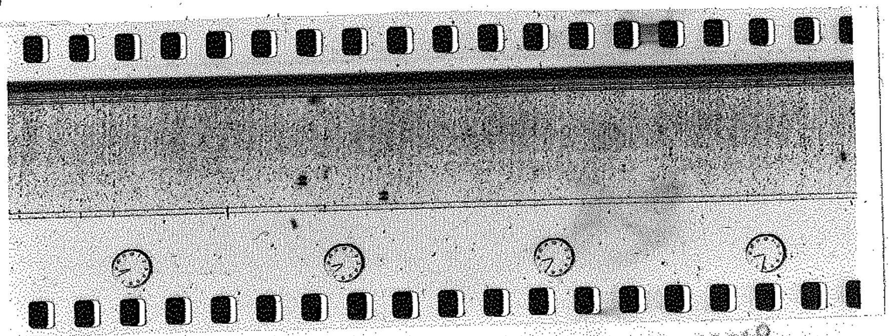

March 6, 1956, 0830 hrs. Aerial Azimuth 292½°.
TX. Pulse Length 26μs. TX. High Tension 13 Kv.
Crystal Control, P.R.F., 150.00 c/s.
Fairly high rate record. Slight background interference.

(d)

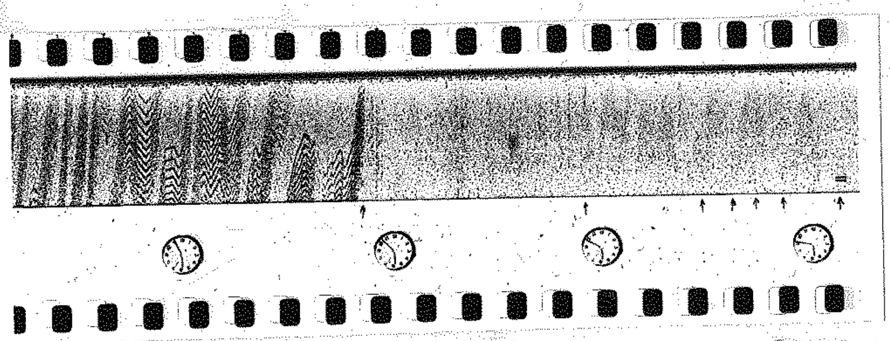

March 11, 1956, 0545 hrs. Aerial Azimuth 292½°.
TX. Pulse Length 3.5μs. TX. High Tension 7.5 Kv.
Crystal Control, P.R.F., 150.00 c/s.
Low rate record. Arrows indicate echoes.
Reasonably bad interference related to mains frequency.

Rolleston: 35mm film recording

Fig. 10

Sample Records from Radiant Measuring Apparatus

(a)

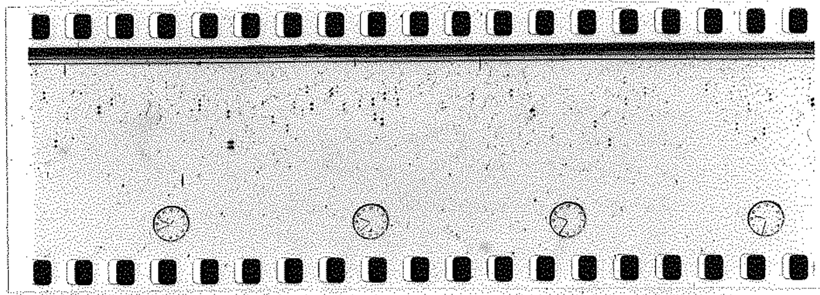

February 10, 1956, 0930 hrs. Aerial Azimuth 292½°.
TX. Pulse Length 26 μs. TX. High Tension 11 Kv.
Free-running Oscillator Control, P.R.F., 146 c/s.
Good high rate record. No interference present.
Note permanent echoes and aircraft echoes at short range.

(b)

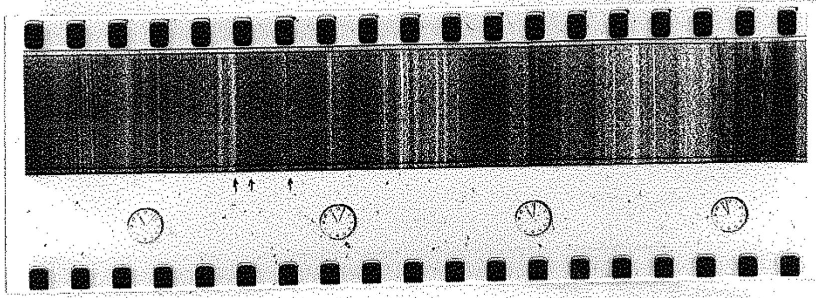

February 26, 1956, 1055 hrs. Aerial Azimuth 292½°.
TX. Pulse Length 3.5 μs. TX. High Tension 13Kv.
Free-running Oscillator Control, P.R.F., 146 c/s.
Low rate record. Arrows indicate echoes.
Reasonably bad interference related to mains frequency.

are separate. They employ small enclosed spark gaps.

The arrangement of lines is shown in diagram 11. The fine wires are located inside and are used to reduce losses and the current in the spark gaps during transmission. It was found that the capacity of the spark-gaps affected the high impedance line. By tuning the lines of the T.B. system carefully it was possible to produce a rejection of signals from the opposite aerial greater than 80 db. This is greater than that of the later circuits, but a high rejection is advantageous as the transmitter is prone to produce noise when the valves start to age, and this is also attenuated, so that it is worthwhile to carry out this adjustment.

The receiver is connected by means of lengths of co-axial cable of 75 Ω impedance.

To ensure the equality of gain of the system the impedance presented to the receiver at the end of the cable was made 75 Ω resistive (measured by a Wayne-Kerr R.F. bridge) by means of a small trimming capacitor connected across the T.R. line, its position and value being adjustable.

5.9 The Receiver.

The receiver proper is one built in 1954 (Fraser 1954, Keay 1955) for use on 69 mc/s. It has a low noise input stage and a bandwidth which can be switched to 60 kc/s or 300 kc/s and has a regulated high tension supply while the filaments are run

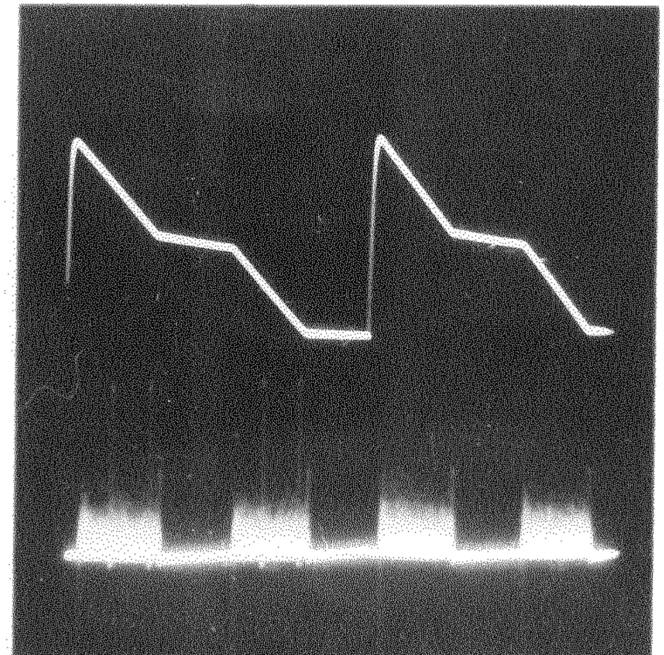

1961: Clif liase with Frank Bateson- under auspices of Royal NZAstronomical Society - who was testing possible sites for an astronomical observatory in the South Island of New Zealand.

1961: they and Prof Brad Wood of the University of Pennsylvania visited the work at the radar meteor work.

1961: Wood, Bateson & Ellyett persuaded the University of Canterbury to enter a cooperative agreement with the University of Pennsylvania to foster astronomical studies.

This subsequently led to the creation of the Mt John Observatory and the birth of astronomy as an academic discipline in New Zealand

1964: Colin Keay with advice from Frank Bateson - already had MSc and PhD at Canterbury - took Leave via scholarships t to take 1 year MSc in Ottawa David Dunlap Observatory Canada acquire grounding in optical astronomy in order to broaden the subjects offered at Canterbury.

The idea was to produce postgraduates in Astronomy in NZ at Canterbury.

1964: Clif set up planetarium in Canterbury Museum

At that time there was rather an emphasis on theoretical Physics at Canterbury with limited support for astronomy (that was to change later).

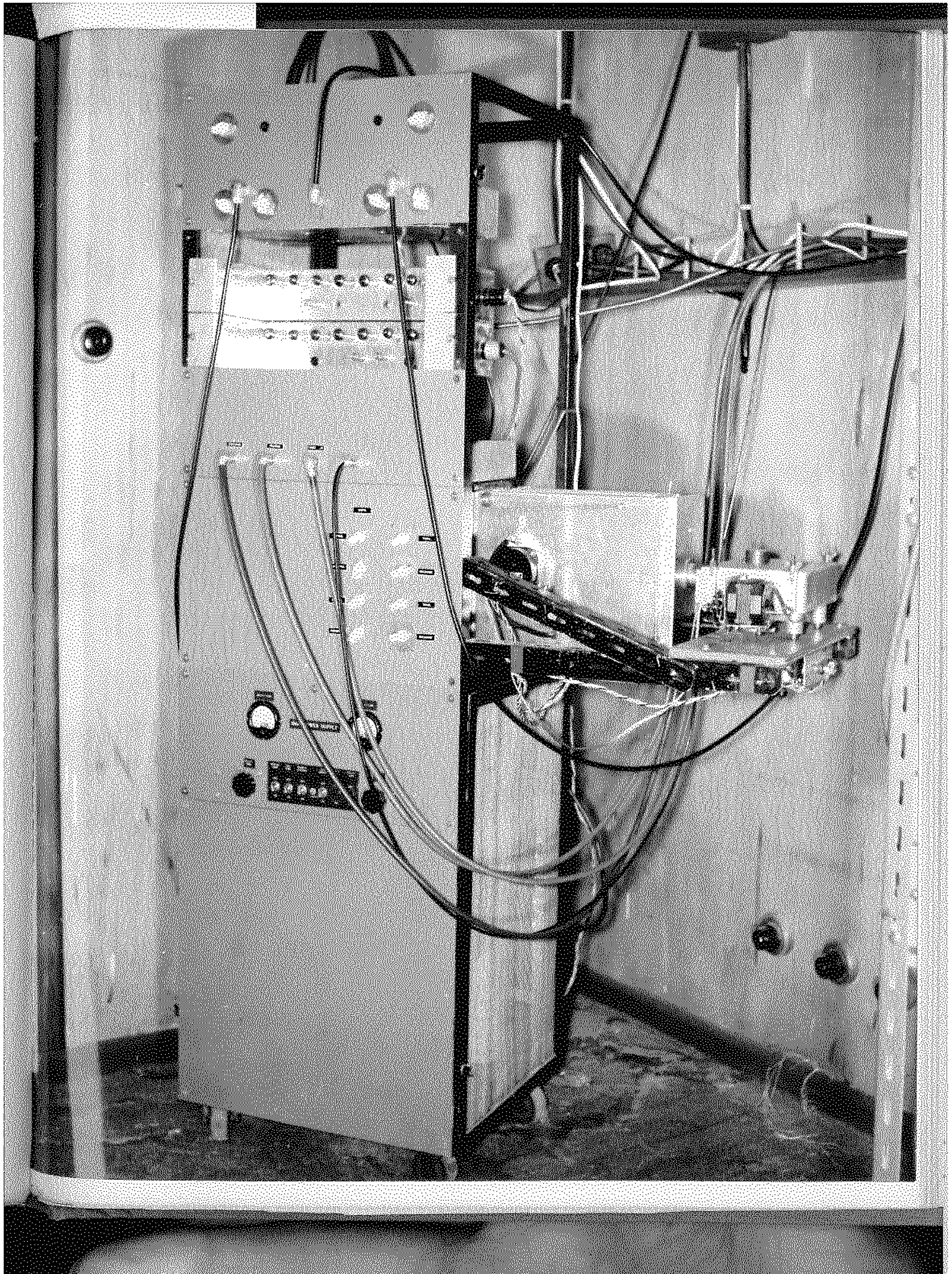

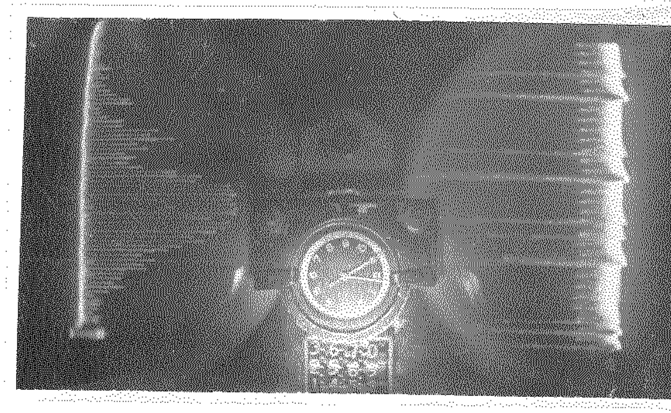

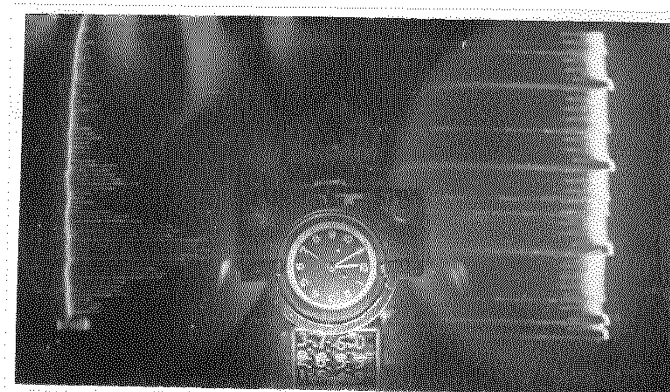

Gross dust distribution

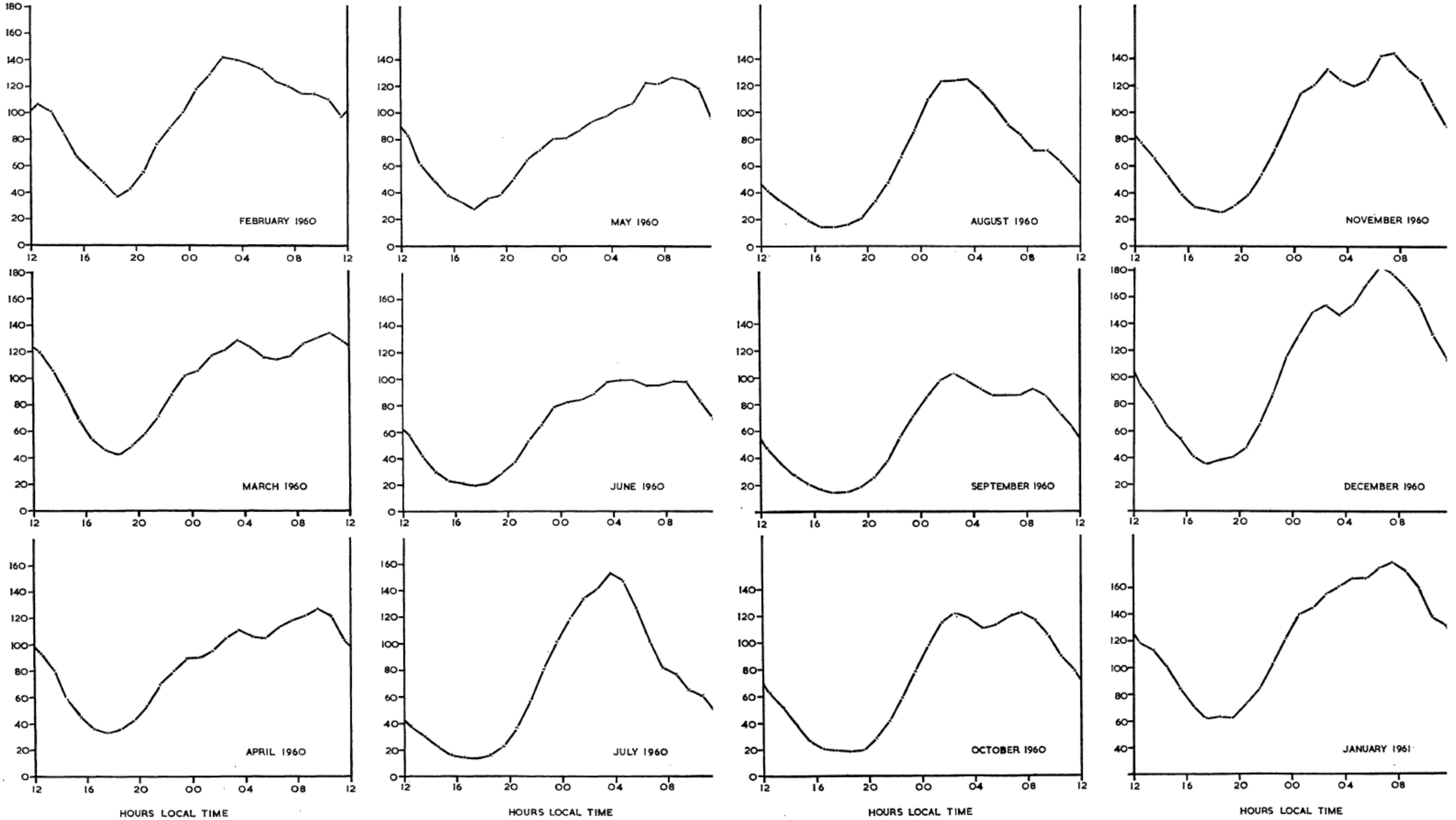

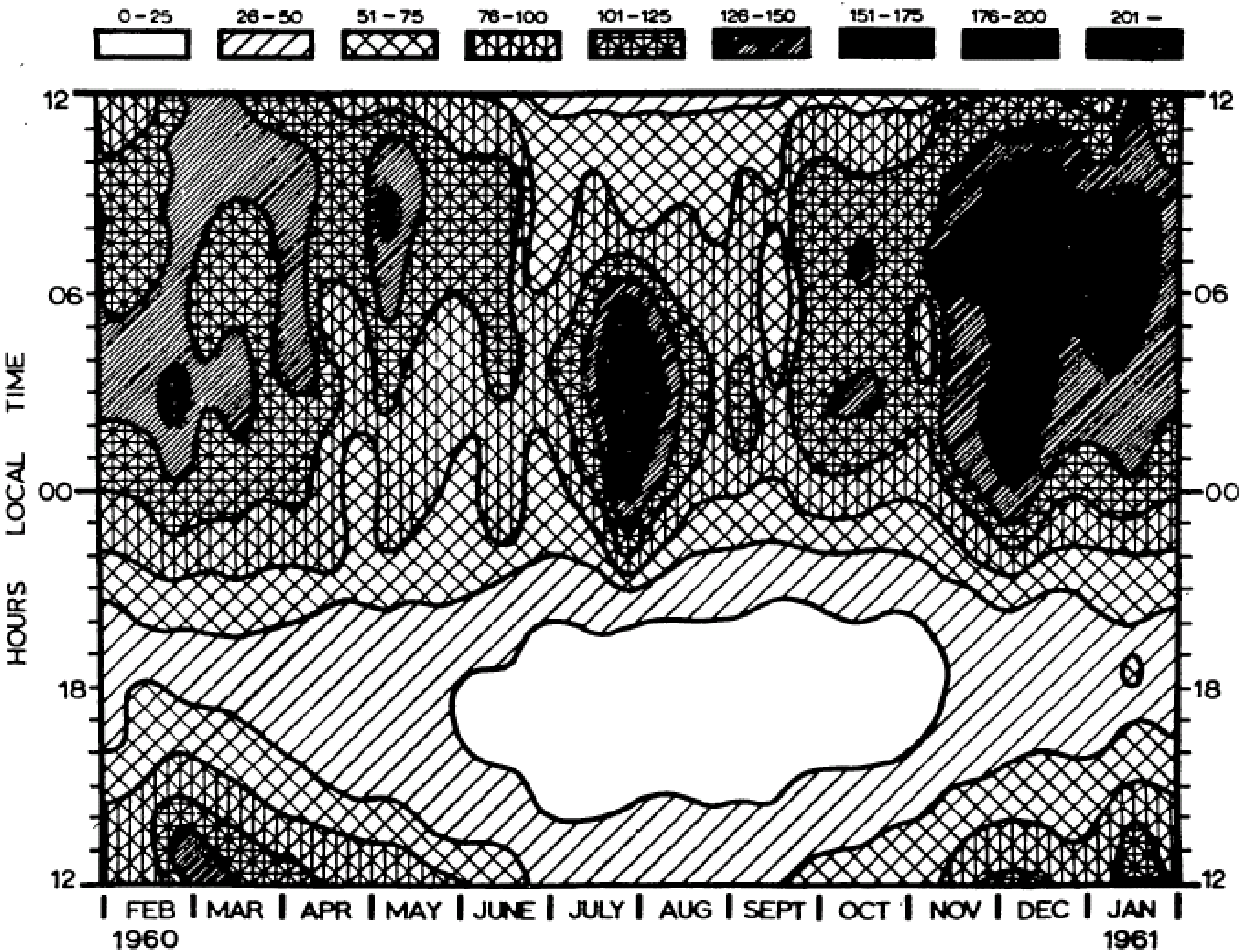

FIG. 3.—*Contours of constant meteor echo rate.*

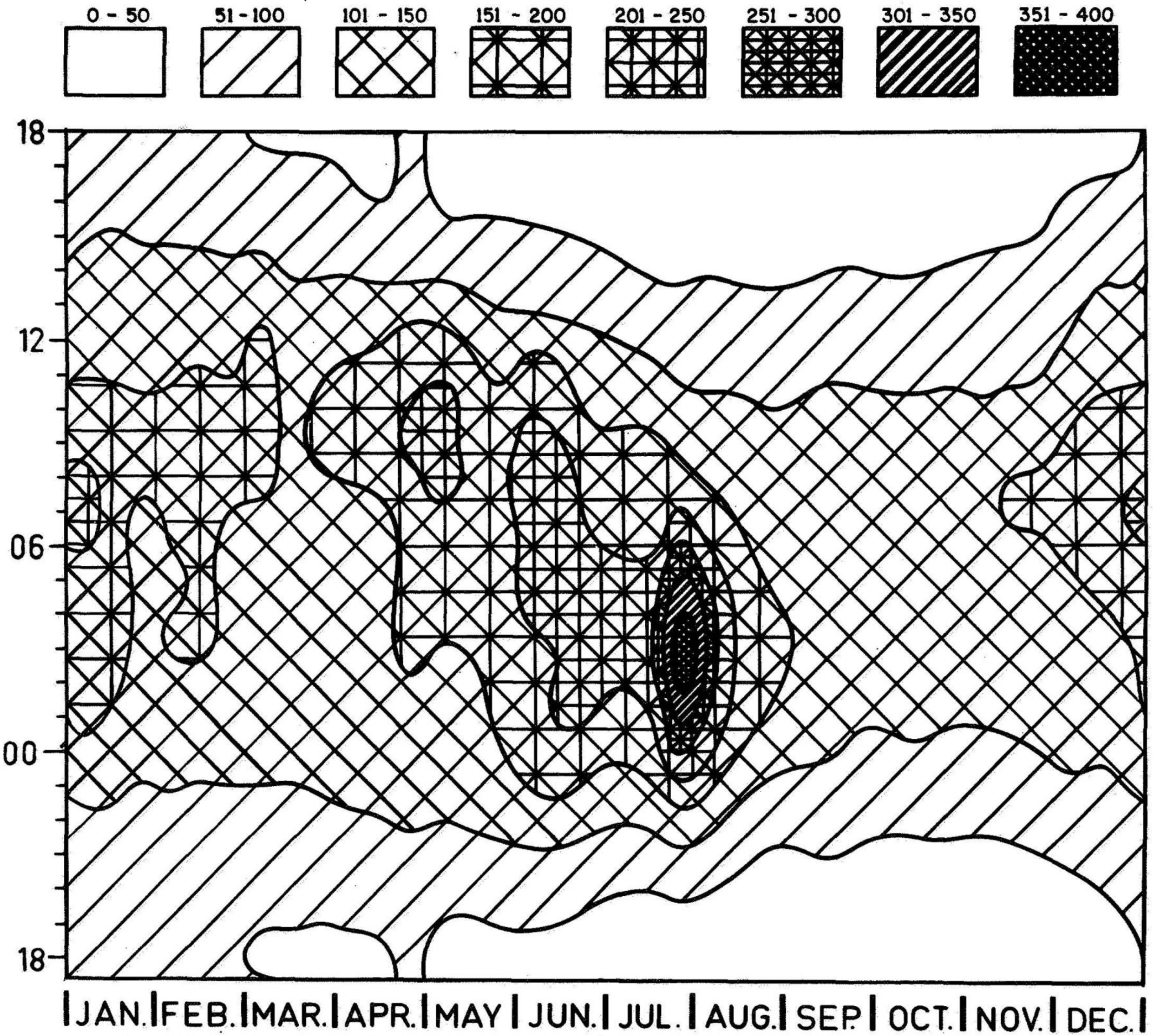

Fig. 4. Contour plot of hourly meteor rates as a function of hour of day

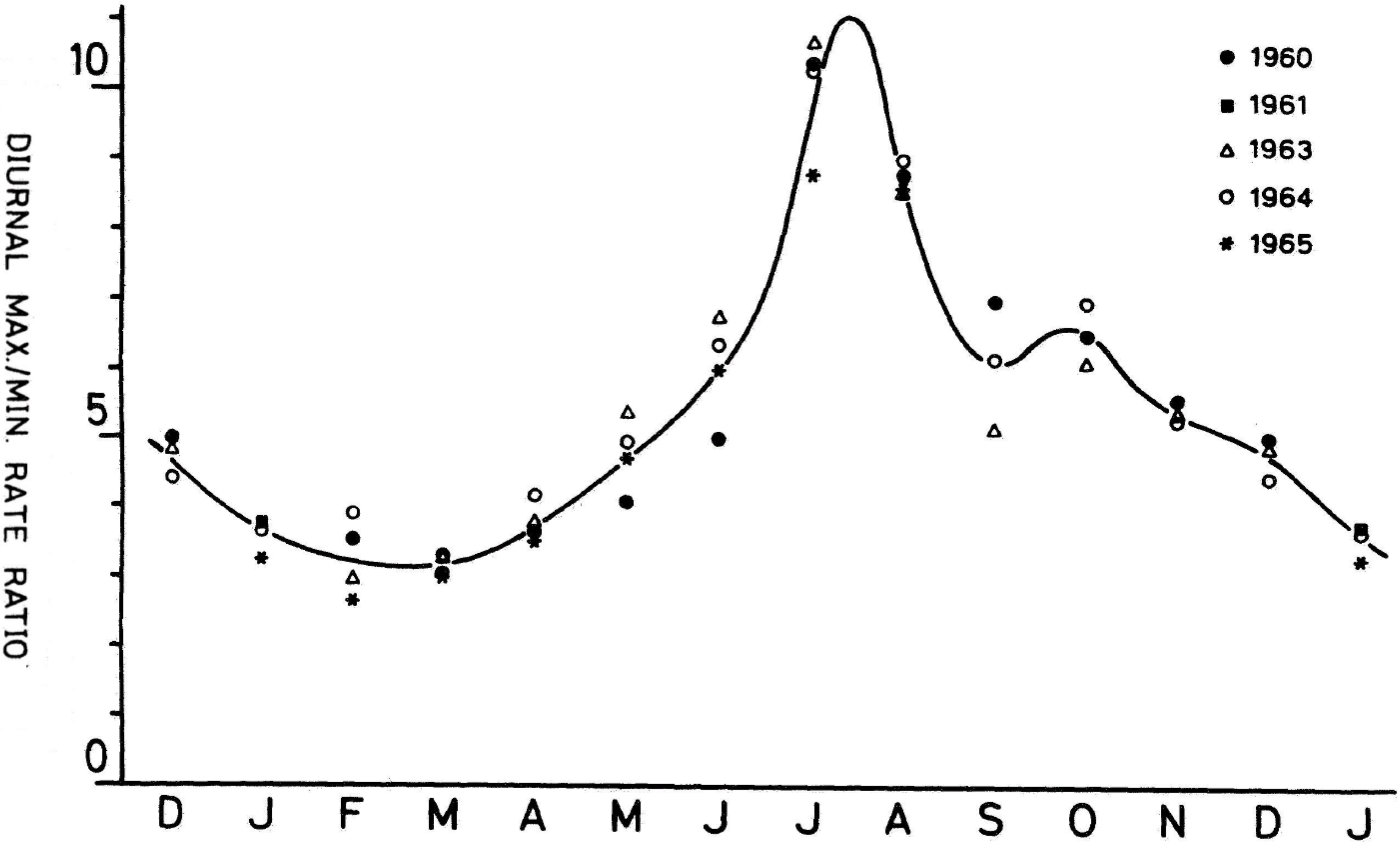

Fig. 12. Annual variation in the diurnal ratio of maximum to minimum meteor rates.

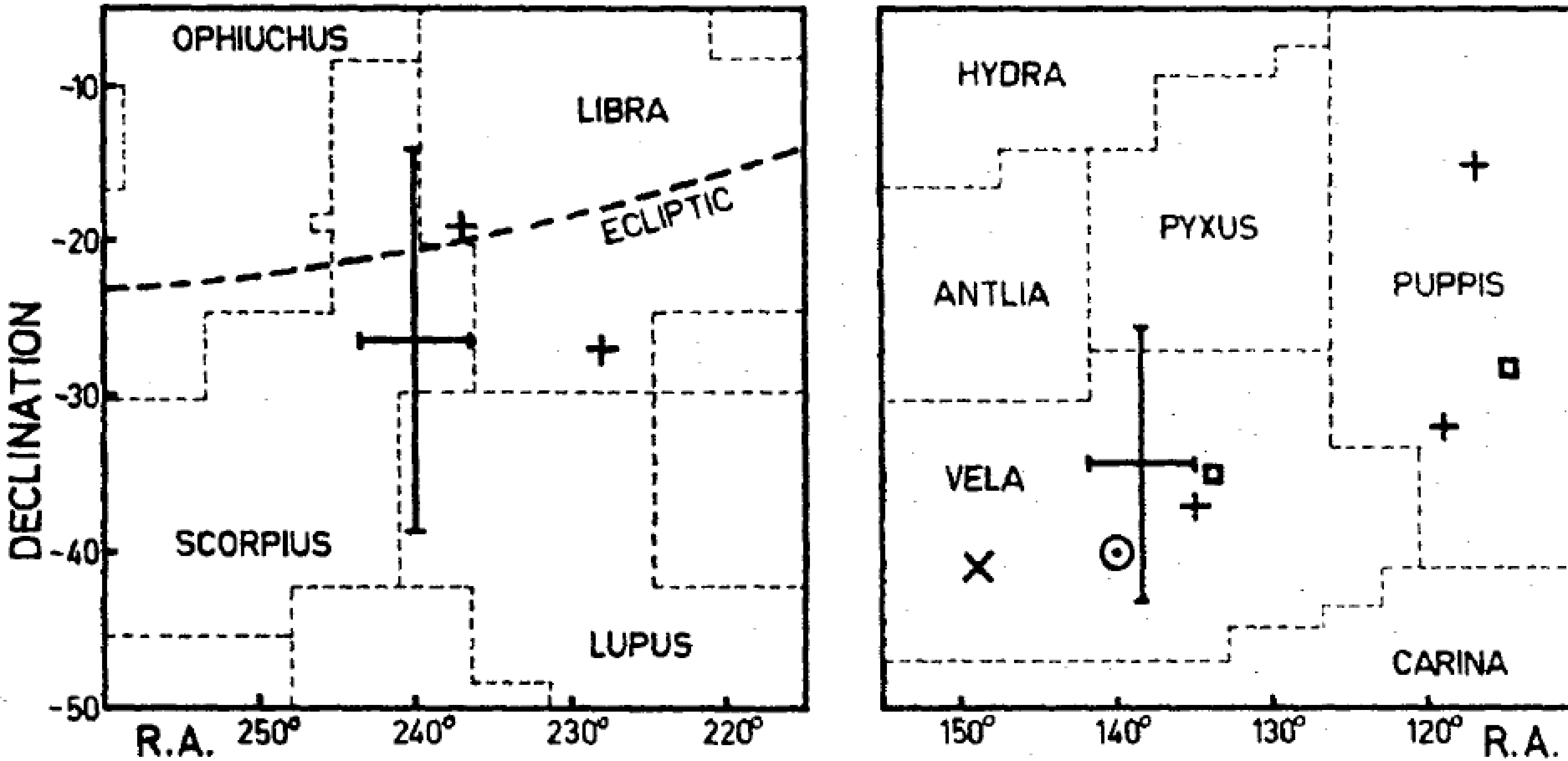

FIG. 9. (a) A plot of the radiant position derived for the L
Scorpid activity together with the positions of Librid ac
(crosses) found by Ellyett, Keay, Roth, and Bennett (1961
the radiant position derived for the Velid activity is s
together with the other Velid–Puppid radiants found by ×
meister (1948); ⊙Weiss (1960); +Ellyett, Keay, Roth and

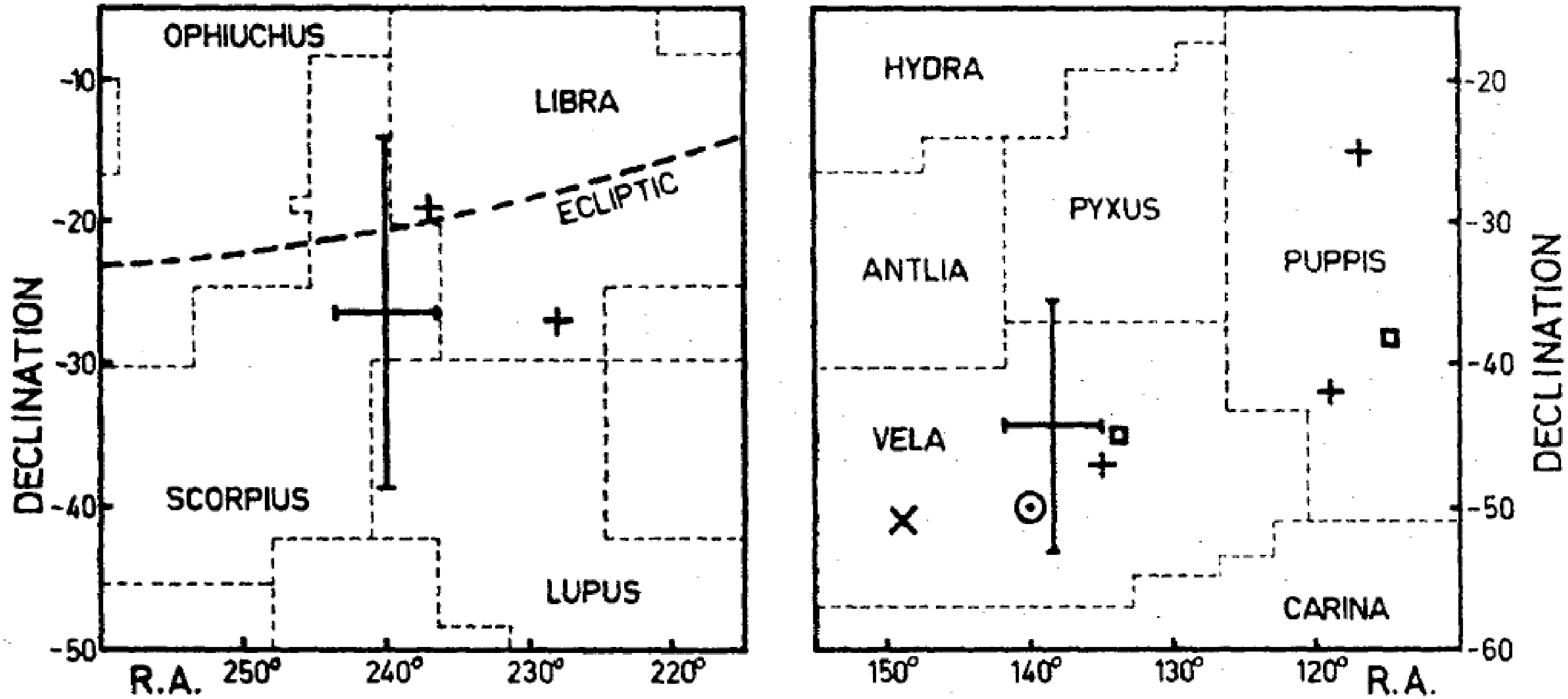

Fig. 9. (a) A plot of the radiant position derived for the Librid–Scorpid activity together with the positions of Librid activity (crosses) found by Ellyett, Keay, Roth, and Bennett (1961); (b) the radiant position derived for the Velid activity is shown together with the other Velid–Puppid radiants found by ✕ Hoffmeister (1948); ⊙ Weiss (1960); + Ellyett, Keay, Roth and Bennett (1961); □ Ellyett and Roth (1964).

1967: Jack Baggaley. Programme on heliocentric orbits.

Individual meteor echo phase + power record ~ 1970

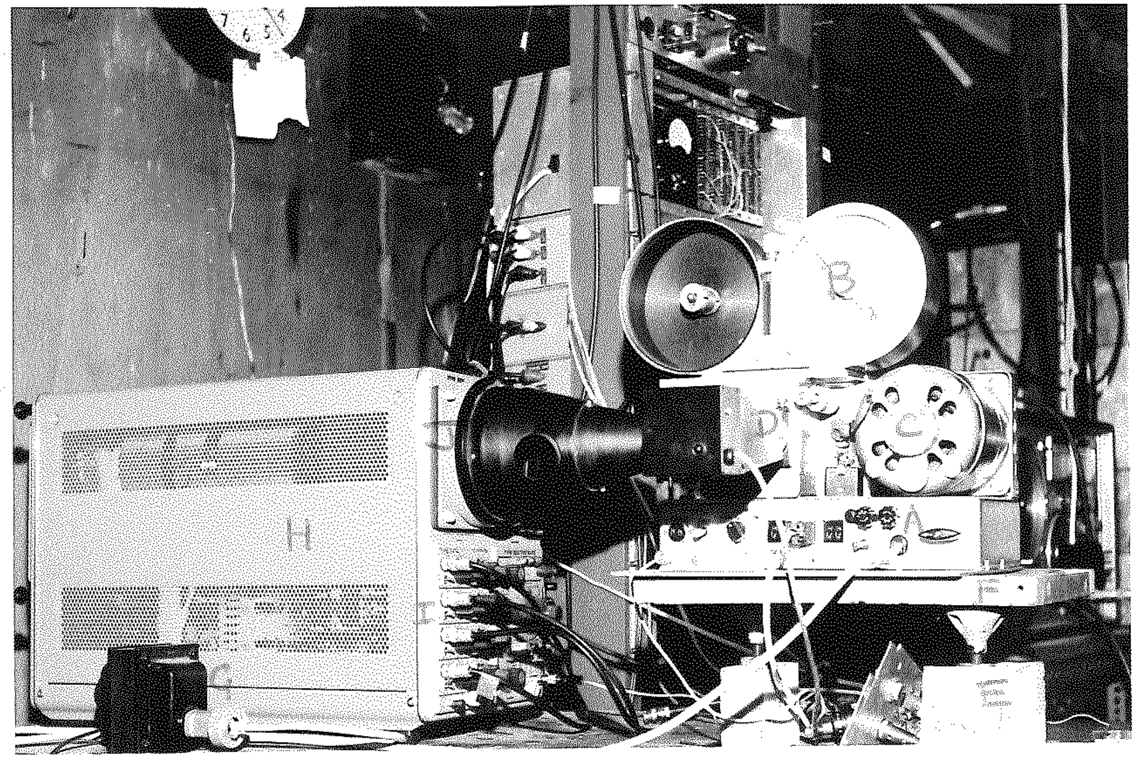

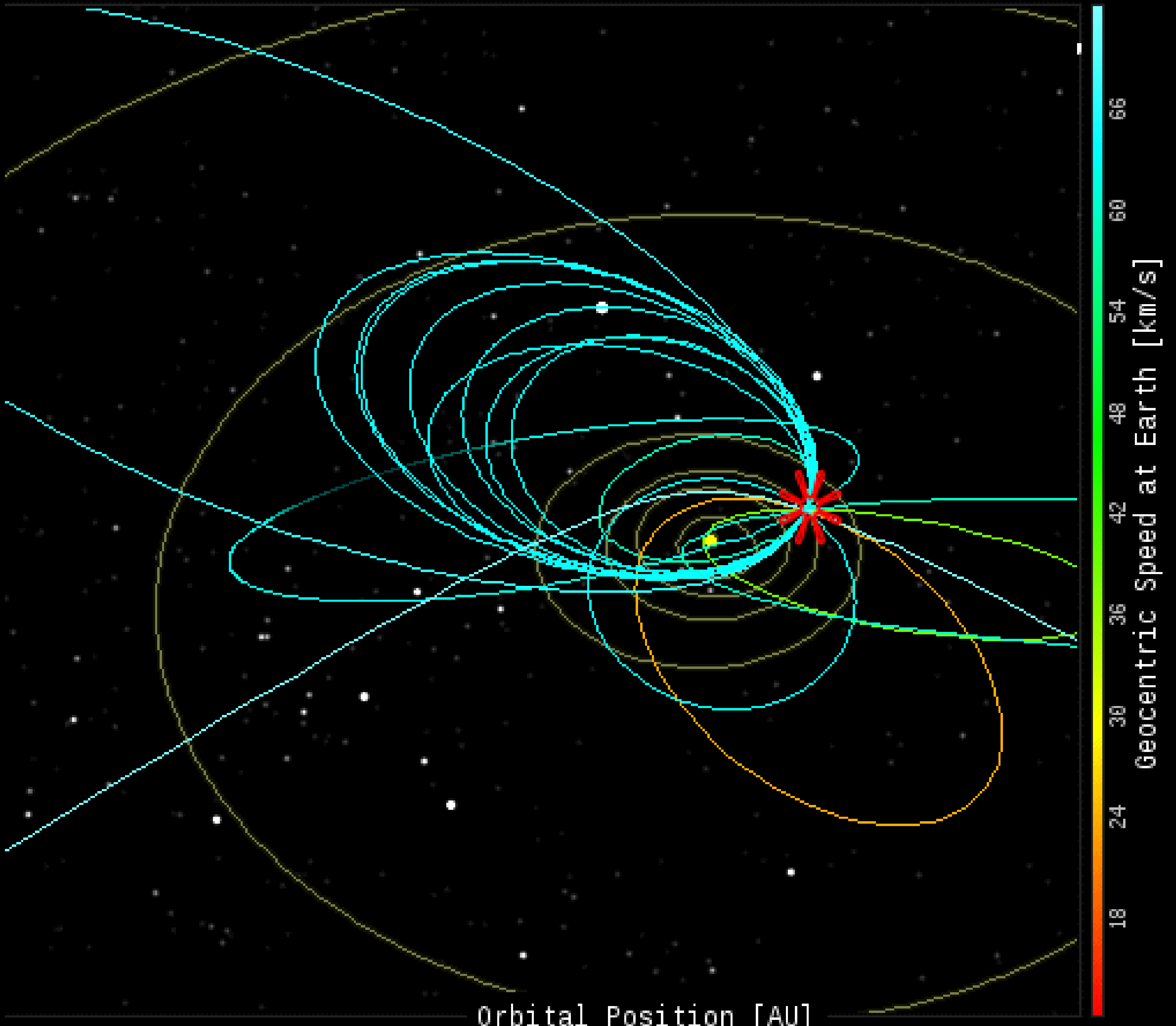

Orbital Position [AU]
Geocentric Speed at Earth [km/s]
66
60
54
48
42
36
30
24
18

orionids

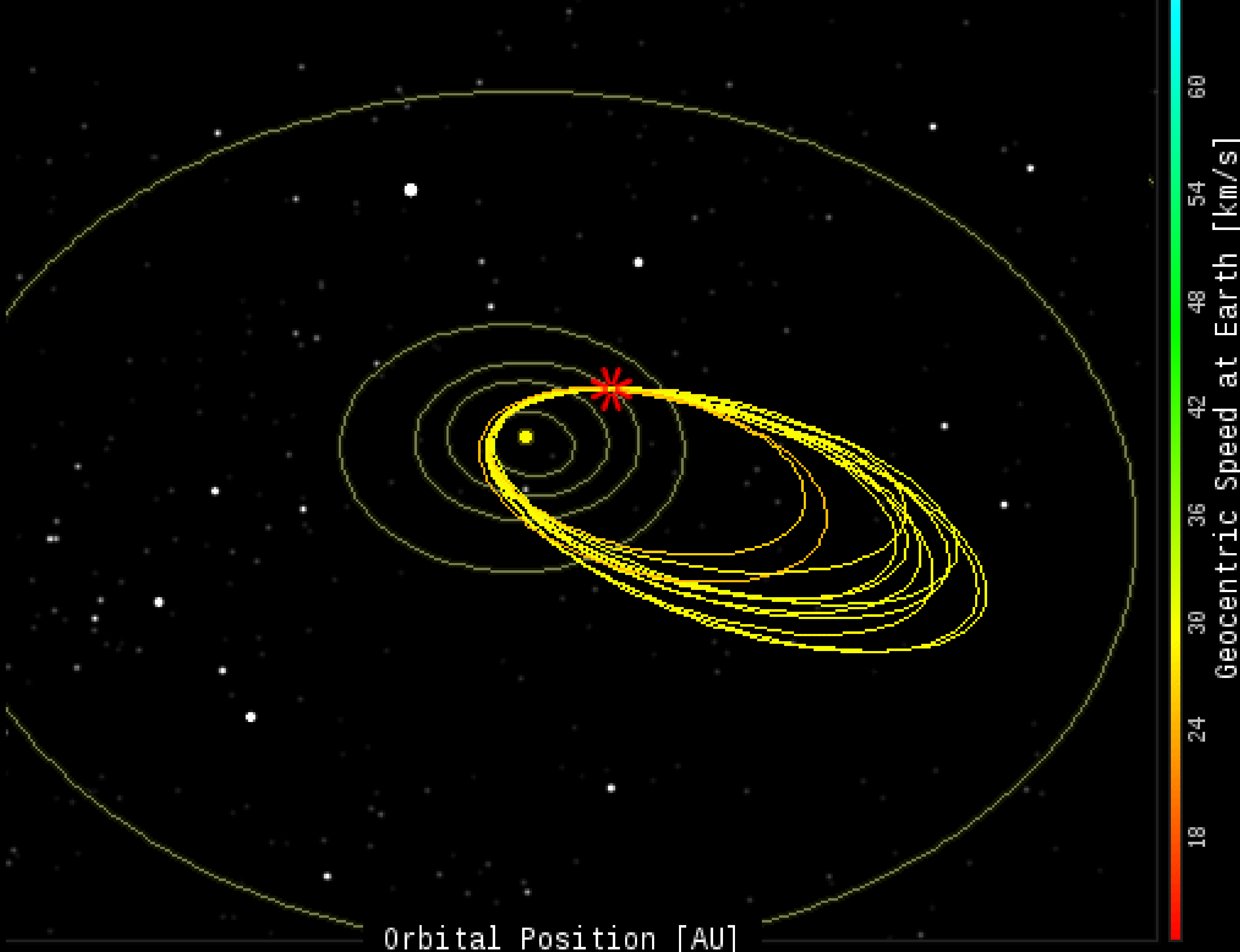
Orbital Position [AU]
Geocentric Speed at Earth [km/s]
18
24
30
36
42
48
54
60

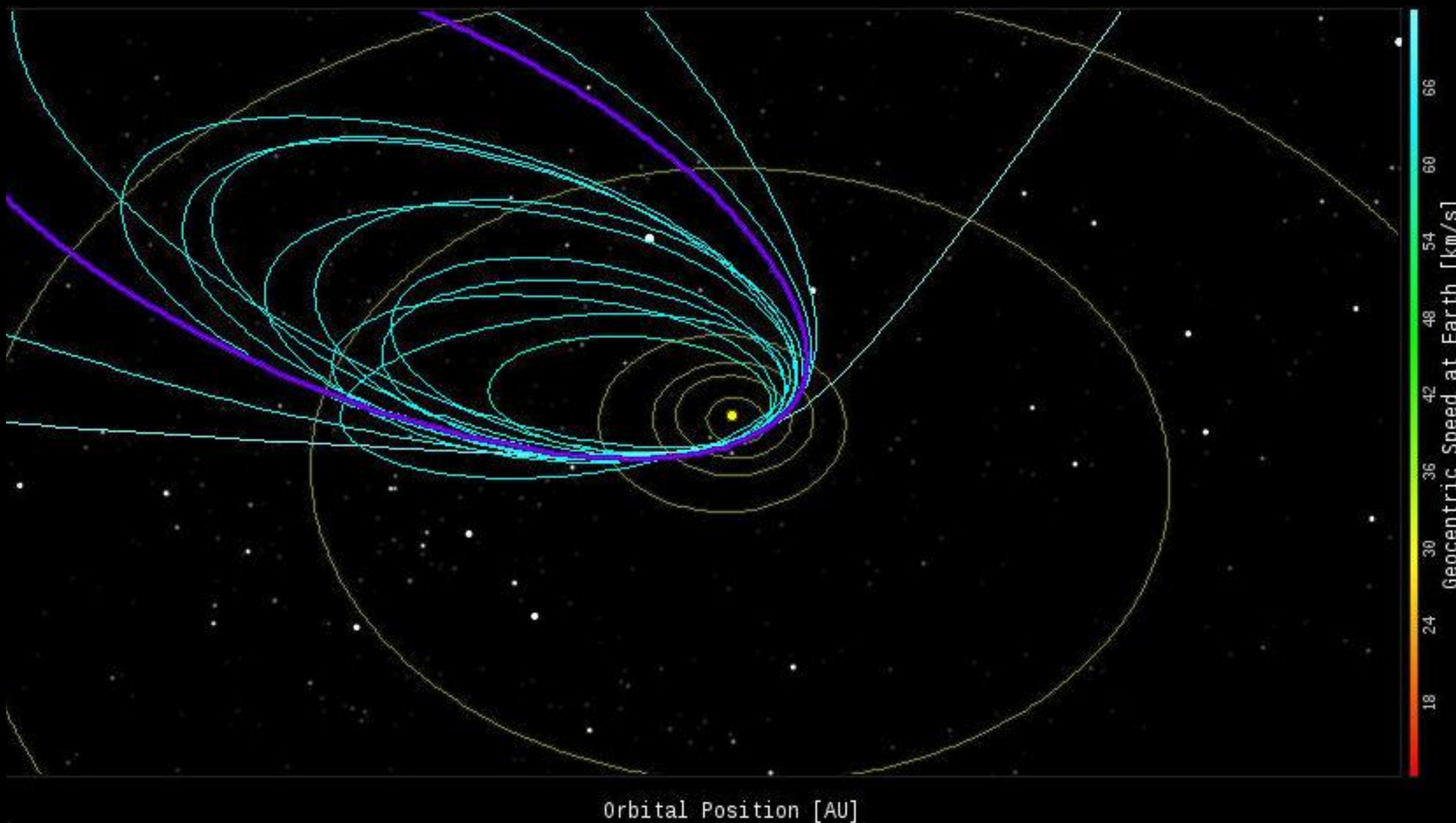
Orbital Position [AU]
Geocentric Speed at Earth [km/s]
18
24
30
36
42
48
54
60
66

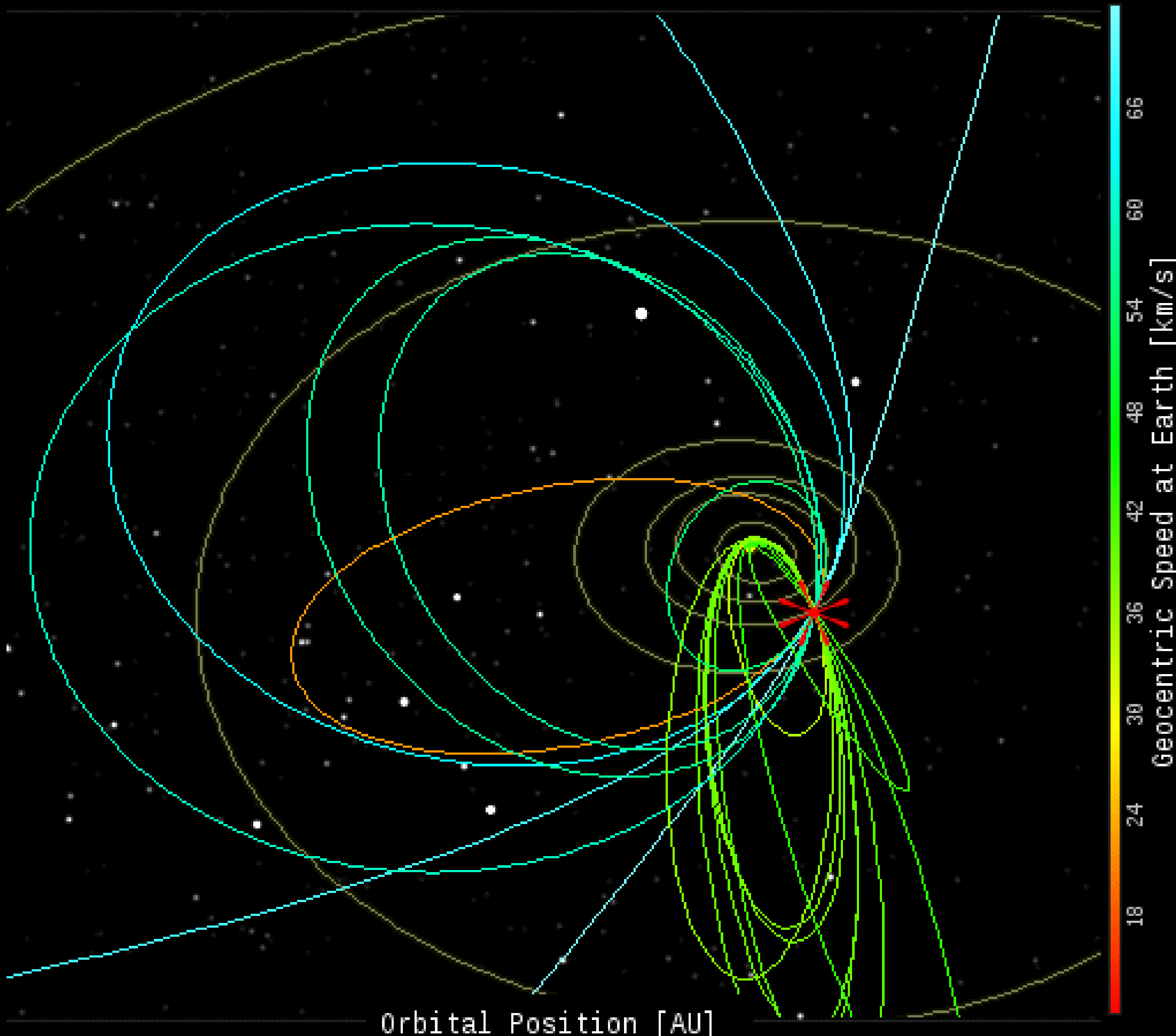

Green 96P Machholz
DeltaAquaid Blue Perseid

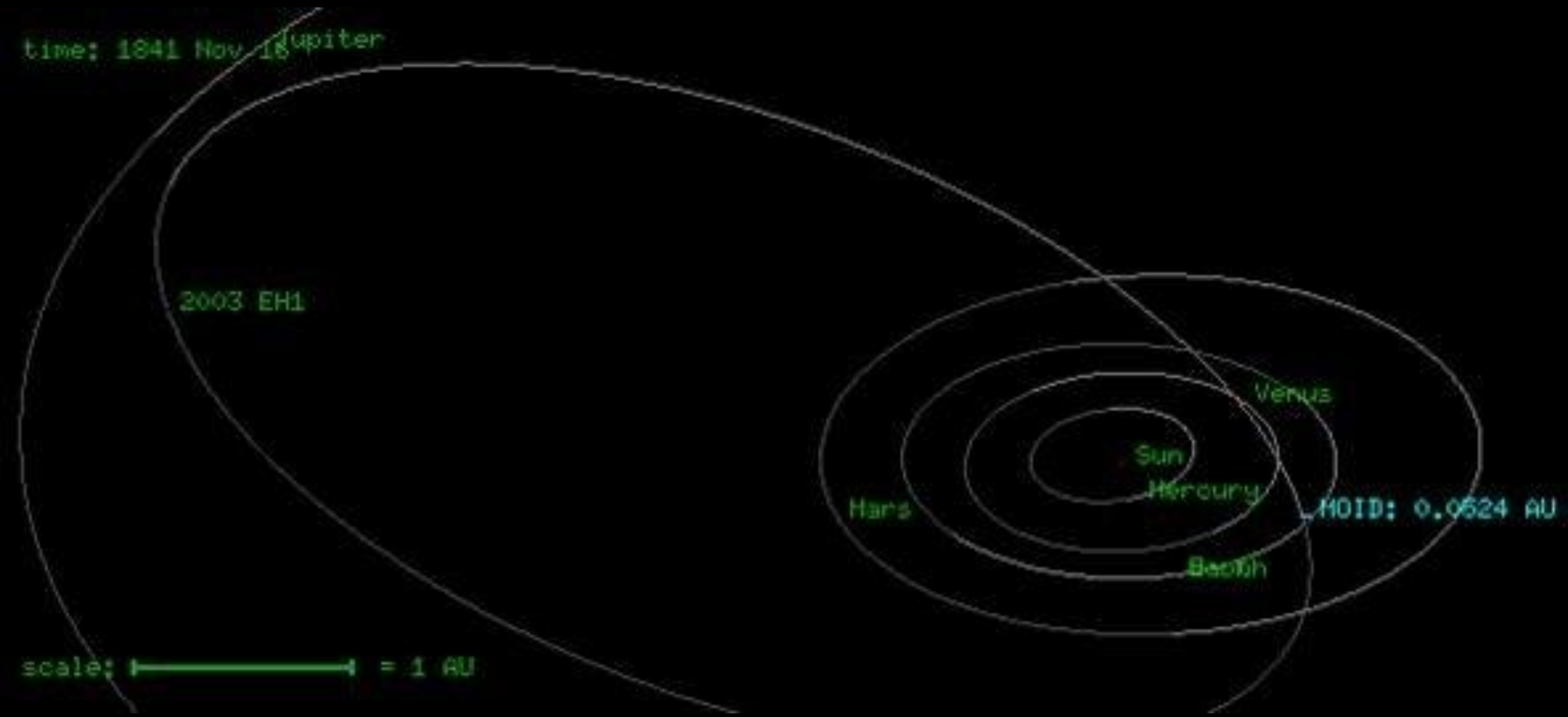

observe-quadrantid-meteor-shower_w

Current Meteoroids, NEAs and Comets

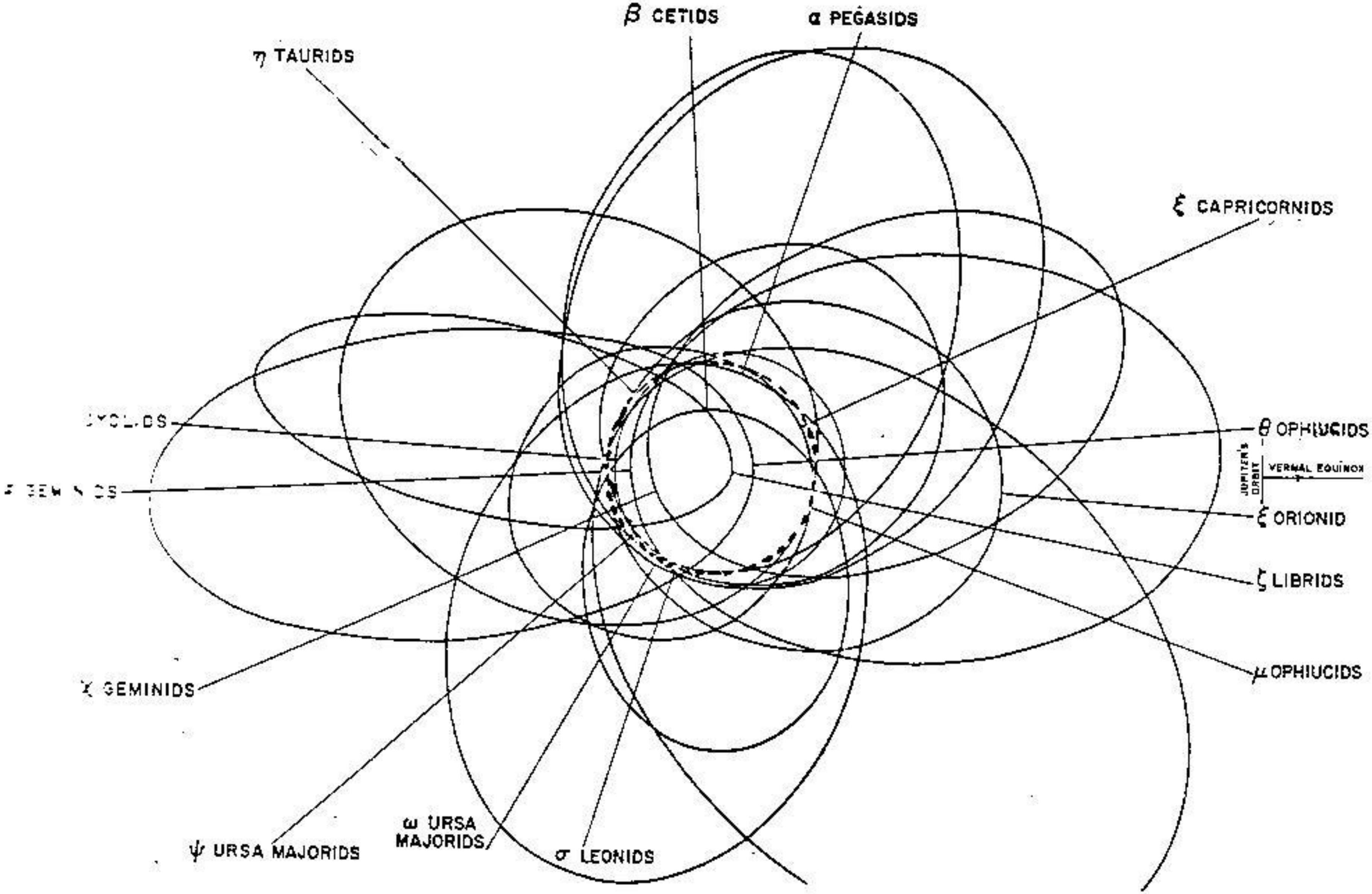

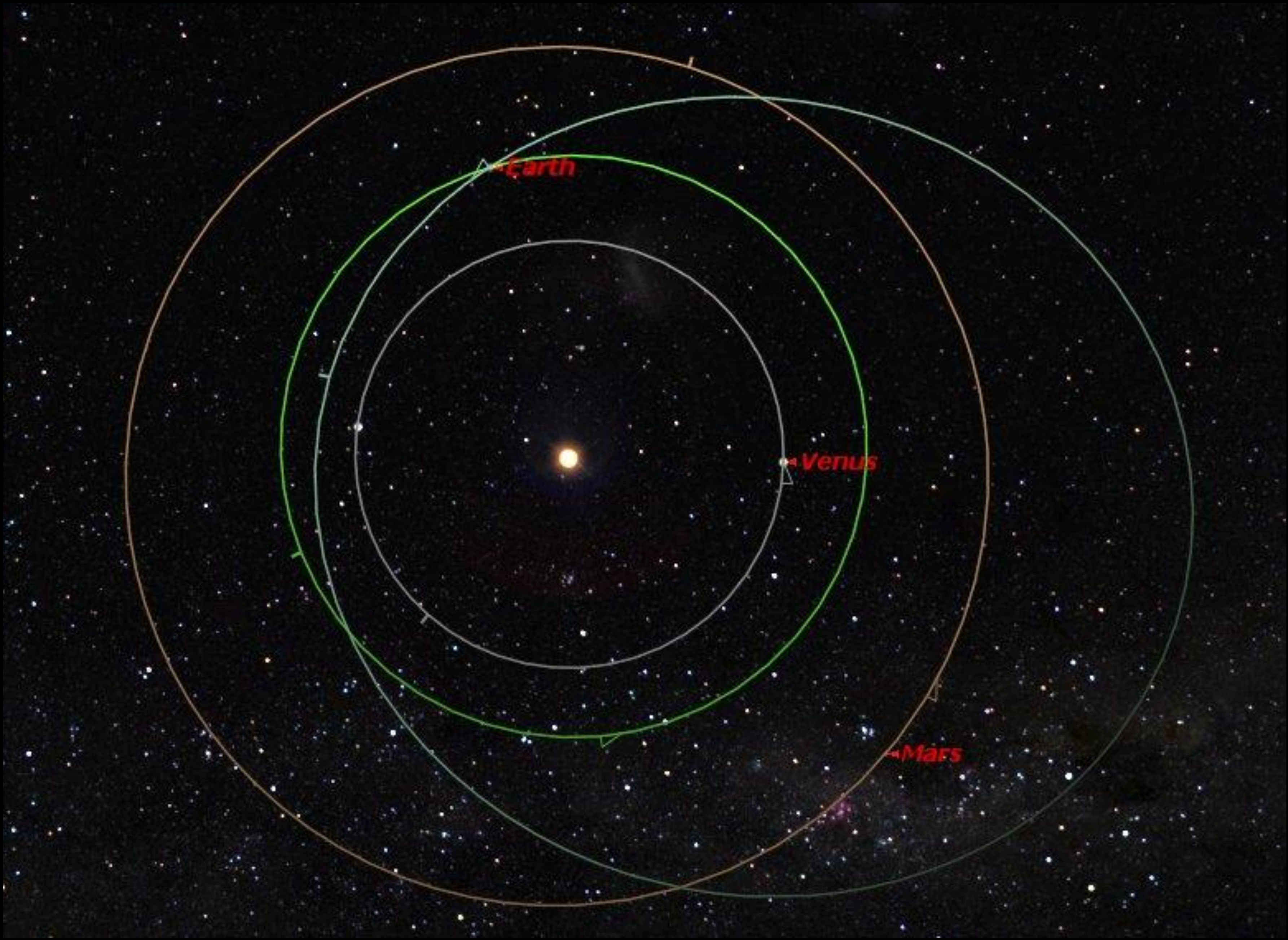
Earth
Venus
Mars

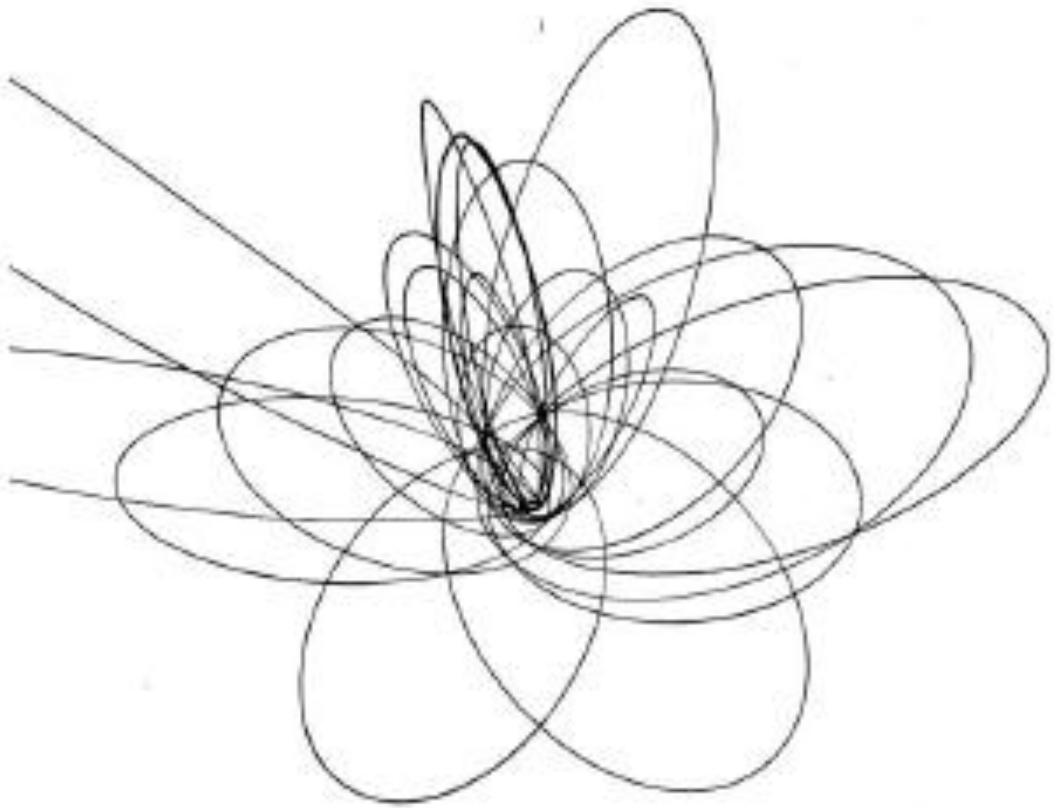

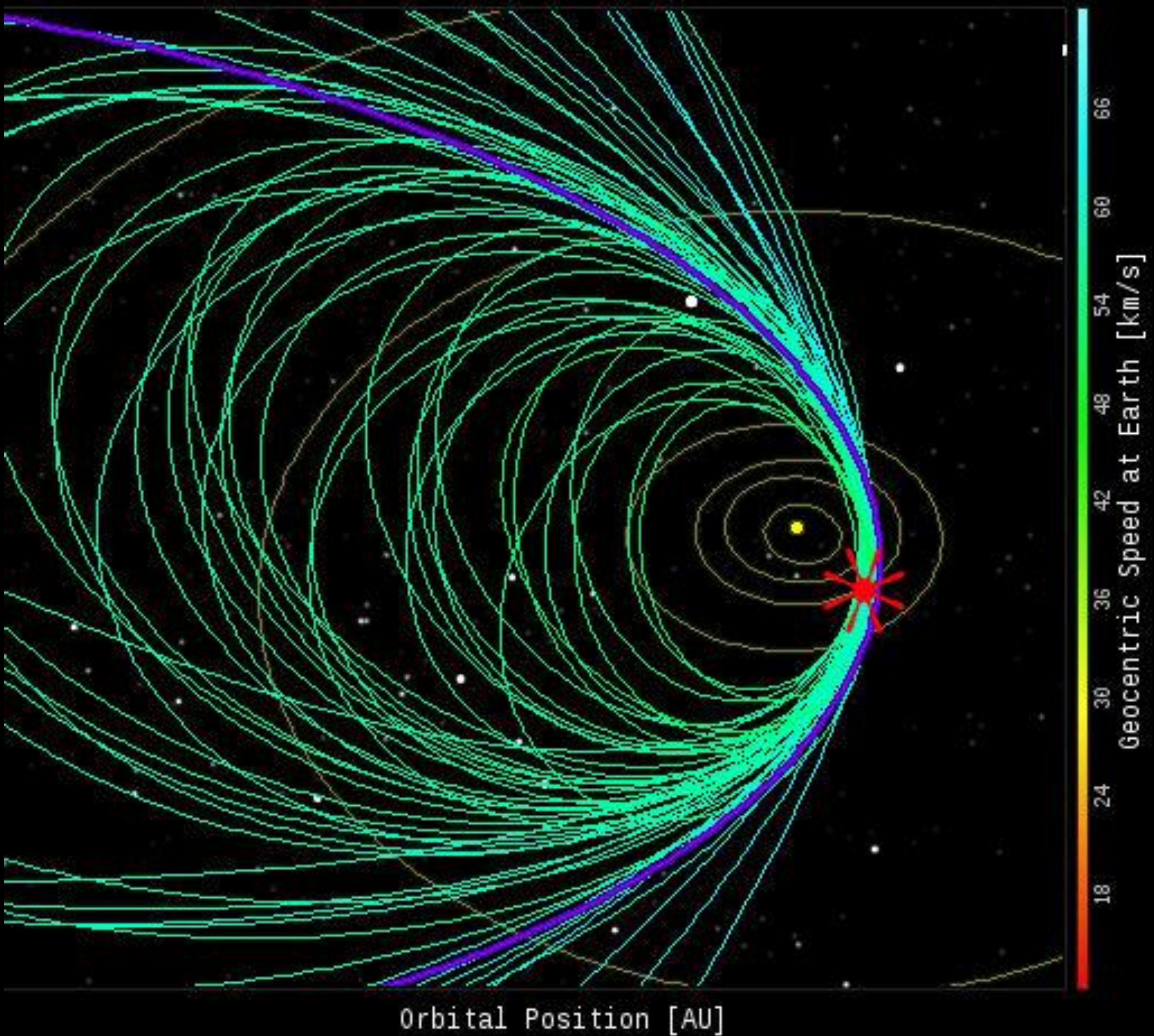

orbits_strip_perseid

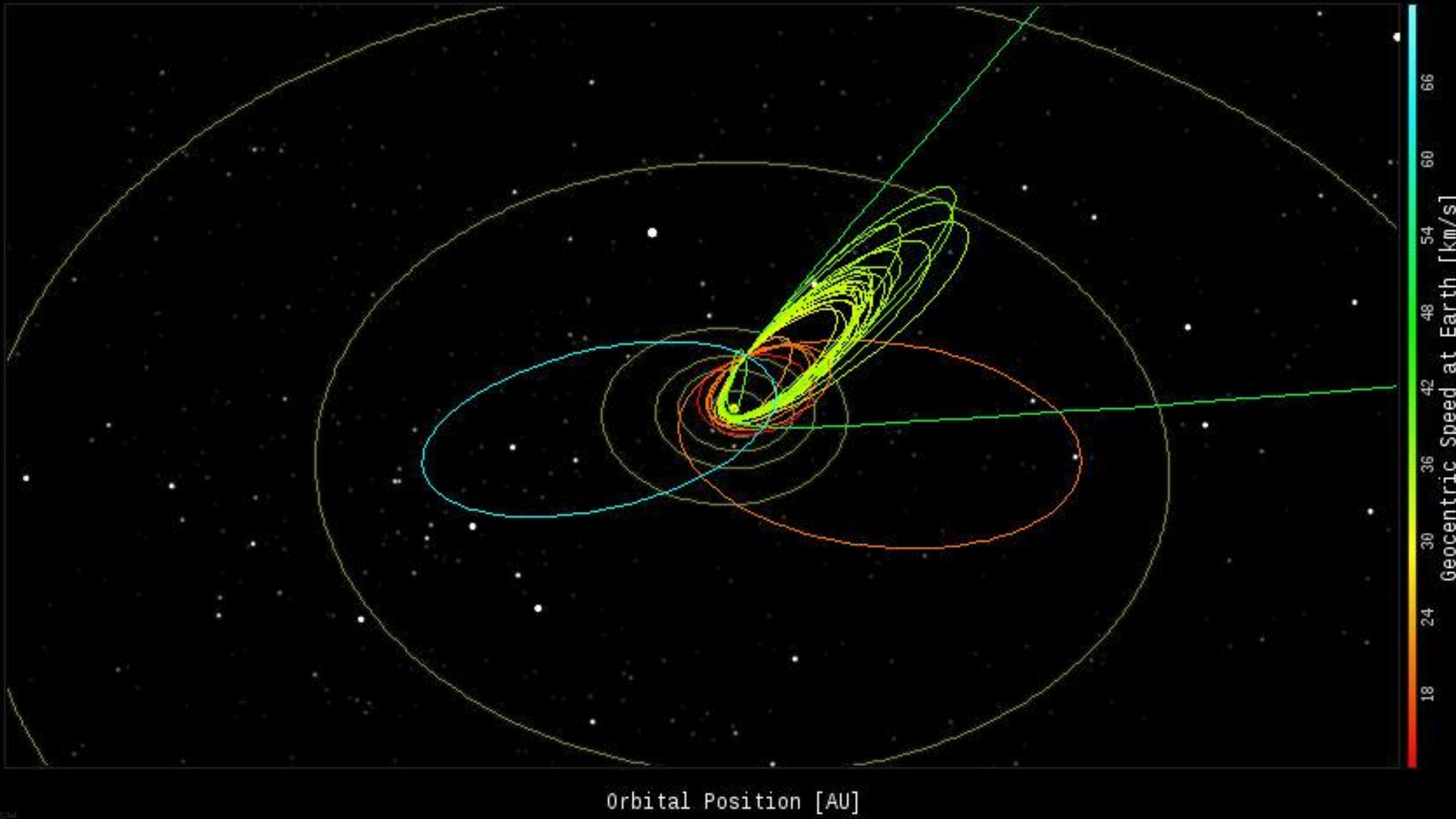

orbitsGreenGeminids same Phaethon.

Three receiving stations separation ~ 8 km

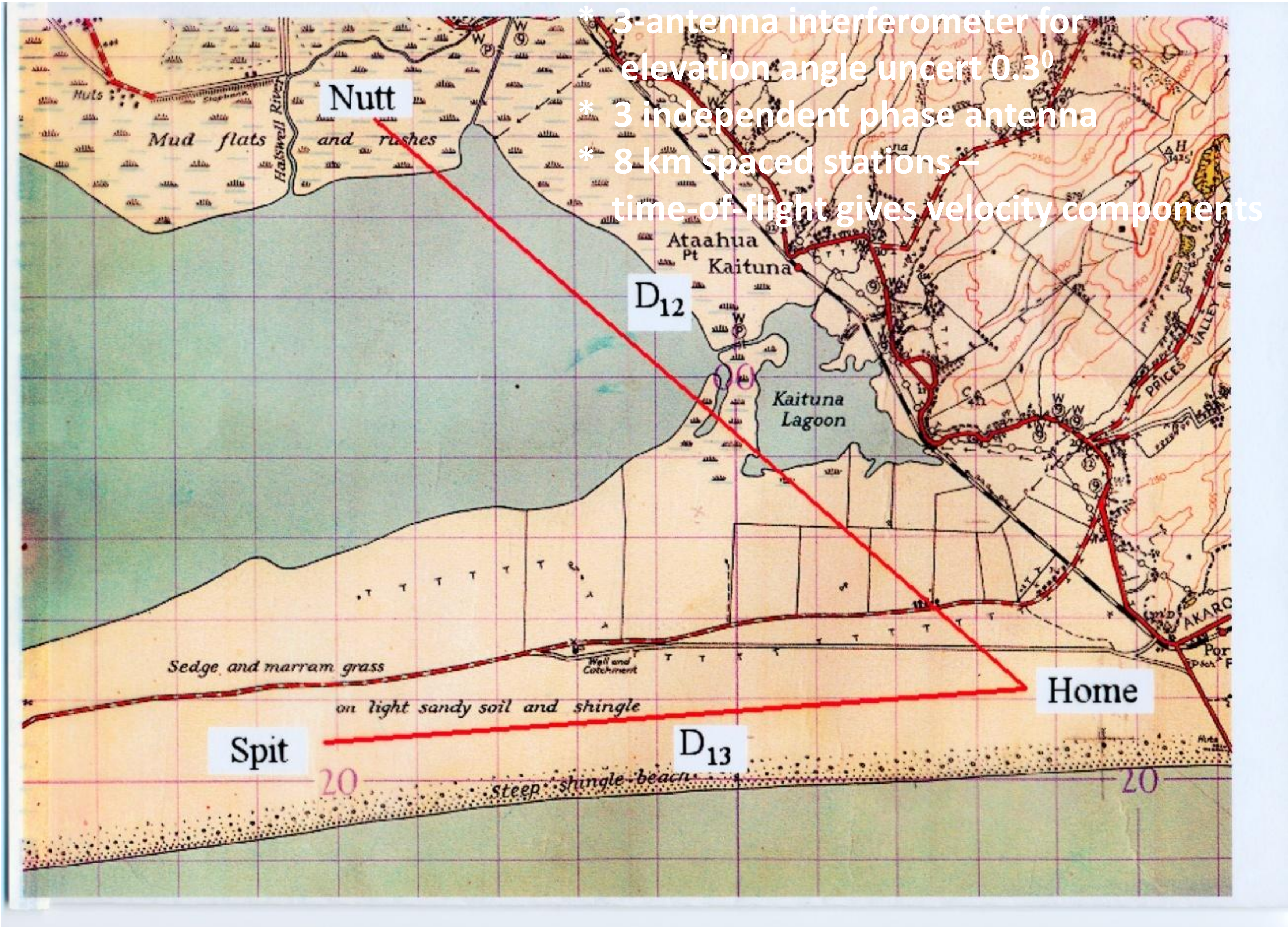

Transverse geometry reflection – specular condition: single transmitter and three receiving stations

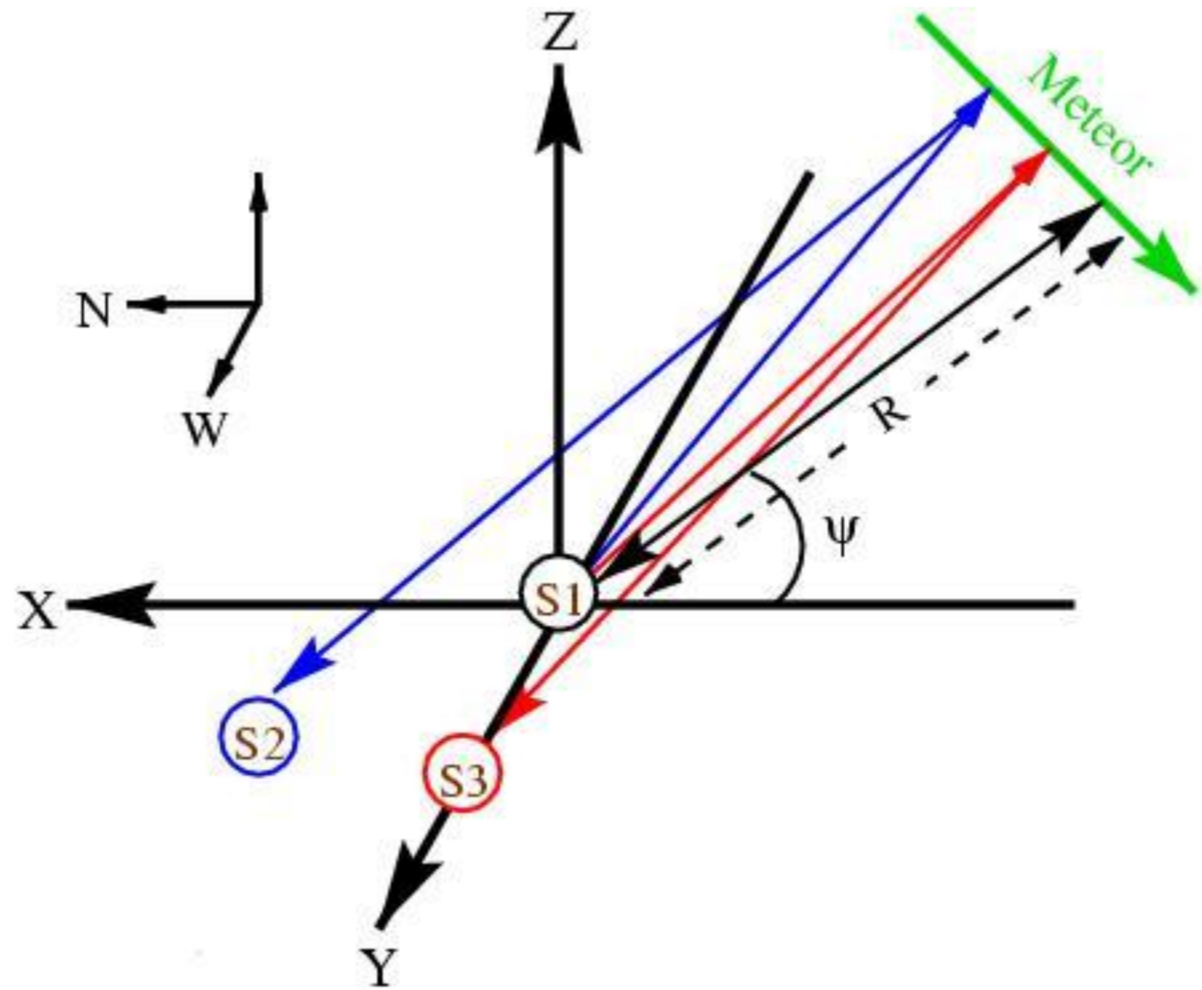

Echo angular position measured by a dual interferometer

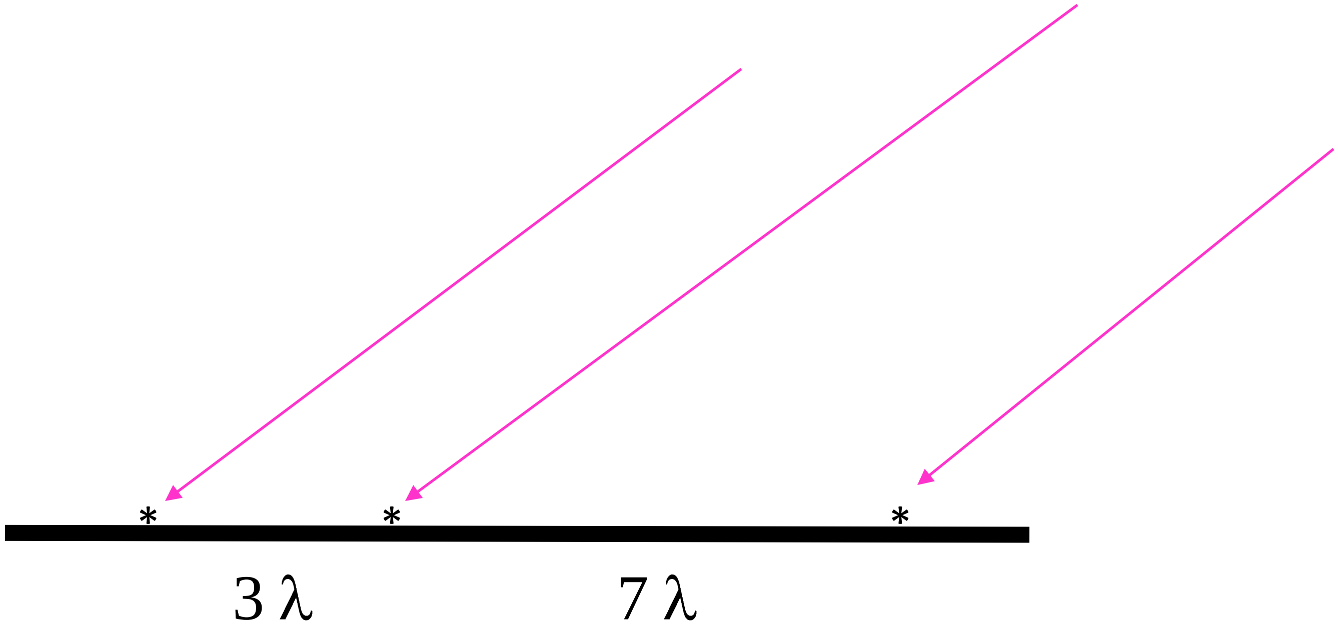

Transmitting antenna - fan beam in E-W meridian

radiation pattern 3° wide in azimuth, 15° - 75° elevation

Transmitting antenna - fan beam in N-S meridian

radiation pattern 3º wide in azimuth, 15º - 75º elevation

Radar echo characteristics

Echo amplitude –

Home site

and

two remote sites

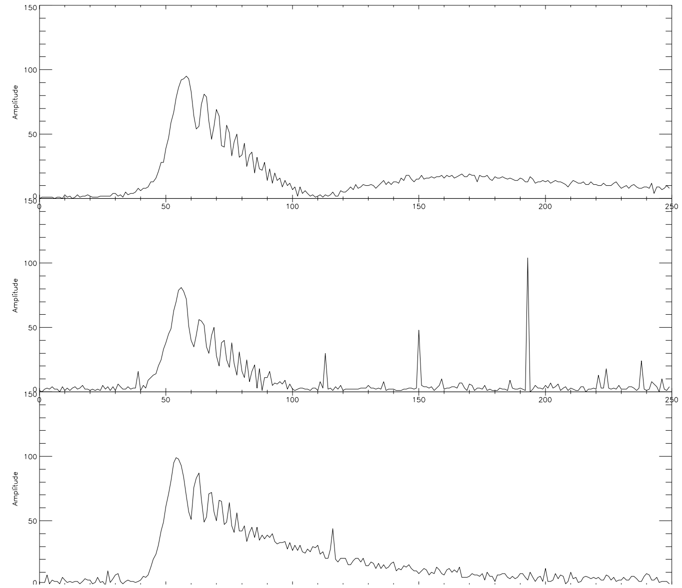

Echo amplitude

Echo phase

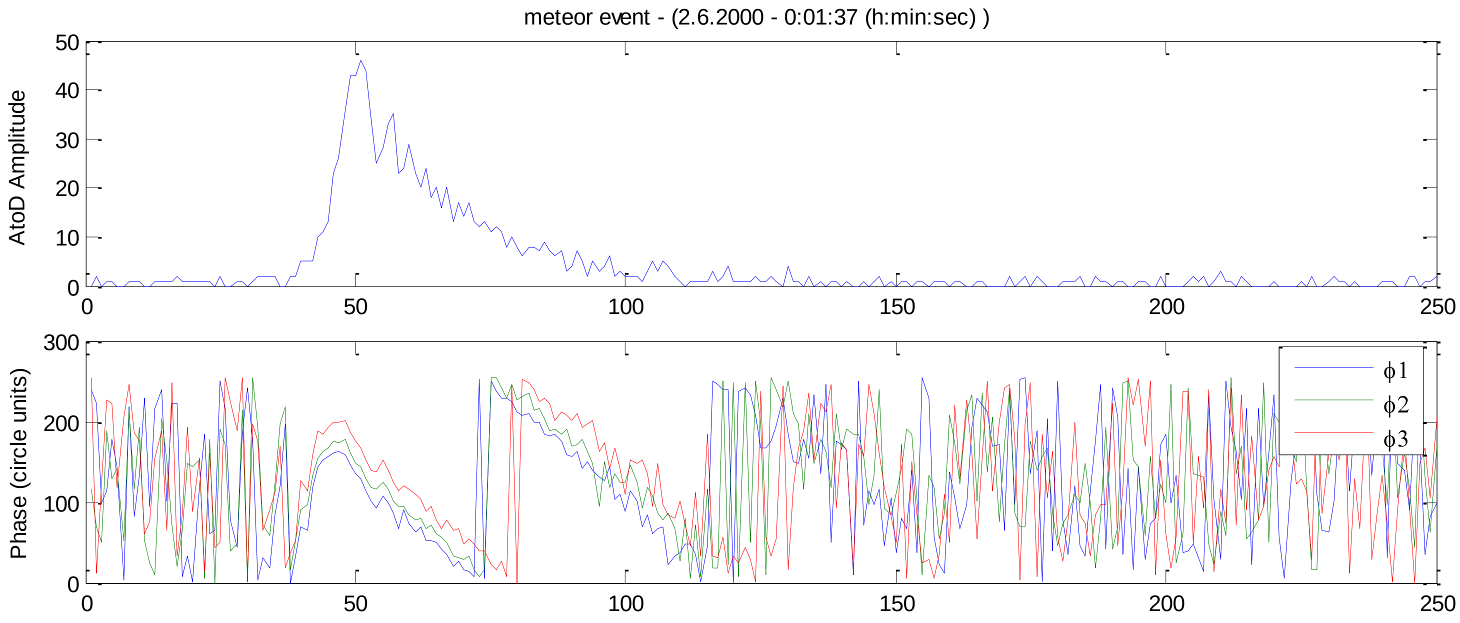

Time, radar pulses

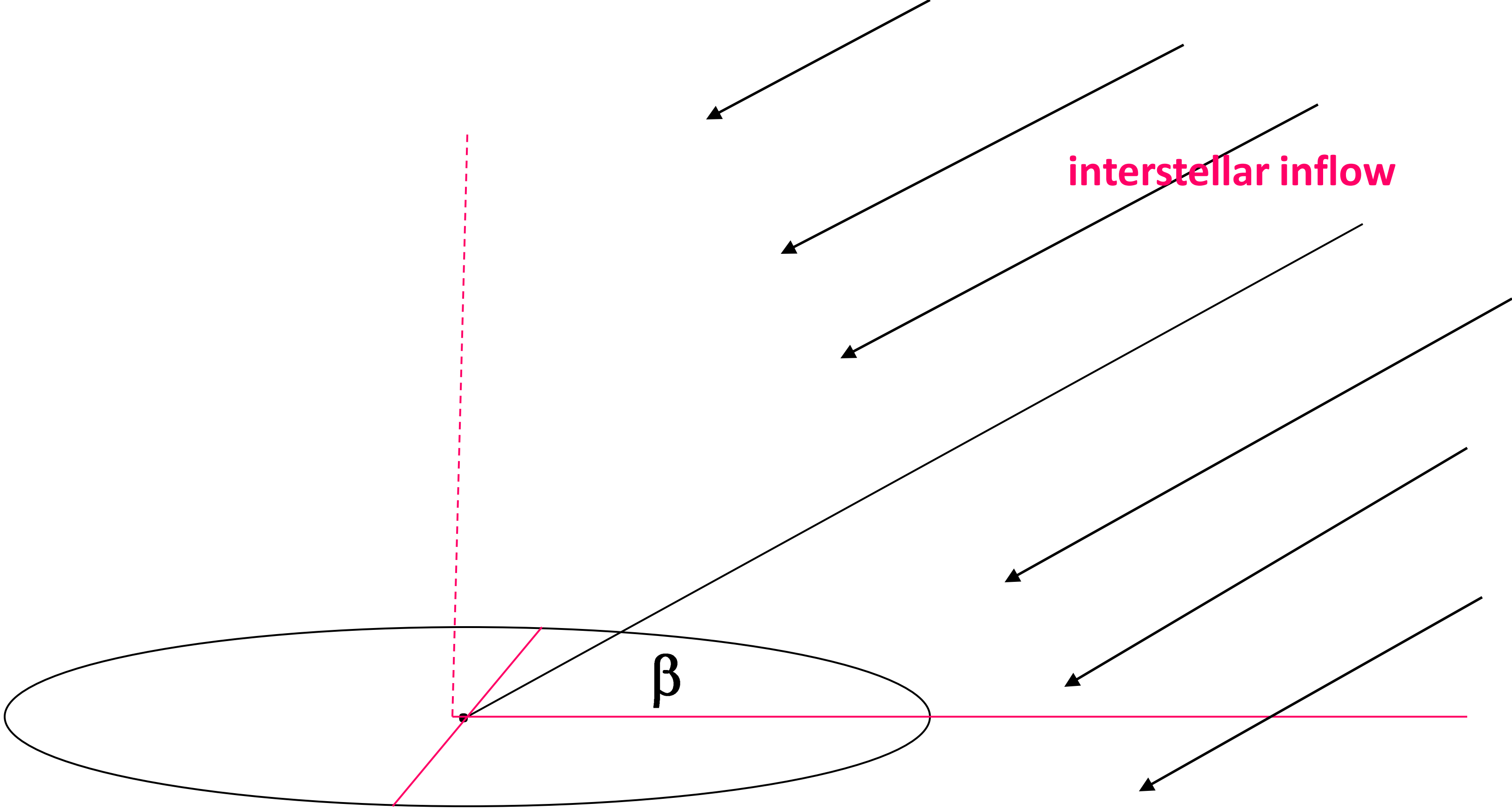

Interstellar dust inflow detected by the annual variation of dust orbital elements

Motion of stars in the solar neighbourhood
in their rotation around the galactic centre

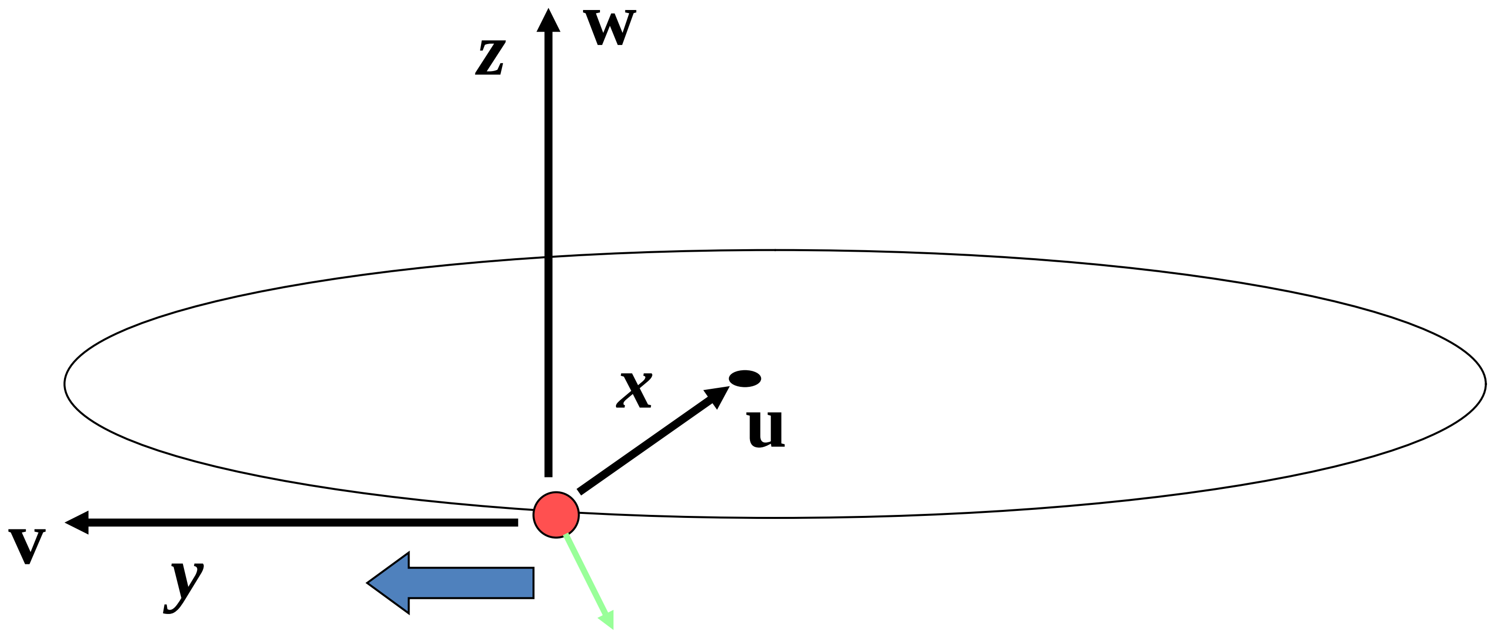

Identifying which star ejected the dust that is detect in the solar system

Motion of Sun and Star

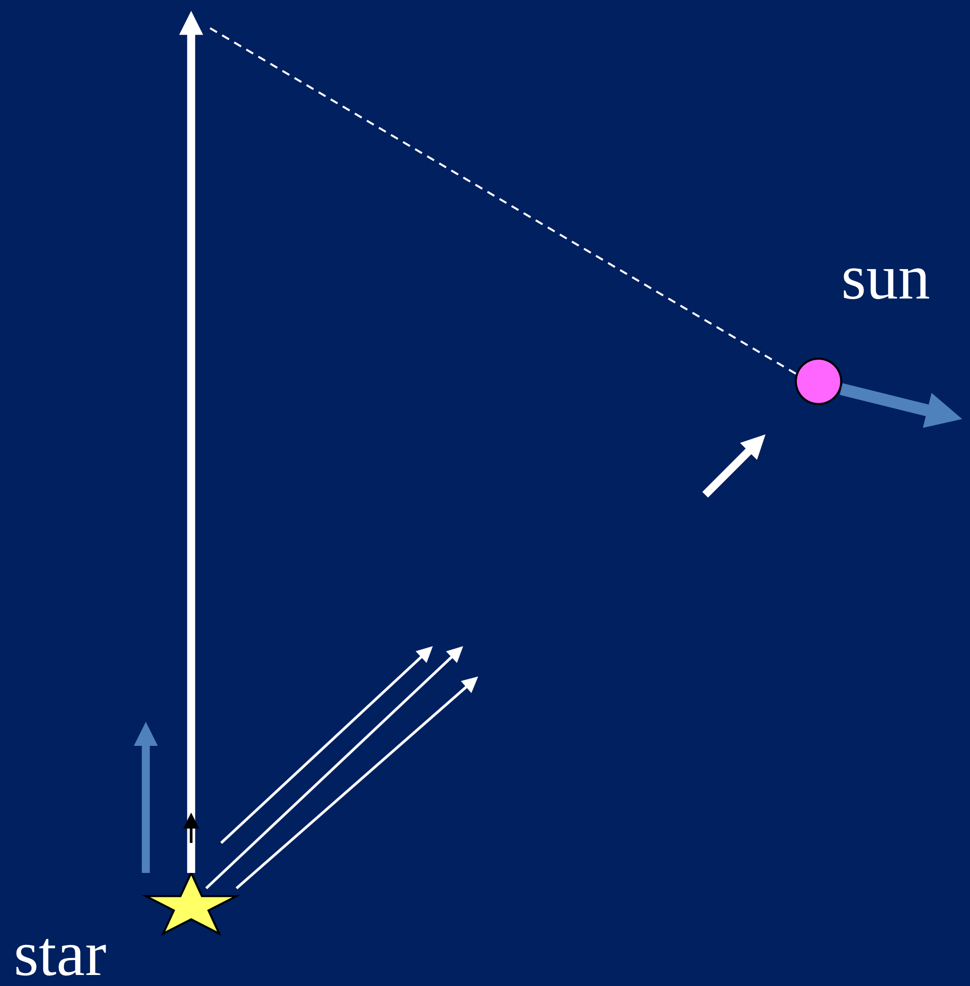

Star ejects dust